

1977

The Investigation Of The Bounds For The Scattering Amplitudes Of Spin 0 And Spin 1/2 Particle Scattering From Symmetry Principles And The Unitarity Condition

Shu-kwing Chan

Follow this and additional works at: <https://ir.lib.uwo.ca/digitizedtheses>

Recommended Citation

Chan, Shu-kwing, "The Investigation Of The Bounds For The Scattering Amplitudes Of Spin 0 And Spin 1/2 Particle Scattering From Symmetry Principles And The Unitarity Condition" (1977). *Digitized Theses*. 1007.
<https://ir.lib.uwo.ca/digitizedtheses/1007>

This Dissertation is brought to you for free and open access by the Digitized Special Collections at Scholarship@Western. It has been accepted for inclusion in Digitized Theses by an authorized administrator of Scholarship@Western. For more information, please contact tadam@uwo.ca, wlsadmin@uwo.ca.



National Library of Canada

Cataloguing Branch
Canadian Theses Division

Ottawa, Canada
K1A 0N4

Bibliothèque nationale du Canada

Direction du catalogage
Division des thèses canadiennes

NOTICE

The quality of this microfiche is heavily dependent upon the quality of the original thesis submitted for microfilm-ing. Every effort has been made to ensure the highest quality of reproduction possible.

If pages are missing, contact the university which granted the degree.

Some pages may have indistinct print especially if the original pages were typed with a poor typewriter ribbon or if the university sent us a poor photocopy.

Previously copyrighted materials (journal articles, published tests, etc.) are not filmed.

Reproduction in full or in part of this film is governed by the Canadian Copyright Act, R.S.C. 1970, c. C-30. Please read the authorization forms which accompany this thesis.

THIS DISSERTATION
HAS BEEN MICROFILMED
EXACTLY AS RECEIVED

AVIS

La qualité de cette microfiche dépend grandement de la qualité de la thèse soumise au microfilmage. Nous avons tout fait pour assurer une qualité supérieure de reproduction.

S'il manque des pages, veuillez communiquer avec l'université qui a conféré le grade.

La qualité d'impression de certaines pages peut laisser à désirer, surtout si les pages originales ont été dactylographiées à l'aide d'un ruban usé ou si l'université nous a fait parvenir une photocopie de mauvaise qualité.

Les documents qui font déjà l'objet d'un droit d'auteur (articles de revue, examens publiés, etc.) ne sont pas microfilmés.

La reproduction, même partielle, de ce microfilm est soumise à la Loi canadienne sur le droit d'auteur, SRC 1970, c. C-30. Veuillez prendre connaissance des formules d'autorisation qui accompagnent cette thèse.

LA THÈSE A ÉTÉ
MICROFILMÉE TELLE QUE
NOUS L'AVONS REÇUE

THE INVESTIGATION OF THE BOUNDS
FOR THE SCATTERING AMPLITUDES OF
SPIN 0 AND SPIN $\frac{1}{2}$ PARTICLE SCATTERING
FROM SYMMETRY PRINCIPLES AND THE UNITARITY CONDITION

by

Shu-Kwing Chan

Department of Applied Mathematics

Submitted in partial fulfillment
of the requirements for the degree of
Doctor of Philosophy

Faculty of Graduate Studies
The University of Western Ontario
London, Ontario

May, 1977

© Shu-Kwing Chan 1977

ABSTRACT

In this work the bounds on some theoretical quantities of the scattering amplitudes (like the relative phase and relative modulus) and the imaginary parts of the spin non-flip and spin flip amplitude for the spin 0 and spin $\frac{1}{2}$ particle scattering have been investigated.

The latter case is related to the existence and uniqueness problem of the solutions of the unitarity equations for the scattering amplitudes.

Some applications of the inequalities of the theoretical scattering quantities for the scattering of spin 0 and spin $\frac{1}{2}$ particles have been carried out. In particular bounds on quantities describing $K^+ p$ scattering are constructed from experimental polarization and differential cross section. With the bounds so established, different sets of phase shifts at 13 different energies between $P_{lab} = .87 \text{ Gev/c}$ and 1.89 Gev/c for $K^+ p$ scattering processes, namely the Cutkosky phase shifts and CERN α, β, γ phase shifts, are compared.

Furthermore these inequalities have been used in the unitarity equations. Different ways of the majorization programs in the imaginary parts of spin non-flip and spin flip amplitudes have been performed. The numerical calculation for the bounds of the $\pi^+ p$, $\pi^- p$ and $K^+ p$ scattering below the inelastic threshold are presented.

ACKNOWLEDGMENT

I am highly indebted to my supervisor, Professor I.A. Sakmar, for introducing this problem and for his constant guidance and instructive advice throughout the investigation of the problem.

I would like to express my gratitude to Professor R.E. Cutkosky for sending me his solutions of the $K^+ p$ partial-wave phase shifts prior to their publication.

This work is supported in part by a grant from the National Research Council of Canada to Professor I.A. Sakmar. This grant and the award of Ontario Graduate Fellowship are gratefully acknowledged.

Finally, I also wish to thank Miss Ruth Lamperd for her accurate typing of the thesis.

TABLE OF CONTENTS

	page
CERTIFICATE OF EXAMINATION	ii
ABSTRACT	iii
ACKNOWLEDGMENTS	iv
LIST OF FIGURES	vii
CHAPTER I -- INTRODUCTION	1
CHAPTER II - THE AMBIGUITIES OF THE SCATTERING AMPLITUDES	7
2.1 The Construction of the Amplitude in the Scattering of the Spinless Particles	7
2.2 The Construction of the Amplitude in the Scattering of the Spin 0 and Spin $\frac{1}{2}$ Particles	14
2.3 Martin-Newton Sufficiency Condition	27
CHAPTER III - THE INEQUALITIES OF THE THEORETICAL QUANTITIES	38
3.1 Introduction	38
3.2 The Bounds of the Theoretical Quantities	39
3.3 Tests for the $K^+ p$ Phase Shifts	46
CHAPTER IV - THE BOUNDS ON THE IMAGINARY PARTS OF THE SCATTERING AMPLITUDES	86
4.1 The Unitarity Equation	86
4.2 The Bound on the Imaginary Part of the Spin Non- Flip Amplitude	101
4.3 The Bound on the Imaginary Part of the Spin Flip Amplitude	124
4.4 The Numerical Investigation of the Physical Processes	138
SUMMARY AND DISCUSSION	167

page

APPENDIX 1 - THE PARTIAL WAVES IN THE CASE OF THE ANTI-LINEAR TRANSFORMATION	169
APPENDIX 2 - THE PARTIAL WAVES IN THE CASE OF THE LINEAR TRANSFORMATION	171
APPENDIX 3 - THE BOUNDS OF THE MODULI OF THE SPIN NON-FLIP AND SPIN FLIP AMPLITUDES	174
APPENDIX 4 - THE BOUNDS OF s DEFINED AS (3.2.6)	177
APPENDIX 5 - THE DERIVATION OF THE COUPLED UNITARITY EQUATIONS FOR SPIN 0 AND SPIN $\frac{1}{2}$ SCATTERING	178
APPENDIX 6 - THE LARGEST VALUE OF $F(\beta)$ DEFINED AS (4.2.8) WITH $a = 1$	186
APPENDIX 7 - THE LARGEST VALUE OF $F(\beta)$ DEFINED AS (4.2.8) WITH $a \leq 1$	189
APPENDIX 8 - THE DISCUSSION OF THE FUNCTION F DEFINED BY (4.2.18).	192
REFERENCES	196
VITA	201

LIST OF FIGURES

	page
Figure 1 The phase shifts δ_1 (solid line) and δ_2 (dashed line) for the transformation $T_1 T_2$	25
Figure 2 Comparison of the $K^+ p$ polarization with the relative phase ($\sin \alpha$) to test the inequality (3.2.9)	50
Figure 3 Comparison of the $K^+ p$ relative magnitude r with their bounds to test the inequalities (3.2.10a) and (3.2.10b)	55
Figure 4 Comparison of the magnitudes of $K^+ p$ amplitudes f and $g \sin \theta$ with their bounds to test the inequalities (3.2.15a) and (3.2.15b)	60
Figure 5 Comparison of the product of the moduli for the $K^+ p$ amplitudes with their bounds to test the inequalities (3.2.16a) and (3.2.16b)	65
Figure 6 Comparison of the sum of the moduli for the $K^+ p$ amplitudes with their bounds to test the inequalities (3.2.17a) and (3.2.17b)	70
Figure 6A The predictions for the rotation parameter R of phase shifts	81
Figure 6B The predictions for the rotation parameter A of phase shifts	82
Figure 7 C.M. momentum of the initial, intermediate and final states	88
Figure 8 The unitarity ellipse	89
Figure 9 Unit vectors in the direction of momenta	95
Figure 10 An example for the polarization curve and the behaviour of $\cos \alpha$	109
Figure 11 Separation of the unitarity ellipse into domains of different signs for the term $\sin \alpha(y) \sin \alpha(x)$	110
Figure 12 Separation of the unitarity ellipse into domains of different signs for the term $\cos \alpha(y) \cos \alpha(x)$	111
Figure 13 The curves for the maximum value of G (4.2.24) with fixed x and y respectively	115
Figure 14 The maximum point of G (4.2.24) in case 1	118

	page
Figure 15 The maximum point of $G(4.2.24)$ in case 2	119
Figure 16 The maximum point of $G(4.2.24)$ in case 3	121
Figure 17 The maximum point of $G(4.2.24)$ in case 4	122
Figure 18 The maximum point of $G(4.2.24)$ in case 5	123
Figure 19 The curves for the maximum value of $G(4.3.8)$ with fixed x and y respectively	130
Figure 20 The maximum point of $G(4.3.8)$ in case 1	132
Figure 21 The maximum point of $G(4.3.8)$ in case 2	133
Figure 22 The maximum point of $G(4.3.8)$ in case 3	134

The author of this thesis has granted The University of Western Ontario a non-exclusive license to reproduce and distribute copies of this thesis to users of Western Libraries. Copyright remains with the author.

Electronic theses and dissertations available in The University of Western Ontario's institutional repository (Scholarship@Western) are solely for the purpose of private study and research. They may not be copied or reproduced, except as permitted by copyright laws, without written authority of the copyright owner. Any commercial use or publication is strictly prohibited.

The original copyright license attesting to these terms and signed by the author of this thesis may be found in the original print version of the thesis, held by Western Libraries.

The thesis approval page signed by the examining committee may also be found in the original print version of the thesis held in Western Libraries.

Please contact Western Libraries for further information:

E-mail: libadmin@uwo.ca

Telephone: (519) 661-2111 Ext. 84796

Web site: <http://www.lib.uwo.ca/>

CHAPTER I

INTRODUCTION

During the last few years the scattering amplitude constructed from the experimental data has been investigated extensively. For energy below the first inelastic threshold the elastic unitarity equation can be considered to be an integral equation for the phase of the scattering amplitude. Since the unitarity equation is a nonlinear integral equation it is not guaranteed that the unitarity equation has a solution or that solution, if it exists, will be unique.

The possible ambiguities in scattering amplitudes, due to the nonlinear character of the unitarity equation, have been studied from two directions.

One is to display explicitly the existing ambiguities. This means to construct a new scattering amplitude from the known scattering amplitude with the same experimental data (total cross section, differential cross section, polarization etc.). Instead of considering the total scattering amplitude one expands the scattering amplitude into partial waves. One can then look for different sets, if possible, of phase shifts that reproduce the same experimental data. For scalar particles scattering the trivial ambiguity which is the simultaneous change of the sign of all phase shifts has been known for a long time. The first non-trivial ambiguity was found by Crichton¹. He gave a very simple example in which two sets of phase shifts (up to D wave) give the same differential cross section. Atkinson, Johnson, Mehta and

de Roo² pointed out it is not a numerical accident. They reproduced it in a more rigorous way. Later Berrends and Ruijsenaars³ constructed systematically pairs of different sets of phase shifts which give the same differential cross section. For SPD wave the construction leads to the Crichton ambiguity. For SPDF wave four different pairs of phase shifts were found. It is expected that as the number of waves increases so do the ambiguities. Other articles on this subject were presented by different authors⁴⁻¹⁰.

Ambiguities in the scattering of spin 0 and spin $\frac{1}{2}$ particles, specifically different sets of phase shifts giving the same differential cross section and polarization, were considered by Puzikov, Ryndin and Smordinskii¹¹, who also introduced the concept of a complete experiment. They pointed out the existence of a generalized Minami ambiguity, i.e. a transformation of the scattering amplitudes leaving the differential cross section, polarization and unitarity condition invariant. Less obvious ambiguities involving S and P waves only were found by Berrends and Ruijsenaars¹². Recently Bruet, Gauthier and Winternitz¹³ presented the possible ambiguities leaving two of the four experimental measurable quantities (differential cross section, polarization, rotation parameter R and A) and unitarity condition invariant. This problem was also studied by Dean and Lee¹⁴, Klepikov and Smorodinskii et al¹⁵⁻¹⁶.

The disadvantage of this approach is that it is only manageable for a small number of partial waves. As we see in Berrends and Ruijsenaars' work^{3,12} it is very complicated both for $L_{\max} = 3$ in spin-less particles scattering case or SP waves in the scattering of spin 0

and spin $\frac{1}{2}$ particles. The other disadvantage is one cannot conclude that all the possible ambiguities have been exposed since other types of ambiguities are still possible constructed by other ways.

The alternative approach is fundamentally more mathematical. It is to solve the unitarity equation directly to determine the phase of the scattering amplitudes. The unitarity equation being a nonlinear integral equation it has not been possible yet to find its solutions under general conditions. But some results, on the existence of solutions under certain conditions and their uniqueness under more stringent conditions, have been found. The existence condition for the solution of the finite dimensional unitarity matrices obtained by discretization of the unitarity integral was studied by Eftimiu¹⁷ and more recently by Tortorella and Leise¹⁸. For spinless particles scattering Martin¹⁹ and Newton²⁰ obtained the sufficiency conditions for existence and uniqueness of an elastic unitarity amplitude with a given differential cross section. They proved that under certain conditions the nonlinear integral equation has the solutions and under more restricted conditions the solution is unique using the fixed point theorem²¹. Atkinson, Johnson and Warnock²² improved the Martin-Newton results on the uniqueness and the iterative construction in the applications of Schauders' theorem. They extended their work to the inelastic region and predict the "continuum ambiguity" with a given differential cross section. Atkinson, Mahoux and Yndurain²³ pursued the investigation by taking into account the analyticity in $\cos \theta$ plane. Specific cases of physical processes were studied by Sakmar²⁴ and Goldberg²⁵. Alvarez-Estrada and Carreras²⁶ proved that the two spin 0

and spin $\frac{1}{2}$ elastic unitarity equations determine uniquely the two scattering amplitudes inside a certain restricted space Ω , once the differential cross section and polarization are given and suitably restricted. There are also three solutions outside Ω obtained through certain transformations. They correspond to the well known trivial and Minami ambiguities and their combinations. Atkinson, Mahoux and Yndurain²⁷ extended their investigation to the scattering of spin 0 and spin $\frac{1}{2}$ particles within the frame work of spinless particle scattering²³. The scattering amplitudes of spin $\frac{1}{2}$ and spin $\frac{1}{2}$ particles were studied by Alvarez-Estrada and Carreras²⁸ and more recently by Manólessou-Grammaticou²⁹.

It must be realized that the Martin-Newton sufficiency condition is very restrictive. In particular it implies automatically $|\delta_\ell| < \frac{\pi}{6}$ for all $\ell > 0$, which means that an amplitude with a resonating $\ell \neq 0$ wave will never fulfill this condition. The numerical investigation of the physical processes^{24,25} and the ambiguities of the phase shift³ show that none of them satisfies the Martin-Newton condition. It is clear that an improvement of this sufficiency condition is needed. The problem of finding the sufficiency condition for the existence of solutions for the unitarity equation is more or less related to maximizing the integral part of the unitarity equation (which leads to the problem of finding an upper bounds of the imaginary parts of the scattering amplitudes from the unitarity condition). For the scattering of spin 0 and spin $\frac{1}{2}$ particles the working amplitudes of Ref. 26 are the transversity amplitudes G_+ and G_- . The differential cross section and polarization data give complete information on the moduli of the

transversity amplitudes $|G_+|$ and $|G_-|$ but nothing about the phases. In order to majorize the integral of the unitarity equations they take the cosine of the phase to be one. This means that all the information on the phases is lost. On the other hand, the moduli of the spin non-flip and spin flip amplitudes $|f|$ and $|g|$ are not determined with the knowledge of the differential cross section D and polarization P neither is the relative phase of f and g . But the upper and lower bounds for the moduli and the relative phase of these amplitudes are determined by D and P^{30-33} . The additional knowledge of the rotation parameter R would determine the relative phase as well as the moduli. The experimental information on D and P is distributed between the three quantities $|f|$, $|g|$ and the relative phase ($\sin \alpha$) in terms of their combinations or as bounds on each of them³⁰. Thus there is too little information on $|f|$ and $|g|$ which are needed in the unitarity equations and too much information on the phase (relative phase) which will be determined by those equations (This observation is due to Sakmar). The other reason to use the spin non-flip and spin flip amplitudes rather than the transversity amplitudes in the derivation of the bounds of the imaginary part for the scattering amplitude is in the simplicity of the unitarity equations and the majorization program. We apply this program later to πp and Kp scatterings.

In this work the tests of $K^+ p$ phase shifts using the bounds of the scattering amplitudes are investigated³⁴. Different sets of phase shifts are compared. The two unitarity equations for spin non-flip and spin flip amplitudes are established. Using the knowledge of the upper and lower bounds of $|f|$, $|g|$ and the relative phase ($\sin \alpha$) determined

by the differential cross section and polarization the bounds on the imaginary parts below the inelastic threshold are obtained from the unitarity condition³⁵.

In chapter II the ambiguities of the scattering amplitudes and the Martin-Newton sufficiency condition are reviewed. The inequalities of the moduli of the spin non-flip amplitudes and spin flip amplitude, relative phase and their combinations are discussed in chapter III. The material in chapter II as well as in the first two sections of chapter III is well known and have been included here as the basis of the following work for the sake of completeness. In section 3.3 of chapter III, testing the restrictions of the inequalities, four different sets of the phase shifts for $K^+ p$ scattering are compared. We give here computer printouts for the bounds of different theoretical quantities as well as their calculated values from the four sets of phase shifts at 13 different energies.

In chapter IV the coupled unitarity-equations of spin non-flip and spin flip amplitudes for the scattering of spin 0 and spin $\frac{1}{2}$ particles are established. The bounds on the imaginary parts of the spin non-flip amplitude and spin flip amplitude are obtained by different ways of majorizations. We also give in this chapter improvements over some of the results of Ref. 35. The numerical comparisons of the bounds with the experimental data are presented here over the entire range of energy for which data was available (including the results of the improved majorizations).

CHAPTER II

THE AMBIGUITIES OF THE SCATTERING AMPLITUDES

2.1 The Construction of the Amplitude in the Scattering of the Spinless Particles.

In the scalar particles scattering process, for example the $\pi - \pi$ and $\alpha - \alpha$ scattering, the experimental measurements are the differential cross section $\frac{d\sigma}{d\Omega}$ and the total cross section σ . Assume that the experimental measurements are infinitely accurate at any fixed energy E and scattering angle θ . In principle one can determine the scattering amplitude up to the overall phase for any fixed value of energy E and scattering angle θ from

$$\frac{d\sigma(E, \theta)}{d\Omega} = |f(E, \theta)|^2 \quad (2.1.1)$$

and the phase of the forward scattering ($\theta = 0$) is determined by optical theorem

$$\text{Im } f(E, 0) = \frac{q_{\text{C.M.}}}{4\pi} \sigma_{\text{Tot.}} \quad (2.1.2)$$

where $f(E, \theta)$ is the scattering amplitude at energy E and scattering angle θ , $q_{\text{C.M.}}$ is the C.M. momentum of the scattering particle, $\frac{d\sigma}{d\Omega}$ and σ are the differential cross section and total cross section respectively.

The scattering amplitude f is a complex quantity.

The partial wave expansion of the scattering amplitude is defined by

$$f(\theta) = \frac{1}{q_{C.M.}} \sum_{\ell=0}^L (2\ell + 1) f_\ell P_\ell(\cos \theta) \quad (2.1.3)$$

$$f_\ell = \frac{\eta_\ell e^{i\delta_\ell} - 1}{2i} \quad (2.1.4)$$

where f_ℓ is the partial wave amplitude of the ℓ -wave, $P_\ell(\cos \theta)$ are the Legendre polynomials of order ℓ , η and δ are real, they represent the inelasticity coefficient and the phase shift respectively. Below the inelastic threshold f_ℓ lies on the unitarity circle. It is $\eta_\ell = 1$, then f_ℓ becomes $e^{i\delta_\ell} \sin \delta_\ell$.

i) trivial ambiguity

The conservation of the probability is origin of the unitarity equation (generalized optical theorem) satisfied by the scattering amplitude below the inelastic threshold

$$\text{Im } f(\vec{n}, \vec{n}) = \frac{q_{C.M.}}{4\pi} \int d\Omega'' f^*(\vec{n}, \vec{n}'') f(\vec{n}'', \vec{n}) \quad (2.1.5)$$

where \vec{n} , \vec{n}' , \vec{n}'' are the directions of the C.M. momentum of the initial final and intermediate states respectively. The details of the unitarity equation are discussed in chapter IV.

In order to satisfy the unitarity equation the phase of the scattering amplitude can no longer be arbitrary. It is obvious that if f is a solution of (2.1.5) so is $-f^*$, the overall sign of real part of scattering amplitude cannot be determined from the unitarity. If we consider the unitarity equation an integral equation for the unknown phase when the modulus of the amplitude is known at all angles the above ambiguity means that if $\psi(\theta)$ is a solution of the equation (2.1.5) then so is $\pi - \psi(\theta)$. This kind of ambiguity is called trivial ambiguity. In terms of the partial wave amplitudes the trivial ambiguity means that the pairs of δ_ℓ and $-\delta_\ell$ give the same differential cross section and satisfy the unitarity condition (2.1.5).

ii) non-trivial ambiguities

In principle the partial wave expansion is an infinite series, but in actual phase shift analysis one always cuts off the series at a finite value of L (L depends on the scattering energy, the higher the energy the larger the number of partial waves). Then the scattering amplitude becomes a polynomial of $\cos \theta$, which can be expressed in terms of its roots F_i (complex) and the forward amplitude $f(0)$

$$f(\theta) = f(0) \prod_{i=1}^L \frac{\cos \theta - F_i}{1 - F_i} \quad (2.1.6)$$

The possible amplitudes $f'(\theta)$ can be obtained from the known amplitude $f(\theta)$ by two types of transformations or their combinations.

$$a) S : \text{Ref}(0) \rightarrow -\text{Ref}(0)$$

(2.1.7)

$$b) T_i : F_i \rightarrow F_i^*$$

which leads to the invariance of the modulus of the scattering amplitude as well as the differential cross section and total cross section.

First we notice the transformation $S \prod_{i=1}^L T_i$ is the trivial ambiguity. Secondly if the transformations A and B are such that their product is a trivial ambiguity then the difference between them is a different sign of the phase shift δ_ℓ . The transformations A and B will therefore be called equivalent. To consider one of them is enough. We have the freedom to choose A or B as convenient as possible.

Not any transformation is physical. The scattering amplitude generated by the transformations should satisfy the unitarity condition below the inelastic threshold. This means that the partial wave amplitudes f'_ℓ obtained by physical transformations are on the unitarity circle. The procedure to construct a new scattering amplitude $f'(\theta)$ from $f(\theta)$ is following. Assume the scattering amplitude $f(\theta)$ has physical partial waves characterized by $\eta_\ell \delta_\ell$ or $\zeta_\ell = \eta_\ell e^{i\delta_\ell}$. The ζ_ℓ are expressed in terms of the roots F_i and the forward scattering amplitude $f(0)$. And then the effect of the transformations generated by (2.1.7) are investigated. We require the $|\zeta_\ell|$ to be invariant. Next we restrict $|\zeta_\ell| = 1$ (this is equivalent to f_ℓ being on the unitarity circle). In this way the specific sets ζ_ℓ and ζ'_ℓ both physical and giving the same differential cross section are found.

For SPD wave case ζ_λ in terms of the roots F_1 and a quantity a defined as $a = 2i q_{C.M.} f(0)$ are,

$$\zeta_2 = \frac{a}{(1 - F_1)(1 - F_2)} \left(\frac{2}{15}\right) + 1$$

$$\zeta_1 = \frac{-a}{(1 - F_1)(1 - F_2)} \left(\frac{F_1 + F_2}{3}\right) + 1 \quad (2.1.8)$$

$$\zeta_0 = \frac{a}{(1 - F_1)(1 - F_2)} \left(F_1 F_2 + \frac{1}{3}\right) + 1$$

The possible transformations are S , T_1 , T_2 , $T_1 T_2$, ST_1 , ST_2 , $ST_1 T_2$.

If we discard the trivial ambiguity and the equivalent transformations this leaves us with the transformations S and ST_1 to be considered.

In the case of the transformation S the invariance of $|\zeta_2|$ leads to $(1 - F_1)(1 - F_2)$ real. The invariance of $|\zeta_1|$ implies $F_1 + F_2$ to be real also. It turns out that the transformation S is the trivial ambiguity, i.e. $\delta_\lambda \rightarrow \delta_\lambda$. It is true for higher partial wave case too.

In the case of transformation ST_1 the invariance of $|\zeta_2|$ requires either F_2 is real or $\frac{a}{1 - F_1} = x$ with x real. In the first case ST_1 is equivalent to $ST_1 T_2$, i.e. trivial ambiguity.

In the latter case the invariance of $|\zeta_1|$ leads to F_2 is real or $x = -3$. Again when F_2 is real it is a trivial ambiguity. The only interesting case is $x = -3$. Under this restriction (2.1.8) becomes

$$\zeta_2 = \frac{\frac{3}{5} - F_2}{1 - F_2}$$

$$\zeta_1 = \frac{1 + F_1}{1 - F_2} \quad (2.1.9)$$

$$\zeta_0 = \frac{-F_2(3F_1 + 1)}{1 - F_2}$$

Imposing the unitarity condition ($|\zeta_\ell| = 1$), we have the following relations

$$|F_2| \cos \psi_2 = \frac{4}{5} \quad (2.1.10)$$

$$2|F_1| \cos \psi_1 = |F_2|^2 - |F_1|^2 - \frac{8}{5} \quad (2.1.11)$$

$$|F_1|^2 = \frac{1}{2}(-|F_2|^2 - \frac{1}{5|F_2|^2} + \frac{8}{5}) \quad (2.1.12)$$

where ψ_1 and ψ_2 are the phases of F_1 and F_2 , respectively. The restriction of $|F_2|^2$ is that $|F_1|^2 \geq 0$, $|\cos \psi_2| \leq 1$ and $|\cos \psi_1| \leq 1$.

The last one means (from (2.1.11) and (2.1.12))

$$h(|F_2|^2) \geq 0 \quad (2.1.13)$$

where $h(|F_2|^2) = -225|F_2|^8 + 520|F_2|^6 - 286|F_2|^4 + 8|F_2|^2 - 1$

$$(2.1.14)$$

which restricts $|F_2|^2$ to the region [0.8389, 1.4498]

Define

$$g(|F_2|^2) = 5(|F_2|^2 - \frac{16}{25})^{\frac{1}{2}}$$

The phase shifts can be in terms of $|F_2|$, h and g as following

$$\delta_2 = \delta'_2 = \arctan g - \frac{1}{2}\pi$$

$$\begin{cases} \delta'_1 \\ \delta'_0 \end{cases} = \pm \frac{1}{2} \arctan \frac{\sqrt{h}}{15|F_2|^4 - 4|F_2|^2 + 1} + \frac{1}{2} \arctan g$$

$$\begin{cases} \delta'_0 \\ \delta'_0 \end{cases} = \pm \frac{1}{2} \arctan \frac{\sqrt{h}}{15|F_2|^4 - \frac{52}{3}|F_2|^2 + 1} + \frac{1}{2} \arctan g$$

$$+ \frac{1}{2} \arccos \frac{4}{5|F_2|^2} \pm \frac{1}{2}\pi \theta\left(\frac{26 + \sqrt{541}}{45} - |F_2|^2\right) + \frac{1}{2}\pi$$

where $\theta(x)$ is a step function $\theta(x) = 1$ when $x > 0$, $\theta(x) = 0$ when $x \leq 0$.

The region of $|F_2|^2$ from 0.8389 to 1.4498 corresponds to a domain of δ_2 from 12.53° to 24.15° . Note that $\delta'_0 = \delta'_0$ and $\delta'_1 = \delta'_1$ (modulo π), at the points $\delta'_2 = 12.53^\circ$ and 24.15° , we see that there is a unique set of phase shifts at $\delta'_2 = 12.53^\circ$ but this set splits into two sets as δ'_2 is increased. At $\delta'_2 = 24.15^\circ$ the phase shifts coincide again (modulo π). Outside this region there are no scattering amplitudes which satisfy the unitarity condition.

2.2 The Construction of the Amplitude in the Scattering of Spin 0 and Spin $\frac{1}{2}$ Particles.

The scattering amplitude for the particles with spin $\frac{1}{2}$ and spin 0 is described by the 2×2 matrix

$$F(\theta) = f(\theta) I + ig(\theta)(\vec{\sigma} \cdot \vec{n}) \quad (2.2.1)$$

where $\vec{\sigma}$ is the spin vector with its components pauli matrices, I is an unit matrix, $\vec{n} = \vec{q}_{C.M.} \times \vec{q}'_{C.M.} / |\vec{q}_{C.M.} \times \vec{q}'_{C.M.}|$ is the unit normal to the scattering plane, $f(\theta)$ and $g(\theta)$ are the spin non-flip and spin flip amplitudes respectively.

The differential cross section and polarization are measured experimentally thus enabling us to determine

$$\frac{d\sigma}{d\Omega} = |f(\theta)|^2 + |g(\theta)|^2 \quad (2.2.2)$$

$$P \frac{d\sigma}{d\Omega} = 2 \operatorname{Im} f(\theta) g^*(\theta) \quad (2.2.3)$$

In the partial wave expansion the spin non-flip and spin flip amplitudes are

$$f(\theta) = \frac{1}{q_{C.M.}} \sum_{l=0}^L [(l+1)f_{l+} + lf_{l-}] P_l(\cos \theta) \quad (2.2.4)$$

$$g(\theta) = \frac{\sin \theta}{q_{C.M.}} \sum_{l=0}^L [f_{l+} - f_{l-}] P'_l(\cos \theta) \quad (2.2.5)$$

where $q_{C.M.}$ is the C.M. momentum, P_l and P'_l are the Legendre Polynomials and their first derivatives respectively, and $f_l^+(f_l^-)$ is the partial wave amplitude with angular momentum l and spin up (down). f_l are defined by

$$f_l = \frac{\zeta_l - 1}{2i} = \frac{\eta_l e^{2i\delta_l} - 1}{2i} \quad (2.2.6)$$

where η_l and δ_l are the inelasticity coefficient and the phase shift respectively.

The constraint of unitarity in terms of partial waves is (with definitions (2.2.4) and (2.2.5))

$$\text{Im } f_{l^\pm} = |f_{l^\pm}|^2 \quad (2.2.7)$$

i) Minami ambiguity

It is obvious the differential cross section and polarization are invariant under one of the following transformations or their combinations.

a) anti linear transformation

$$f(\theta) \rightarrow -f^*(\theta) \quad (2.2.8)$$

$$g(\theta) \rightarrow g^*(\theta)$$

b) linear transformation

$$\begin{pmatrix} f'(\theta) \\ g'(\theta) \end{pmatrix} = \begin{pmatrix} \cos \psi & \sin \psi \\ -\sin \psi & \cos \psi \end{pmatrix} \begin{pmatrix} f(\theta) \\ g(\theta) \end{pmatrix} \quad (2.2.9)$$

in particular $\psi = 0$.

In terms of partial waves the anti linear transformation (2.2.8) is equivalent to replacing $f_{\ell+}^*$ by (Appendix 1)

$$f'_{\ell+} = -(f_{\ell+}^* + 2\ell f_{\ell-}^*)/(2\ell + 1) \quad (2.2.10)$$

$$f'_{\ell-} = -[2(\ell + 1)f_{\ell+}^* - f_{\ell-}^*]/(2\ell + 1)$$

and the linear transformation (2.2.9) with $\psi = 0$ becomes (Appendix 2)

$$f'_{\ell+} = [2(\ell + 2)f_{\ell+1+} - f_{\ell+1-}]/(2\ell + 3) \quad (2.2.11)$$

$$f'_{\ell-} = [2(\ell - 1)f_{\ell-1-} + f_{\ell-1+}]/(2\ell - 1)$$

The combination of the transformations (2.2.10) and (2.2.11) leads to the Minami transformation

$$f_{\ell\pm}^M = -f_{\ell+1\mp}^* \quad (2.2.12)$$

It is easy to show that the amplitudes obtained by the

transformation (2.2.10) or (2.2.11) violate unitarity condition (2.2.7); only the Minami transformation (2.2.12) survives.

ii) non-trivial ambiguities

It is similar to the scalar particle scattering case. We choose the transversity amplitudes defined by

$$G_+(\theta) = f(\theta) + ig(\theta) \quad (2.2.13)$$

$$G_-(\theta) = f(\theta) - ig(\theta) \quad (2.2.14)$$

The relation between the transversity amplitudes and the differential cross section and polarizations are

$$\frac{d\sigma}{d\Omega} = \frac{1}{2}(|G_+|^2 + |G_-|^2) \quad (2.2.15)$$

$$P \frac{d\sigma}{d\Omega} = \frac{1}{2}(|G_+|^2 - |G_-|^2) \quad (2.2.16)$$

Because of the partial wave expansion (2.2.4) and (2.2.5) we have the relations $f(\theta) = f(-\theta)$ and $g(\theta) = -g(-\theta)$. From the definitions of the two transversity amplitudes (2.2.13) and (2.2.14) they are connected by

$$G_-(\theta) = G_+(-\theta) \quad (2.2.17)$$

From the partial wave expansion (2.2.4) and (2.2.5) one can write the spin non-flip and spin flip amplitudes in the forms

$$f(\theta) = \sum_{l=0}^L f_l P_l(\cos \theta) \quad (2.2.18)$$

$$g(\theta) = \sin \theta \sum_{l=0}^{L-1} g_l P_l(\cos \theta) \quad (2.2.19)$$

In practice the partial wave expansion is cut off at a finite number L , in this case $f(\theta)$ is a polynomial of degree L in $\cos \theta$ and $g(\theta)$ is a polynomial of degree $L - 1$ in $\cos \theta$ which is multiplied by $\sin \theta$. We can represent the functions $f(\theta)$ and $g(\theta)$ as rational functions of $t = \tan \frac{1}{2} \theta$, because

$$\sin \theta = \frac{2 \tan \frac{1}{2} \theta}{1 + \tan^2 \frac{1}{2} \theta} = \frac{2t}{1 + t^2} \quad (2.2.20)$$

$$\cos \theta = \frac{1 + \tan^2 \frac{1}{2} \theta}{1 + \tan^2 \frac{1}{2} \theta} = \frac{1 + t^2}{1 + t^2}$$

Hence we obtain,

$$G(\theta) = \frac{A(t)}{(1 + t^2)^L} \quad (2.2.21)$$

where

$$A(t) = \sum_{n=0}^{2L} a_n t^n \quad (2.2.22)$$

It is a polynomial of degree $2L$ in t .

Finding the roots F_i of the polynomial (2.2.22) we can write

$$A(t) = f(0) \prod_{i=1}^{2L} \left(1 - \frac{t}{F_i}\right) \quad (2.2.23)$$

then

$$G_+(t) = \frac{f(0)}{(1+t)^{2L}} \prod_{i=1}^{2L} \left(1 + \frac{t}{F_i}\right) \quad (2.2.24)$$

because of the relation (2.2.17) we have

$$G_-(t) = G_+(-t) = \frac{f(0)}{(1-t)^{2L}} \prod_{i=1}^{2L} \left(1 + \frac{t}{F_i}\right) \quad (2.2.25)$$

The invariance of $|G_+(t)|$ and $|G_-(t)|$ are obtained when one performs the following transformations or their combinations

$$1) S : \text{Ref}(0) \rightarrow -\text{Ref}(0) \quad (2.2.26)$$

$$2) T : F_i \rightarrow F_i^* \quad (2.2.27)$$

$$3) R_m \text{ and } R_{-m}$$

$$R_m : G(t) = \frac{t^m}{1+t} G(t) \quad (2.2.28)$$

$$R_{-m} : G(t) = \frac{(1+t)^m}{1-t} G(t)$$

These transformations raise the order of the polynomial (2.2.22)

from $2L$ to $2L + 2m$. The additional $2m$ roots are $i = \sqrt{-1}$ for R_m and $-i = -\sqrt{-1}$ for R_{-m} . The corresponding transformations for $G_-(t)$ are

$$\begin{aligned} R_m : G'_-(t) &= \left(\frac{i-t}{i+t}\right)^m G_-(t), \\ R_{-m} : G'_-(t) &= \left(\frac{i-t}{i+t}\right)^m G_-(t). \end{aligned} \quad (2.2.29)$$

For the transformation R_{-1}

$$G'_+(t) = \left(\frac{i-t}{i+t}\right) G_+(t) = (\cos \theta - i \sin \theta) G_+(\theta). \quad (2.2.30)$$

$$G'_-(t) = \left(\frac{i-t}{i+t}\right) G_-(t) = (\cos \theta + i \sin \theta) G_-(\theta)$$

In terms of $f(\theta)$ and $g(\theta)$ we have

$$f'(\theta) = f(\theta) \cos \theta + g(\theta) \sin \theta$$

$$g'(\theta) = -f(\theta) \sin \theta + g(\theta) \cos \theta$$

This is the linear transformation (2.2.9).

The combination of the transformation (2.2.26) and (2.2.27)

$\sum_{i=1}^{2L} T_i$ gives

$$G'_+(0) = -G^*_+(0)$$

(2.2.31)

$$G'_-(0) = -G^*_-(0)$$

From the relation (2.2.13) and (2.2.14) we have

$$f'(0) = -f^*(0)$$

(2.2.32)

$$g'(0) = g^*(0)$$

It turns out to be the antilinear transformation (2.2.8). So the transformation $R_{-1} S \prod_{i=1}^{2L} T_i$ is the Minami ambiguity.

We notice that not all the scattering amplitudes constructed with the transformations satisfy the unitarity condition. The procedure of constructing a unitarity amplitude is as follows. First write down the partial wave amplitude (or ζ_j) in terms of the forward amplitude and the roots F_i . Secondly consider all possible transformations and then impose the unitarity condition $|\zeta_j| = |\zeta_j'| = 1$.

In the simplest case only S and P waves are involved. The connection between ζ_j , a defined by $a = 2i q_{\text{C.M.}} f(0)$ and the roots F_i is given by

$$\zeta_j = 1 + \frac{1}{2} a \left(1 + \frac{1}{F_1 F_2} \right)$$

(2.2.33)

$$\zeta_1^+ = 1 + \frac{1}{6} a \left(1 + \frac{-1 + i(F_1 + F_2)}{F_1 F_2} \right) \quad (2.2.34)$$

$$\zeta_1^- = 1 + \frac{1}{6} a \left(1 - \frac{1 + 2i(F_1 + F_2)}{F_1 F_2} \right) \quad (2.2.35)$$

The transformations we have to consider are ST_1T_2 , S, T_1T_2 , T_1 and ST_1 . The remaining transformations are either equivalent or the Minami ambiguity.

1) Transformation ST_1T_2

According to (2.2.31) and (2.2.32) this transformation is an anti linear transformation. The amplitudes generated by this transformation never satisfy the unitarity condition except when the polarization $P = 0$ (in that case $g(\theta) = 0$).

2) Transformation S

ζ_j and ζ'_j have the form

$$\zeta_j = 1 + a C_j \quad (2.2.36)$$

$$\zeta'_j = 1 + a^* C_j$$

both a and C_j are complex. $|\zeta_j| = |\zeta'_j|$ requires either a or C_j is real. If a is real the transformation S is an identical transformation. If C_j are real it makes the transformation S the same as ST_1T_2 .

3) Transformation $T_1 T_2$

$|\zeta_0^+|$ does not change under the transformation $T_1 T_2$ when a is real or $F_1 F_2 = \frac{1}{y}$ is real. The first case makes $T_1 T_2$ equal to $S T_1 T_2$ and.

therefore uninteresting. For the second case the condition that $|\zeta_1^+|$ remain invariant implies that

$$i \frac{6}{a} + i(1-y) = x, \quad (2.2.39)$$

where x is real. The invariance of $|\zeta_1^-|$ is guaranteed by unitarity.

By defining $G = \frac{1}{F_1} + \frac{1}{F_2}$ we obtain

$$\zeta_0^+ = \frac{x + 2i + 4iy}{iy - i + x} \quad (2.2.40)$$

$$\zeta_1^+ = \frac{x - G}{iy - i + x} \quad (2.2.40)$$

$$\zeta_1^- = \frac{x + 2G}{iy - i + x}$$

The effect of $T_1 T_2$ is replacement of G by G^* .

The unitarity condition $|\zeta_j| = |\zeta'_j| = 1$ leaves only two values for y and give the representation in terms of a parameter Z .

a) $y = -1, Z = -\frac{1}{3x}$

$$\zeta_0^+ = 1, \zeta_1^+ = \frac{1 + 3\sqrt{2}Z e^{ix}}{1 + 6iz}, \zeta_1^- = \frac{1 - 6\sqrt{2}Z e^{ix}}{1 + 6iz} \quad (2.2.41)$$

$$\cos x = \frac{3z}{\sqrt{2}} \quad |z| \leq \frac{1}{3} \sqrt{2}$$

$$b) \quad y = -\frac{1}{5} \quad z = -\frac{1}{5x}$$

$$\zeta_0^+ = \frac{1 - 6i z}{1 + 6i z} \quad \zeta_1^+ = \frac{1 + 3\sqrt{2} z e^{ix}}{1 + 6i z} \quad \zeta_1^- = \frac{1 - 6\sqrt{2} z e^{ix}}{1 + 6i z} \quad (2.2.42)$$

$$\cos x = \frac{3z}{\sqrt{2}} \quad |z| \leq \frac{1}{3} \sqrt{2}$$

The transformation $T_1 T_2$ now changes x into $-x$.

Following the same procedure which is more complicated, the parameters of the transformation T_1 and the transformation ST_1 are found. Each transformation has two different ranges of parameter. The actual values of the phase shifts δ_j and δ'_j which leave the differential cross section, polarization and unitarity invariant are presented in the table 1. The corresponding curves for phase shifts of transformation $T_1 T_2$ are shown in Figure 1. If we drew the curves in the three dimensional space δ_0^+, δ_1^+ and δ_1^- different curves correspond different kinds of transformation. Given a point δ on such a curve the same transformation will pick up another point δ' on the same curve which leaves the differential cross section polarization and unitarity condition invariance. If the curves do not intersect the only two-fold ambiguity δ and δ' exists. If two curves I and II intersect at δ then at least there is one point where the three-fold ambiguity exists. In the case S and P waves one can see that the curves do not intersect. This means that only two fold ambiguity exists. But the rigorous proof has not been given.

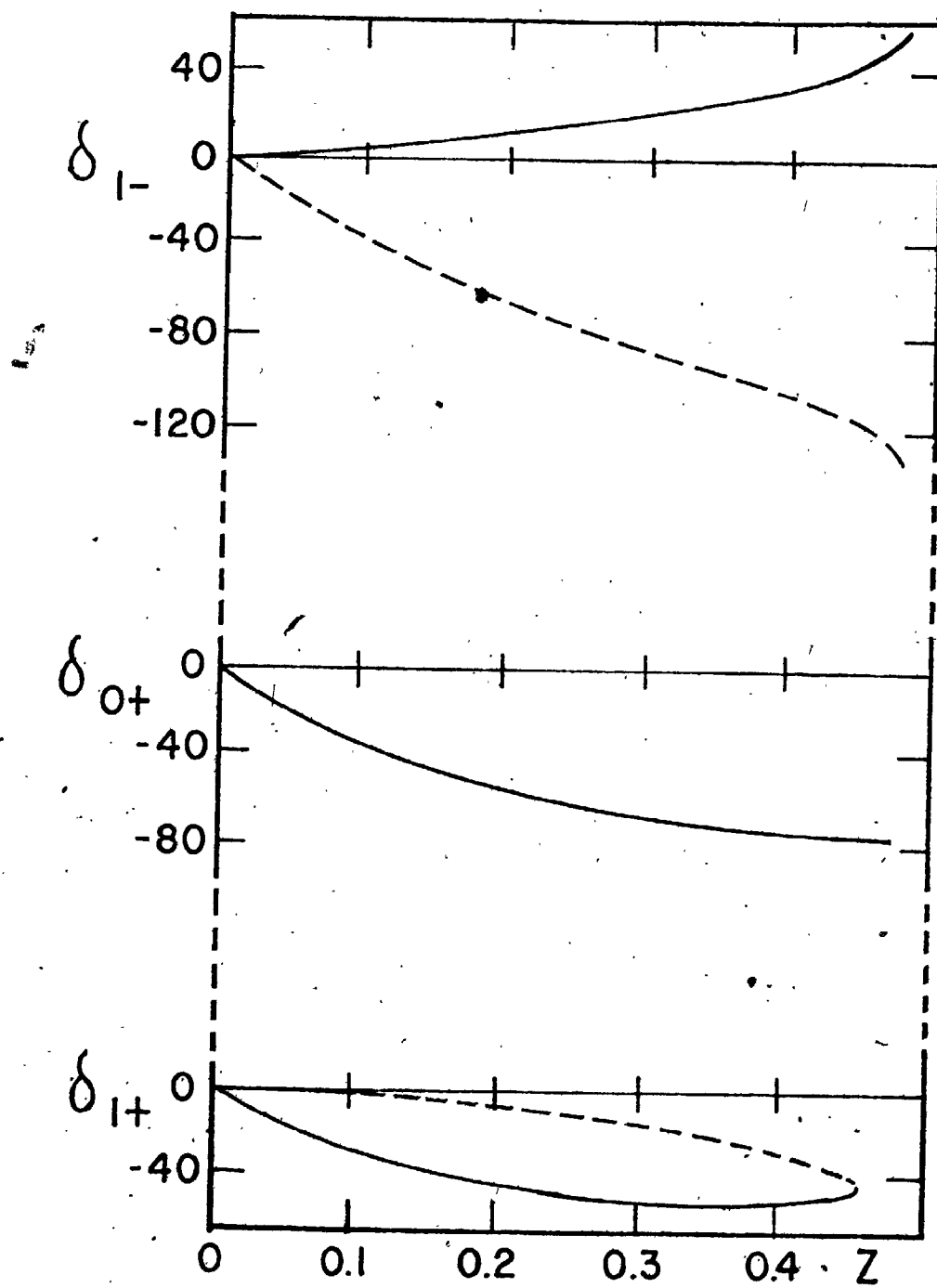


Figure 1. The phase shifts δ_i (solid line) and δ'_i (dashed line) for the transformation $T_1 T_2$.

TABLE 1

A SCHEMATIC DISPLAY OF THE SETS OF PHASE SHIFTS
WITH RESPECT TO THE CURVE PARAMETERS

Parameter	δ_{0+}	δ_{1+}	δ_{1-}
$T_1 T_2 : z$ $\frac{1}{3} \sqrt{2}$	0	-45.0 -35.3	70 54.7 (-π)
$T_1 T_2 : z$ $\frac{1}{3} \sqrt{2}$	-70.5	-45.0 -35.3	54.7 (-π)
-0.50143 $T_1 : x$ 0	75.2 96.5 90 83.5 0	16.9 22.3 0 -22.3 -16.9	-41.4 -90 0 -138.6 (+π)
0.50143 $T_1 : x$ 0	-75.2 (+π)	-16.9	-138.6 (+π)
0.8139 $T_1 : x$ 1.6158	-8.3 35.34 35.27 -141.6 (+π)	56.3 71.8 19.5 22.5	-59.2 -173.3 (+π)
-0.8525 $ST_1 : x$ 0	-8.4 27.3 -90 0 -27.3 -171.6 (+π)	20.0 23.3 0 -23.3 -20.0	-45.2 0 -90 45.2 (-π)
-0.9198 -1.4578 $ST_1 : x$ -0.485 -0.54034	-87.8 -130.8 -35.3 -35.6 16.6 -4.7	81.6 148.6 17.0 114.6 38.7 123.7 27.7 78.4	-74.8 -162.6 4.7 -70.8

It is likely that for higher L-values the number of ambiguities increases. Both the number of transformations and the number of representations increase. The shape of the curves in the space of the phase shifts is not clear. Whether the curves of different transformations intersect or not is not known.

2.3 Martin-Newton Sufficiency Condition.

The existence and uniqueness of the unitary amplitude which fits the experimental data can be considered directly from the unitarity equation. In the simplest case which is that of spin zero elastic scattering at an energy below the first inelastic threshold the unitarity equation is given in (2.1.5).

$$\text{Im } f(\vec{n}', \vec{n}) = \frac{q_{\text{C.M.}}}{4\pi} \int d\omega'' f^*(\vec{n}', \vec{n}'') f(\vec{n}'', \vec{n}) \quad (2.3.1)$$

Define

$$f(\vec{n}', \vec{n}) = \frac{1}{q_{\text{C.M.}}} A(\cos \theta) \quad (2.3.2)$$

$$\text{and } A(\cos \theta) = A(x) = |A(x)| e^{i\psi(x)}$$

where $\psi(x)$ is the phase of $A(x)$.

Then the unitarity equation has the form

$$\sin \psi(x) = \int \int dy dz H(x, y, z) \cos[\psi(y) - \psi(z)] \quad (2.3.3)$$

where

$$H = \frac{1}{2\pi} \frac{|A(y)| |A(z)|}{|A(x)| \sqrt{1 - x^2 - y^2 - z^2 + 2xyz}} \quad (2.3.4)$$

Since the modulus of $A(x)$ is given by the differential cross section if there is a solution for ψ of the unitarity equation (2.3.3) then the unitary amplitudes are completely determined. This means that finding a unitary amplitude is equivalent to solve the unitarity equation for ψ . But the unitarity equation (2.3.3) is a non-linear equation. Our understanding of this class of equations is still at a very primitive level. Because of lack of the knowledge to handle this type of equations one concentrates to finding the condition under which the equation has solutions and the solution is unique, if it exists.

In general modern mathematics provides the method to find the existence and uniqueness condition of the solution for the non-linear integral equation

$$\psi(x) = \int_{\Omega} F[x, y, \psi(y)] dy \quad (2.3.5)$$

in the function space, i.e. in a space the points of which are certain functions. The right hand side of the integral equation (2.3.5) defines a functional space operation which maps a set of functions $\psi(x)$, i.e. a set of points of the function space, to the points $x(x)$ of this space according to the formula.

$$x(x) = \int_{\Omega} F[x, y, \psi(y)] dy \quad (2.3.6)$$

The problem of the solution of the integral equation (2.3.5) can be thought geometrically as finding a point ψ of the function space which corresponds to itself under the mapping (2.3.6); this point is called the fixed point of function space with respect to the operation (2.3.6) or in general

$$\psi = A(\psi) \quad (2.3.7)$$

There are theorems for finding the conditions under which solutions of (2.3.7) exist and are unique. They are:

The Schauder theorem: If in a Banach space a continuous operation transforms a closed convex set of points into a compact subset, then there exists at least one fixed point of the operation, i.e. there exists at least one solution for equation (2.3.7).

The principle of the contraction mapping: Let A be an operator in a Banach space E and A map a subset S of E into itself for every x_1 and x_2 in S we have

$$||A(x_1) - A(x_2)|| \leq \alpha ||x_1 - x_2||$$

the positive constant α being smaller than unity, and independent of the pair x_1 and x_2 , then there exists an unique point x of the space which satisfies the equation

$$x = A(x)$$

We give the explanation of these theorems and the definition of the mathematical terms in the following example.

Consider the general non-linear integral equation

$$\psi(x) = \int_{\Omega} F[x, y, \psi(y)] dy \quad (2.3.8)$$

with the assumption that F is defined and continuous with respect to the set of variables in the closed and bounded domain

$$[x \in \Omega, y \in \Omega, |\psi| \leq R]$$

Let us find under what conditions the operation

$$x(x) = A[\psi(x)] = \int_{\Omega} F[x, y, \psi(y)] dy \quad (2.3.9)$$

satisfies the assumptions of the Schauder theorem.

Consider a function space E the points of which are all real continuous functions $\psi(x)$ defined in the closed set Ω . If we define the norm

$$\|\psi\| = \sup_{x \in \Omega} |\psi(x)|$$

then the function space is a complete normed vector space, or Banach

space. In this space a set s of points satisfy

$$\|\psi\| = \delta(\psi, 0) \leq R$$

where $\delta(\psi, 0)$ is the length of ψ in the Banach space.

Let ψ_1 and ψ_2 be arbitrary points of s , i.e.

$$\|\psi_1(x)\| \leq R \quad \|\psi_2(x)\| \leq R$$

then every point of the line segment joining these points is defined by

$$(1 - \alpha)\psi_1 + \alpha\psi_2$$

where $0 \leq \alpha \leq 1$ and we have

$$\|(1 - \alpha)\psi_1 + \alpha\psi_2\| \leq (1 - \alpha)\|\psi_1\| + \alpha\|\psi_2\| \leq R$$

then all points of this segment belong to s and this set is convex.

Now the operation (2.3.9) is defined in s and maps every point $\psi \in s$ to a point $x \in E$. The fixed point operation (2.3.9) is exactly the solution of the integral equation (2.3.8).

Since E is a Banach space, to prove the existence of a fixed point on the basis of Schauder's theorem, it is sufficient to establish the

reactions. To construct the scattering amplitude from dynamics a number of theoretical models have been used, for example the direct channel resonance model, Regge pole model, absorption or Regge cut model etc.. At low energies, a partial wave decomposition is often used. There are several phase shift analysis methods. They are the Energy-independent phase shift analysis⁴², Energy-dependent phase shift analysis⁴³ and lately the accelerated convergence expansion analysis (ACE)⁴⁴. There are many sets of phase shift presented by different groups using different methods. The phase shifts are constructed as to fit the differential cross section and polarization on the average as best as possible but without the knowledge of the bounds of the theoretical quantities. From the view point of the bounds the theoretical quantities constructed from the phase shift analysis should be inside the bound. The bounds provide the criteria to choose one set of the phase shifts among possible sets which lead to the same observed P and D. The bounds do not tell us how large a quantity should be as long as it is between its lower and upper allowed limits. But they do tell us things like, for instance, the one set of the phase shifts has been obtained at the expense of making the relative angle between the spin non-flip and spin flip amplitudes as small as allowed.

3.2 The Bounds of the Theoretical Quantities.

To describe the scattering process there are different pairs of scattering amplitudes we can use. One such pair is the transversity amplitudes G_+ and G_- ^{12,26}. The absolute values of the transversity amplitudes are completely determined by the differential cross section

defined in the same bounded domain, contains a uniformly convergent sequence of functions i.e. compact. The equicontinuity is defined as

follows: For any ϵ if there exists a number $n(\epsilon)$ such that all functions $f(x)$ satisfy $|f(x') - f(x'')| < \epsilon$ when $|x' - x''| < n$, we show that $|x(x') - x(x'')| < \epsilon$ when $|x' - x''| < n$ as follows:

Since F is a continuous function such that

$$|F[x', y, \psi(y)] - F[x'', y, \psi(y)]| < \frac{\epsilon}{y} \quad \text{when } |x' - x''| < n$$

so

$$|x(x') - x(x'')| \leq \int_{\Omega} |F[x', y, \psi(y)] - F[x'', y, \psi(y)]| dy$$

$$\leq \epsilon \quad \text{when } |x' - x''| < n$$

Then $x(x)$ is equicontinuous and hence the set s' of all transformed points of set s is compact.

The first property restricts the right hand side of the operation (2.3.9) to be

$$\left| \int_{\Omega} F[x, y, \psi(y)] dy \right| < R$$

Then it maps the set s into itself.

In particular we can write the unitarity equation (2.3.4) in the following form

$$\psi(x) = \sin^{-1} \int \int dz dy H(x, y, z) \cos[\psi(y) - \psi(z)]$$

The operation corresponds to

$$\chi(x) = \sin^{-1} \int \int dz dy H(x, y, z) \cos[\psi(y) - \psi(z)]$$

If we define the norm as

$$\|\psi(x)\| = \sup_{-1 \leq x \leq 1} |\psi(x)|$$

and restrict

$$0 \leq \psi \leq \frac{\pi}{2}$$

Since $H(x, y, z) \cos[\psi(y) - \psi(z)]$ is a continuous function the only restriction to satisfy the assumptions of the Schauder theorem is that this mapping should map $\|\psi\|$ into itself. i.e.

$$\sup_{-1 \leq x \leq 1} \left\{ \int dy dz H(x, y, z) \cos[\psi(y) - \psi(z)] \right\} \leq 1$$

Since

$$\sup_{-1 \leq x \leq 1} \left\{ \int dy dz H(x, y, z) \cos[\psi(x) - \psi(z)] \right\}$$

$$\leq \sup_{-1 \leq x \leq 1} \int dy dz H(x, y, z)$$

the obvious sufficiency condition of the existence of the solution for the unitarity equation is

$$\sin \mu = \sup_{-1 \leq x \leq 1} \int \int dy dz H(x, y, z) \leq 1$$

In order to improve this sufficiency condition one can majorize

$$\int \int dy dz H(x, y, z) \cos[\psi(y) - \psi(z)]$$

to replace $\sin \mu$. It leads to the problem of finding the upper bound of the imaginary part in chapter IV. For the uniqueness problem we use the principle of the contraction mapping. Let

$$x_1(x) = \sin^{-1} \int \int dy dz H(x, y, z) \cos[\psi_1(y) - \psi_1(z)] dy dz$$

$$\text{and } x_2(x) = \sin^{-1} \int \int dy dz H(x, y, z) \cos[\psi_2(y) - \psi_2(z)] dy dz$$

$$|x_2(x) - x_1(x)| = |\sin^{-1} \int \int dy dz H(x, y, z) \cos[\psi_2(y) - \psi_2(z)] -$$

$$-\sin^{-1} \int \int dy dz H(x, y, z) \cos[\psi_1(y) - \psi_1(z)]|$$

$$\leq (1 - \sin^2 \mu)^{\frac{1}{2}} \int \int dy dz H(x, y, z) |\cos[\psi_2(y) - \psi_2(z)] -$$

$$-\cos[\psi_1(y) - \psi_1(z)]|$$

$$\leq (1 - \sin^2 \mu)^{\frac{1}{2}} \int \int dy dz H(x, y, z) |[\psi_2(y) - \psi_2(z)] -$$

$$= |\psi_1(y) - \psi(z)|$$

$$\leq 2(1 - \sin^2 \mu)^{-\frac{1}{2}} \int \int dy dz H(x, y, z) |\psi_2(y) - \psi_1(y)|$$

here we use the fact

$$\left| \frac{\sin^{-1} \beta - \sin^{-1} \alpha}{\beta - \alpha} \right| < \left| \frac{d}{d\beta} \sin^{-1} \beta \right| = \left| \frac{1}{(1 - \beta^2)^{\frac{1}{2}}} \right|$$

$$\leq (1 - \sin^2 \mu)^{-\frac{1}{2}}$$

where

$$\beta = \int \int dy dz H(x, y, z) \cos[\psi_1(y) - \psi_1(z)]$$

$$\alpha = \int \int dy dz H(x, y, z) \cos[\psi_2(y) - \psi_2(z)]$$

and $\sin \mu \geq \beta$ or α

and in the last step the symmetry property of $H(x, y, z)$ with respect to y, z has been used. This inequality can be written in terms of the norm

$$\|x_1 - x_2\| \leq 2(1 - \sin^2 \mu)^{\frac{1}{2}} \sin \mu \|\psi_1 - \psi_2\|$$

In order to meet the requirement of contraction mapping it must be

$$2(1 - \sin^2 \mu)^{\frac{1}{2}} \sin \mu \leq 1$$

solving this inequality leads to the sufficiency condition of the unique solution for the unitarity equation:

$$\sin \mu \leq \frac{1}{\sqrt{5}} \approx .447$$

Martin¹⁹ has improved this bound for the sufficiency condition of the uniqueness problem as

$$\sin \mu \leq .79$$

CHAPTER III

THE INEQUALITIES OF THE THEORETICAL QUANTITIES

3.1 Introduction.

The experimentally measurable quantities for $0^{-\frac{1}{2}+} \rightarrow 0^{-\frac{1}{2}+}$ processes, for example the πN and KN scattering, are the total cross section σ_{Tot} , the differential cross section D , polarization P and the rotation parameters R and A . For local measurements there are only three independent quantities since these measurable quantities have a relation $R^2 + A^2 + P^2 = 1$. The experimental differential cross section data in πN scattering cases are known with good precision. Also in last decade accurate polarization measurements have been performed³⁶⁻⁴⁰. But measurements of the rotation parameters are still in the primary stage⁴¹. They are not reliable and even the sign is not determined. On the other hand the theoretical quantities spin non-flip and spin flip amplitudes represent four real quantities which can be taken as the absolute values and phases of the scattering amplitudes. Three independent measurements are not enough to completely determine the scattering amplitudes. If we use only the reliable local measurements, differential cross section and the polarization, the scattering amplitudes cannot be completely determined from these local measurements. But we can restrict the scattering amplitudes to certain ranges, the bounds of the theoretical values of the scattering amplitudes.

In the elementary particle physics, one would like to be able to determine experimentally the amplitudes in the S-matrix of the particle

reactions. To construct the scattering amplitude from dynamics a number of theoretical models have been used, for example the direct channel resonance model, Regge pole model, absorption or Regge cut model etc.. At low energies, a partial wave decomposition is often used. There are several phase shift analysis methods. They are the Energy-independent phase shift analysis⁴², Energy-dependent phase shift analysis⁴³ and lately the accelerated convergence expansion analysis (ACE)⁴⁴. There are many sets of phase shift presented by different groups using different methods. The phase shifts are constructed as to fit the differential cross section and polarization on the average as best as possible but without the knowledge of the bounds of the theoretical quantities. From the view point of the bounds the theoretical quantities constructed from the phase shift analysis should be inside the bound. The bounds provide the criteria to choose one set of the phase shifts among possible sets which lead to the same observed P and D. The bounds do not tell us how large a quantity should be as long as it is between its lower and upper allowed limits. But they do tell us things like, for instance, the one set of the phase shifts has been obtained at the expense of making the relative angle between the spin non-flip and spin flip amplitudes as small as allowed.

3.2 The Bounds of the Theoretical Quantities.

To describe the scattering process there are different pairs of scattering amplitudes we can use. One such pair is the transversity amplitudes G_+ and G_- ^{12,26}. The absolute values of the transversity amplitudes are completely determined by the differential cross section

and polarization as

$$|G_{\pm}|^2 = \frac{1}{2} D(1 \pm |P|) \quad (3.2.1)$$

where G_{\pm} , D and P are the transversity amplitudes, differential cross section and polarization at a fixed scattering angle respectively. But the phases of the transversity amplitudes are completely unknown when the differential cross section and polarization are known.

One pair of scattering amplitudes commonly used are the spin non-flip amplitude f and spin flip amplitude g. They are derived from the symmetry principle (rotation and time reversal invariance and parity conservation). The derivation are given in Chapter IV. They are

$$F(E, Z) = f(Z, Z) + i \vec{\sigma} \cdot \vec{n} g(E, Z) \quad (3.2.2)$$

Here \vec{n} is the normal vector to scattering plane ($\vec{n} = \vec{n}_i \times \vec{n}_f$) and θ the scattering angle ($\cos \theta = Z$). \vec{n}_i and \vec{n}_f are the unit vectors in the momentum directions of the initial and final scattered particles (pion or kaon). $\vec{\sigma}$ is the Pauli spin matrix vector.

We define the theoretical quantities, the relative magnitude r, the relative phase α and the product m and the sum s of the magnitudes f and $g \sin \theta$, as follows,

$$r = \frac{|f|}{|g|} \quad (3.2.3)$$

$$\alpha = \arg(f) - \arg(g) \quad (3.2.4)$$

$$m = |f| |g| \sin \theta \quad (3.2.5)$$

$$s = |f| + |g| \sin \theta \quad (3.2.6)$$

The relations between the experimental quantities D and P and the theoretical quantities are,

$$\frac{d\sigma}{d\Omega} = |f|^2 + |g|^2 \sin^2 \theta \quad (3.2.7)$$

$$\begin{aligned} P &= \frac{2 \operatorname{Im} f g^* \sin \theta}{|f|^2 + |g|^2 \sin^2 \theta} = \frac{2 \sin \theta \sin \alpha |f| |g|}{|f|^2 + |g|^2 \sin^2 \theta} \\ &= \frac{2 \sin \alpha}{\frac{r}{\sin \theta} + \frac{\sin \theta}{r}} \end{aligned} \quad (3.2.8)$$

In the last relation the denominator of the right hand side is always positive with minimum value of two in the physical region $0 \leq \theta \leq \pi$ ($1 \geq \sin \theta \geq 0$). It is easy to get the bound for $\sin \alpha$

$$|P| \leq |\sin \alpha| \quad \text{or} \quad \frac{|\sin \alpha|}{P} \geq 1 \quad (3.2.9)$$

Eq. (3.2.9) indicates that $|P|$ is the lower bound of $|\sin \alpha|$. If we have full polarization ($P = \pm 1$) then $\sin \alpha$ becomes ± 1 . $\sin \alpha$ and P have the same sign as $\sin \alpha = 0$ if P cross zero. Solving for r in Eq. (3.2.8) using $|\sin \alpha| \leq 1$ we obtain bounds of the relative magnitude

$$r \leq r_+ = \frac{\sin \theta}{|P|} (1 + \sqrt{1 - P^2}) \quad (3.2.10a)$$

$$r \leq r_- = \frac{\sin \theta}{|P|} (1 - \sqrt{1 - P^2}) \quad (3.2.10b)$$

Thus the experimental knowledge of P alone restricts the (theoretically) allowed $\sin \alpha$ and r .

When we take into account the differential cross section and use the bounds of r , the bounds of $|f|^2$ and $|g|^2 \sin^2 \theta$ can be obtained.

$$\frac{d\sigma}{d\Omega} = D = |f|^2 + |g|^2 \sin^2 \theta$$

$$D = |f|^2 \left(1 + \frac{\sin^2 \theta}{r^2}\right) = |g|^2 \sin^2 \theta \left(\frac{r^2}{\sin^2 \theta} + 1\right)$$

$$|f|^2 = \frac{D}{1 + \frac{\sin^2 \theta}{r^2}} \quad (3.2.11)$$

$$|g|^2 \sin^2 \theta = \frac{D}{\frac{r^2}{\sin^2 \theta} + 1} \quad (3.2.12)$$

$$\frac{D}{1 + \frac{\sin^2 \theta}{r_-^2}} \leq |f|^2 \leq \frac{D}{1 + \frac{\sin^2 \theta}{r_+^2}} \quad (3.2.13)$$

$$\frac{D}{1 + \frac{\sin^2 \theta}{r_+^2}} \leq |g|^2 \sin^2 \theta \leq \frac{D}{1 + \frac{\sin^2 \theta}{r_-^2}} \quad (3.2.14)$$

It turns out that the upper (lower) bounds of $|f|$ and $|g| \sin \theta$ are the same (see appendix 3).

$$\begin{aligned} |f|_+, |g|_+ \sin \theta &= \sqrt{\frac{D}{2}} (1 + \sqrt{1 - P^2}) \\ &= \frac{\sqrt{D}}{2} (\sqrt{1 + |P|} + \sqrt{1 - |P|}) \end{aligned} \quad (3.2.15a)$$

$$\begin{aligned} |f|_-, |g|_- \sin \theta &= \sqrt{\frac{D}{2}} (1 - \sqrt{1 - P^2}) \\ &= \frac{\sqrt{D}}{2} (\sqrt{1 + |P|} - \sqrt{1 - |P|}) \end{aligned} \quad (3.2.15b)$$

From (3.2.8)

$$PD = 2|f||g| \sin \theta \sin \alpha$$

$$PD = 2m \sin \alpha$$

$$m_+ = \frac{PD}{2 \sin \alpha} \geq m_- = \frac{PD}{2} \quad (3.2.16a)$$

$$\text{and since } \frac{\sin \alpha}{P} \geq 1 \quad \therefore m = \frac{PD}{2 \sin \alpha} \leq \frac{D}{2} = m_+ \quad (3.2.16b)$$

then $\frac{PD}{2}$ and $\frac{D}{2}$ are the lower and upper bounds of m respectively. When we search for the upper and lower bounds of s we notice that there is a relation between $|f|$ and $|g| \sin \theta$. They cannot reach their upper (lower) bounds simultaneously.

$$D = |f|^2 + |g|^2 \sin^2 \theta$$

$$|g| \sin \theta = \sqrt{D - |f|^2}$$

$$\text{and } s = |f| + \sqrt{D - |f|^2}$$

The upper and lower bounds either satisfy $\frac{\partial s}{\partial |f|} = 0$ or on the boundary of $|f|$ region (i.e. $|f| = \sqrt{\frac{D}{2}(1 + \sqrt{1 - P^2})}$). They are (see appendix 4)

$$s \leq s_+ = \sqrt{2D} \quad (3.2.17a)$$

$$s \geq s_- = \sqrt{D(1 + P)} \quad (3.2.17b)$$

We summarize these bounds in the following

	$ \sin \alpha $	r	$ f $	$ g \sin \theta$	m	s
upper bound	1	$\frac{\sin \theta}{ P }(1 + \sqrt{1 - P^2})$	$\sqrt{\frac{D}{2}(1 + \sqrt{1 - P^2})}$	$\frac{D}{2}$	$\sqrt{2D}$	
lower bound	$ P $	$\frac{\sin \theta}{ P }(1 - \sqrt{1 - P^2})$	$\sqrt{\frac{D}{2}(1 - \sqrt{1 - P^2})}$	$\frac{D P }{2}$	$\sqrt{D(1 + P)}$	

From a theoretical point of view we can get the bounds in terms of any two of the four measurable quantities P , D , R and A .

The definitions of the rotation parameters R and A are

$$R = \frac{2 \operatorname{Re} f g^* \sin \theta}{|f|^2 + |g|^2 \sin^2 \theta} = \frac{2|f||g| \sin \theta \cos \alpha}{|f|^2 + |g|^2 \sin^2 \theta} \quad (3.2.18)$$

$$A = \frac{|f|^2 - |g|^2 \sin^2 \theta}{|f|^2 + |g|^2 \sin^2 \theta} = \frac{r^2 - \sin^2 \theta}{r^2 + \sin^2 \theta} \quad (3.2.19)$$

From (3.2.19) we have

$$r = \sin \theta \sqrt{\frac{1+A}{1-A}} \quad (3.2.20)$$

then r is uniquely determined by A alone.

From (3.2.18) we have the inequality

$$\frac{\cos \alpha}{R} \leq 1 \quad |\cos \alpha| \leq |R| \quad (3.2.21)$$

$|R|$ is a lower bound of $|\cos \alpha|$.

And again the upper and lower bounds of the relative magnitude can be written in terms of R alone

$$r_+ = \frac{\sin \theta}{|R|} (1 + \sqrt{1 - R^2}) \quad (3.2.22a)$$

$$r_- = \frac{\sin \theta}{|R|} (1 - \sqrt{1 - R^2}) \quad (3.2.22b)$$

We compare (3.2.22) with (3.2.10); the larger $|P|$ or $|R|$ are the better the bound is.

A together with B determine $|f|$ and $|g| \sin \theta$ uniquely

$$|f| = \sqrt{\frac{D(1+A)}{2}} \quad |g| \sin \theta = \sqrt{\frac{D(1-A)}{2}} \quad (3.2.23)$$

The relative phase α is found from equations (3.2.18) and (3.2.8)

$$\frac{\sin \alpha}{P} = \frac{1}{\sqrt{P^2 + R^2}} \quad \text{and} \quad \frac{\cos \alpha}{R} = \frac{1}{\sqrt{P^2 + R^2}} \quad (3.2.24)$$

We get these bounds from the relation between the theoretical quantities and the experimental quantities and to maximize (minimize) it. So it is model independent and good for any energy and any $0^- \frac{1+}{2} \rightarrow 0^+ \frac{1+}{2}$ process. (πN , $K N$ etc.).

3.3 Test of the $K p$ Phase Shifts.

πN and KN scattering processes fall in the category of $0^- \frac{1+}{2} \rightarrow 0^+ \frac{1+}{2}$ processes. πN scattering has been investigated by Liu and Sakmar³³. Here we test the $K p$ scattering in more details. We choose the experimental data of the differential cross section and polarization presented by CERN group³⁹. Though it is not the latest data we have, it is best suited for our purpose since these experimental data on P and D covers the entire scattering region at the median energy (the incident momentum is between 0.86 Gev/c to 2.74 Gev/c) with small errors in the polarization measurements. The energy-independent phase shift solutions are found using these data by CERN group. Solutions at different momenta were linked together by the "shortest path" method⁴². It is shown that the solutions are not unique and 3 sets with paths call α , β , and γ are obtained. Recently Cutkosky obtained a set of phase shifts

using the energy independent accelerated convergence expansion (ACE) analysis in which the higher partial waves are constructed from the lower partial waves^{45,46}. We compare these 4 sets of phase shifts with the bounds at the 13 incident lab. momentum between 0.86 Gev/c and 1.89 Gev/c (Even though the CERN data goes up to 2.74 Gev/c we did not use them above 1.89 Gev/c because Cutkosky phase shifts go only up to this energy).

First we use the experimental P and D from CERN group to obtain the bounds of r , $|f|$, $|g| \sin \theta$, m and s from equations (3.2.10), (3.2.15), (3.2.16) and (3.2.17). Next we reconstruct $\sin \alpha$, r , $|f|$, $|g| \sin \theta$, m and s from α , β , γ and Cutkosky's phase shift solutions.

The scattering amplitudes are expanded in partial-wave amplitudes in the usual form

$$f(E, z) = \frac{1}{q_{C.M.}} \sum_{\ell} [(\ell + 1)f_{+} + \ell f_{-}] P_{\ell}(z) \quad (3.3.1)$$

$$g(E, z) = \frac{1}{q_{C.M.}} \sum_{\ell} [f_{+} - f_{-}] P_{\ell}(z) \quad (3.3.2)$$

The values of ℓ are up to and including H waves in CERN phase shifts and 14 in the Cutkosky solutions.

In order to get a better comparison with the bounds we calculate the error bars of these bounds from the error bars of the experimental P and D.

$$\begin{aligned}
 \Delta |f|_+ &= \Delta |\epsilon|_- \stackrel{\text{def}}{=} \Delta |g|_+ \sin \theta = \Delta |g|_- \sin \theta \\
 &= \frac{1}{4} \left[\frac{(1 + |P|)\Delta D + D\Delta P}{\sqrt{D(1 + |P|)}} + \frac{(1 - |P|)\Delta D + D\Delta P}{\sqrt{D(1 - |P|)}} \right] \\
 &\quad (3.3.3)
 \end{aligned}$$

$$\Delta m_+ = \frac{\Delta D}{2} \quad \text{and} \quad \Delta m_- = \frac{|P|\Delta D + D\Delta P}{2} \quad (3.3.4)$$

$$\Delta s_+ = \frac{\Delta D}{\sqrt{2D}} \quad \text{and} \quad \Delta s_- = \frac{(1 + |P|)\Delta D + D\Delta P}{2\sqrt{D(1 + |P|)}} \quad (3.3.5)$$

where ΔD and ΔP are the errors for the differential cross section and polarization respectively.

The trivial upper bounds for $|f|_+$ and $|g|_+ \sin \theta$ obtained directly from equation (3.2.7) are:

$$|f|_+ = \frac{1}{D^2} \quad \text{and} \quad |g|_+ \sin \theta = \frac{1}{D^2} \quad (3.3.6)$$

It is obvious that they are the limit cases equation (3.2.15a) when $r_+ \rightarrow \infty$ and $r_- \rightarrow 0$ (i.e. $P \rightarrow 0$).

The acceptable solutions of phase shifts should satisfy the bounds over the entire scattering angle region at all incident momentum. In the cases of violations of the bounds either the solutions need a reexamination or more accurate measurements at the violated points are needed.

We have tested the bounds at 13 incident momentum from 0.87 Gev/c to 1.89 Gev/c. Computer graph printout are obtained for all energies. Give all results in Figures 2, 3, 4, 5 and 6. We show the comparison of the bounds with Cutkosky solutions and CERN α , β and γ paths respectively.

We observe the following features:

Cutkosky phase shifts:

$\sin \alpha$)

Here we are comparing $\sin \alpha$ constructed from the phase shifts, on the one hand with the experimental polarization, on the other hand with the polarization constructed from phase shifts. Both should be lower than $\sin \alpha$. Cutkosky solution satisfies this bound except at some odd experimental points where P turns out to be larger than $\sin \alpha$. One striking feature of Cutkosky's solution is that his $\sin \alpha$ not only follows the general shape of the polarization but at almost all energies it is practically equal to P over a large angle region except for forward direction. This makes one suspect that $|f| = |g| \sin \theta$ (see equation (3.2.8)). But notice that our definition of r is $|f|/|g|$ and not $|f|/|g| \sin \theta$. Actually r for Cutkosky's solution as can be seen from the figures is close to one. But this is not the ratio of $|f|$ and $|g| \sin \theta$. It turns out that a small percentage difference between P and $\sin \alpha$ give a very large percentage difference between $|f|$ and $|g| \sin \theta$ (see equation (3.2.8)).

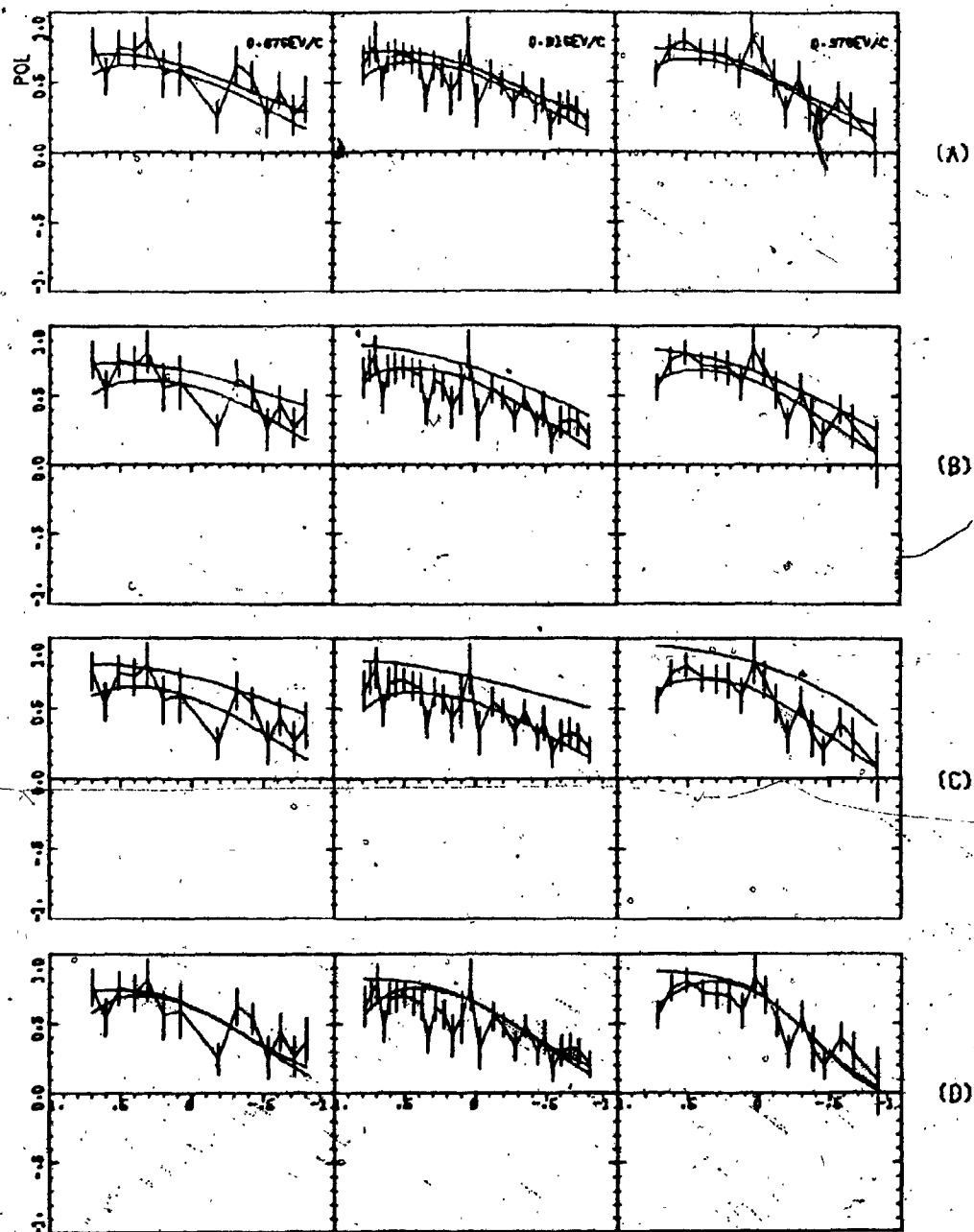


Figure 2.1. Comparison of the $K^+ p$ polarization with the relative phase ($\sin \alpha$) to test the inequality (3.2.9). The experimental polarizations with error bars are taken from Ref. 39 and the relative phases are constructed from (A) Cutkosky phase shifts, (B) CERN α solutions, (C) CERN β solutions and, (D) CERN γ solutions at $P_{\text{lab.}} = .87 \text{ Gev}/c$, $.91 \text{ Gev}/c$ and $.97 \text{ Gev}/c$ respectively. The upper line shows $\sin \alpha$, the lower line the polarization constructed from the phase shifts. Experimental points are connected to guide the eye only.

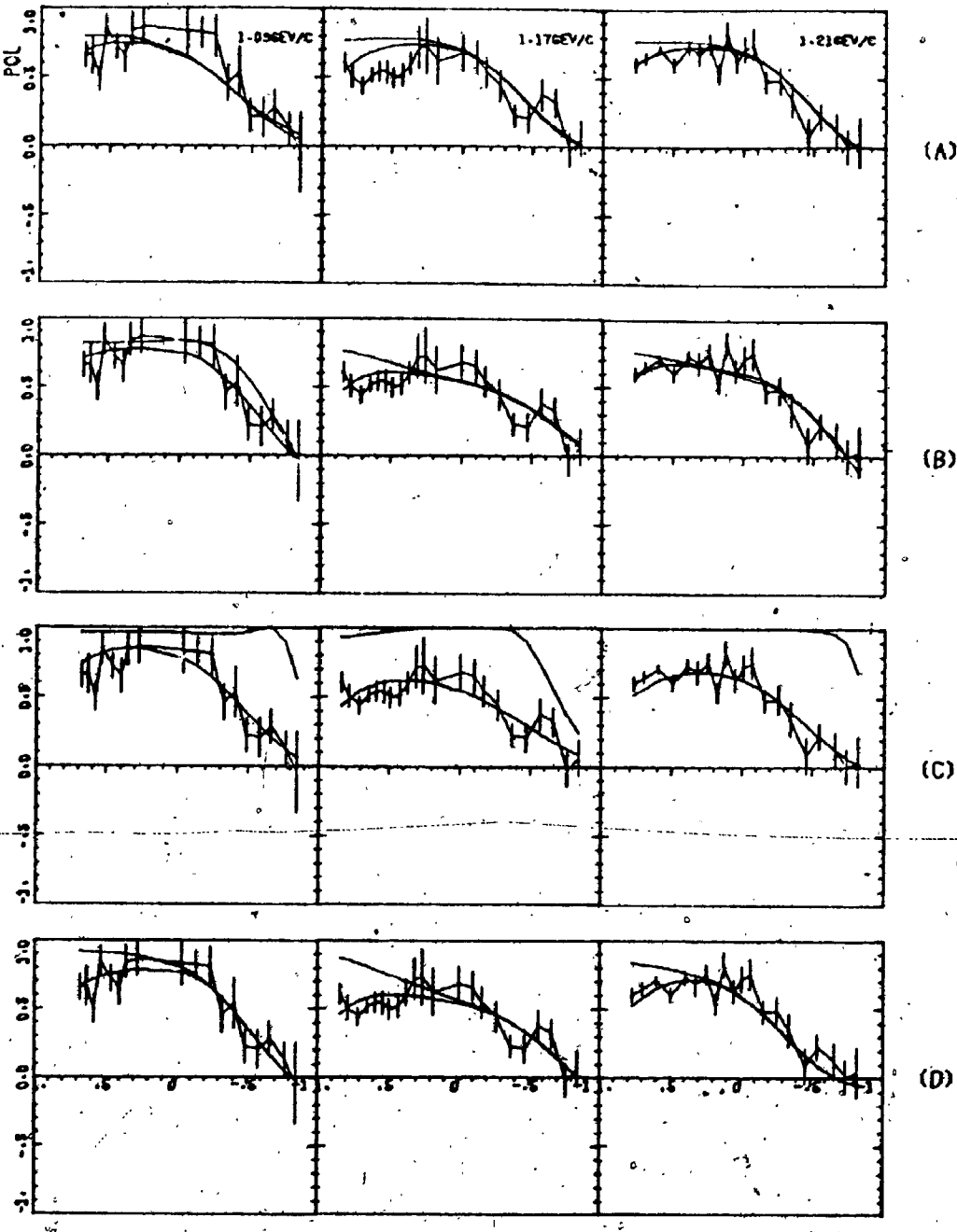


Figure 2.2. Comparison of the $K^+ p$ polarization with the relative phase ($\sin \alpha$) to test the inequality (3.2.). The experimental polarizations with error bars are taken from Ref. 39 and the relative phases are constructed from (A) Cutkosky phase shifts, (B) CERN α solutions, (C) CERN β solutions and, (D) CERN γ solutions at $P_{\text{lab.}} = 1.09 \text{ Gev}/c$, $1.17 \text{ Gev}/c$ and $1.21 \text{ Gev}/c$ respectively. The upper line shows $\sin \alpha$, the lower line the polarization constructed from the phase shifts. Experimental points are connected to guide the eye only.

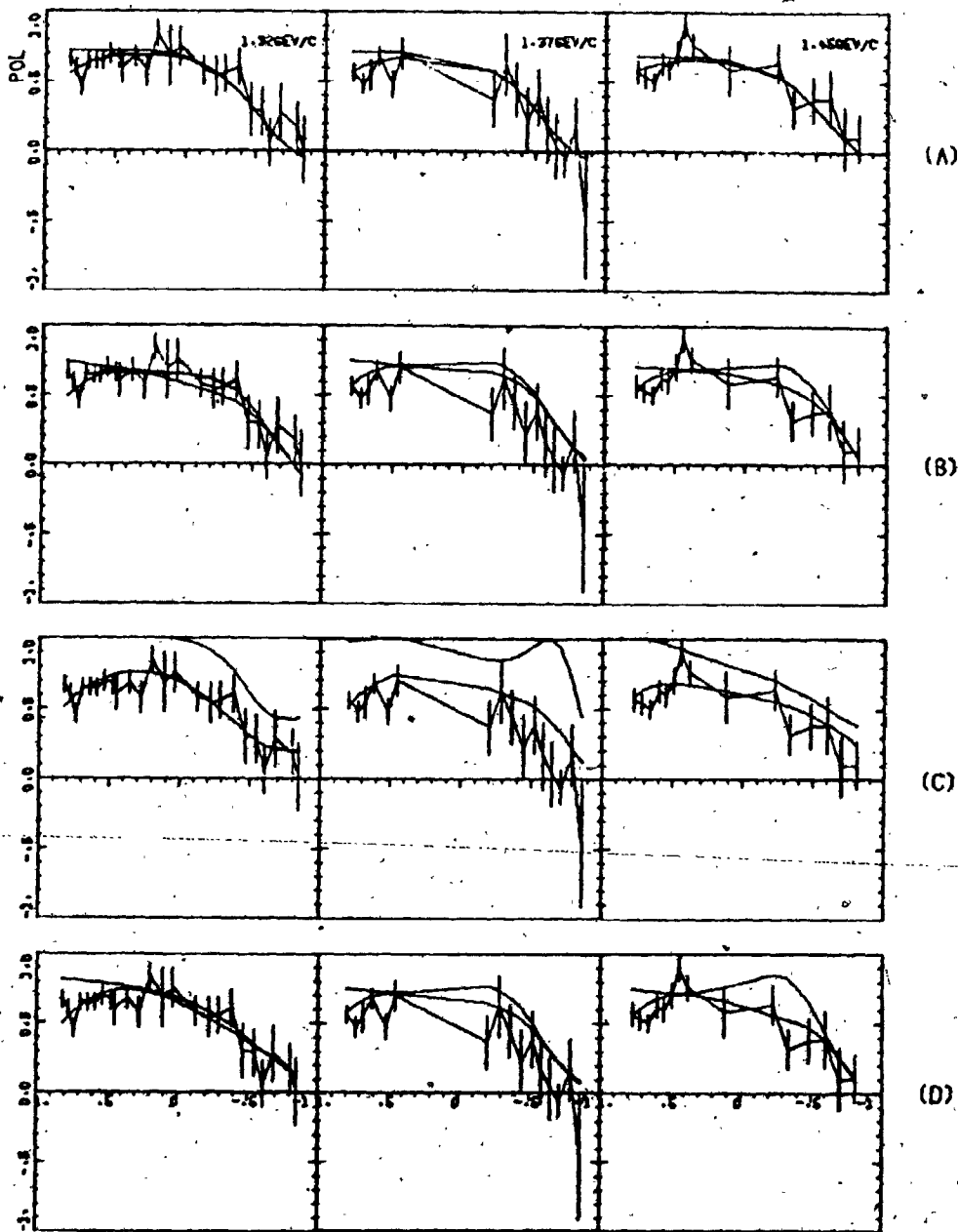


Figure 2.3. Comparison of the $K^+ p$ polarization with the relative phase ($\sin \alpha$) to test the inequality (3.2.9). The experimental polarizations with error bars are taken from Ref. 39 and the relative phases are constructed from (A) Cutkosky phase shifts, (B) CERN α solutions, (C) CERN β solutions and, (D) CERN γ solutions at $P_{\text{lab}} = 1.32 \text{ Gev}/c$, $1.37 \text{ Gev}/c$ and $1.45 \text{ Gev}/c$ respectively. The upper line shows $\sin \alpha$, the lower line the polarization constructed from the phase shifts. Experimental points are connected to guide the eye only.

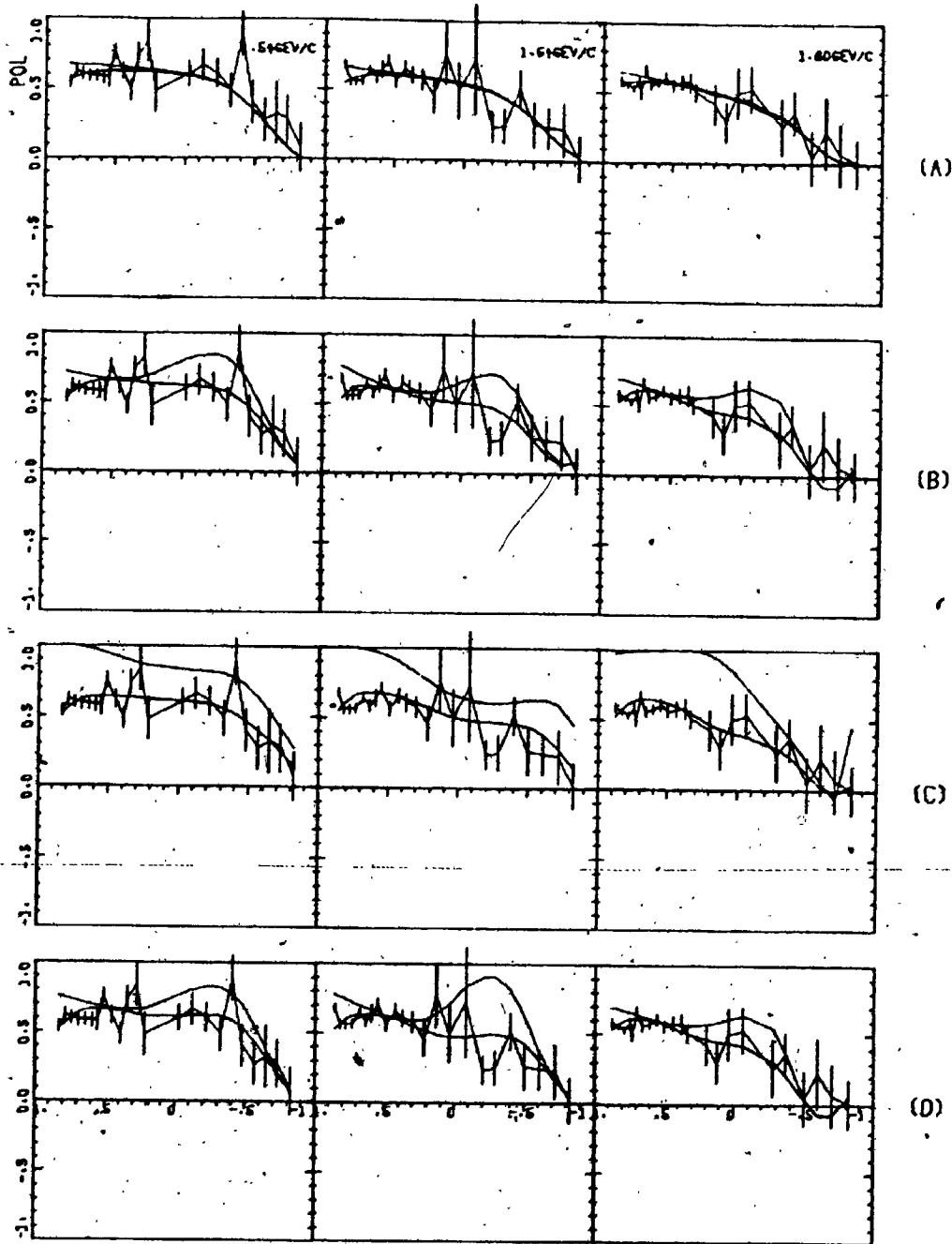


Figure 2.4. Comparison of the $K^+ p$ polarization with the relative phase ($\sin \alpha$) to test the inequality (3.2.9). The experimental polarizations with error bars are taken from Ref. 39 and the relative phases are constructed from (A) Cutkosky phase shifts, (B) CERN α solutions, (C) CERN β solutions and, (D) CERN γ solutions at $P_{\text{lab.}} = 1.54 \text{ Gev}/c$, $1.64 \text{ Gev}/c$ and $1.80 \text{ Gev}/c$ respectively. The upper line shows $\sin \alpha$, the lower line the polarization constructed from the phase shifts. Experimental points are connected to guide the eye only.

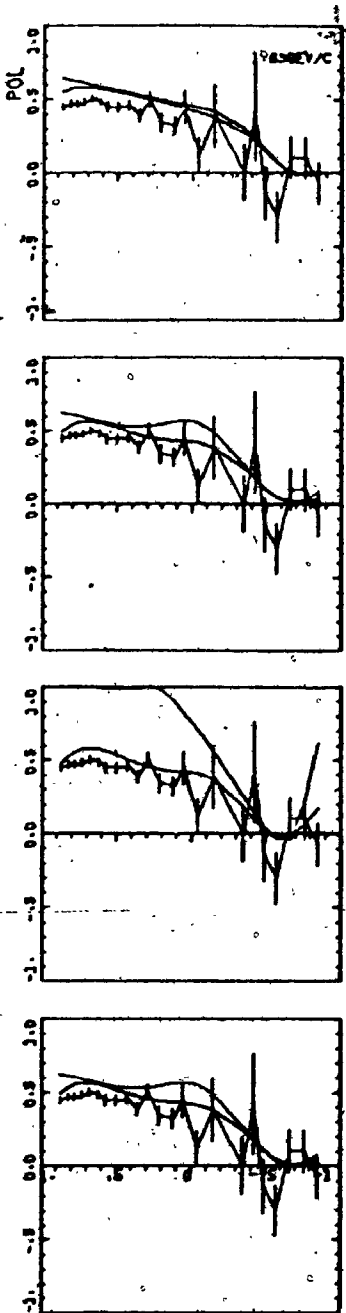


Figure 2.5. Comparison of the $K^+ p$ polarization with the relative phase ($\sin \alpha$) to test the inequality (3.2.9). The experimental polarizations with error bars are taken from Ref. 39 and the relative phases are constructed from (A) Cutkosky phase shifts, (B) CERN α solutions, (C) CERN β solutions and, (D) CERN γ solutions at $P_{lab} = 1.89$ GeV/c. The upper line shows $\sin \alpha$, the lower line the polarization constructed from the phase shifts. Experimental points are connected to guide the eye only.

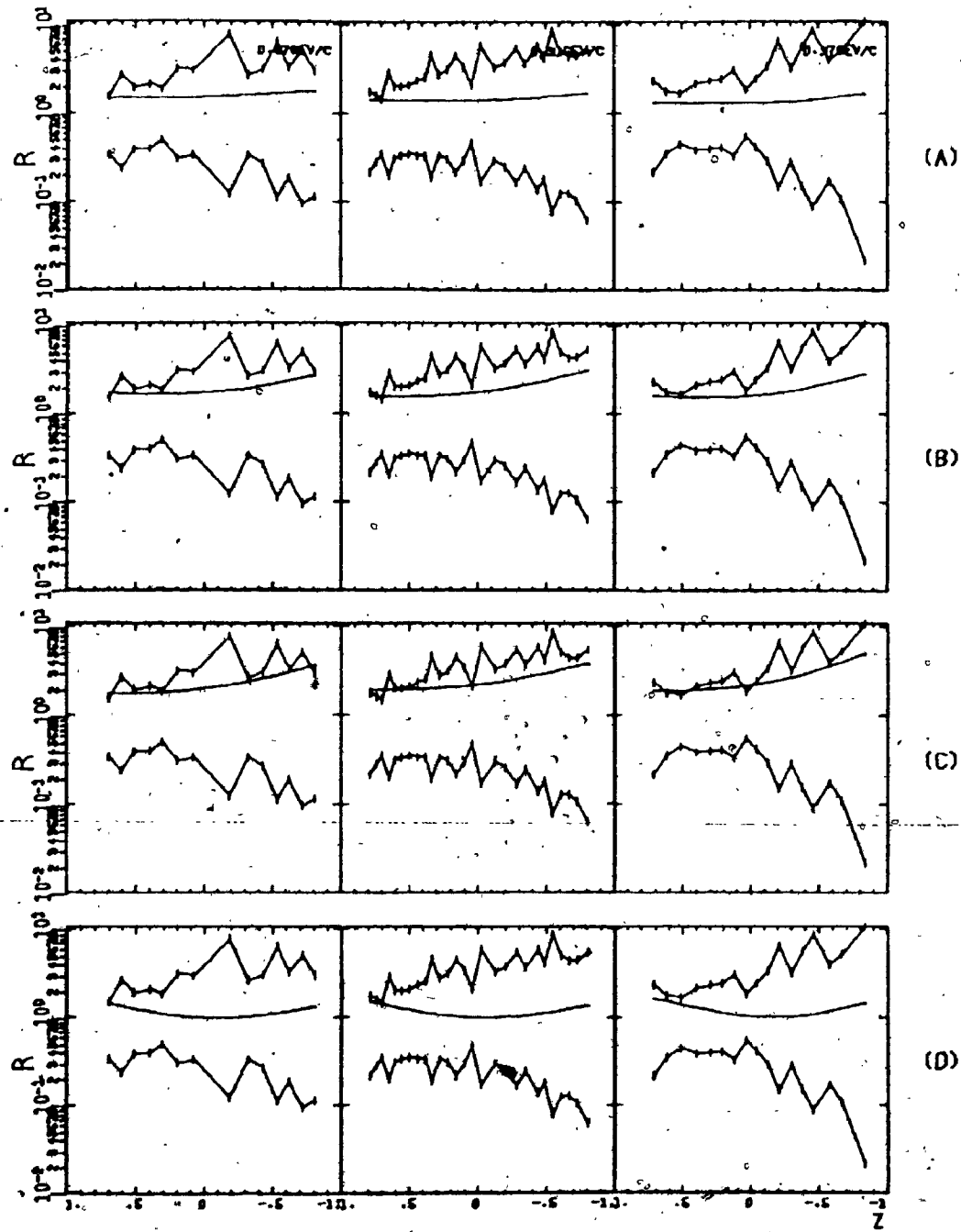


Figure 3.1. Comparison of the $K^+ p$ relative magnitude r with their bounds to test the inequalities (3.2.10a) and (3.2.10b). r are constructed from (A) Cutkosky phase shifts; (B) CERN α solutions, (C) CERN β solutions and, (D) CERN γ solutions and their upper and lower bound are found from P of Ref. 39 at $P_{lab} = .87 \text{ Gev}/c$, $.91 \text{ Gev}/c$ and $.97 \text{ Gev}/c$ respectively. Experimental points are connected to guide the eye only.

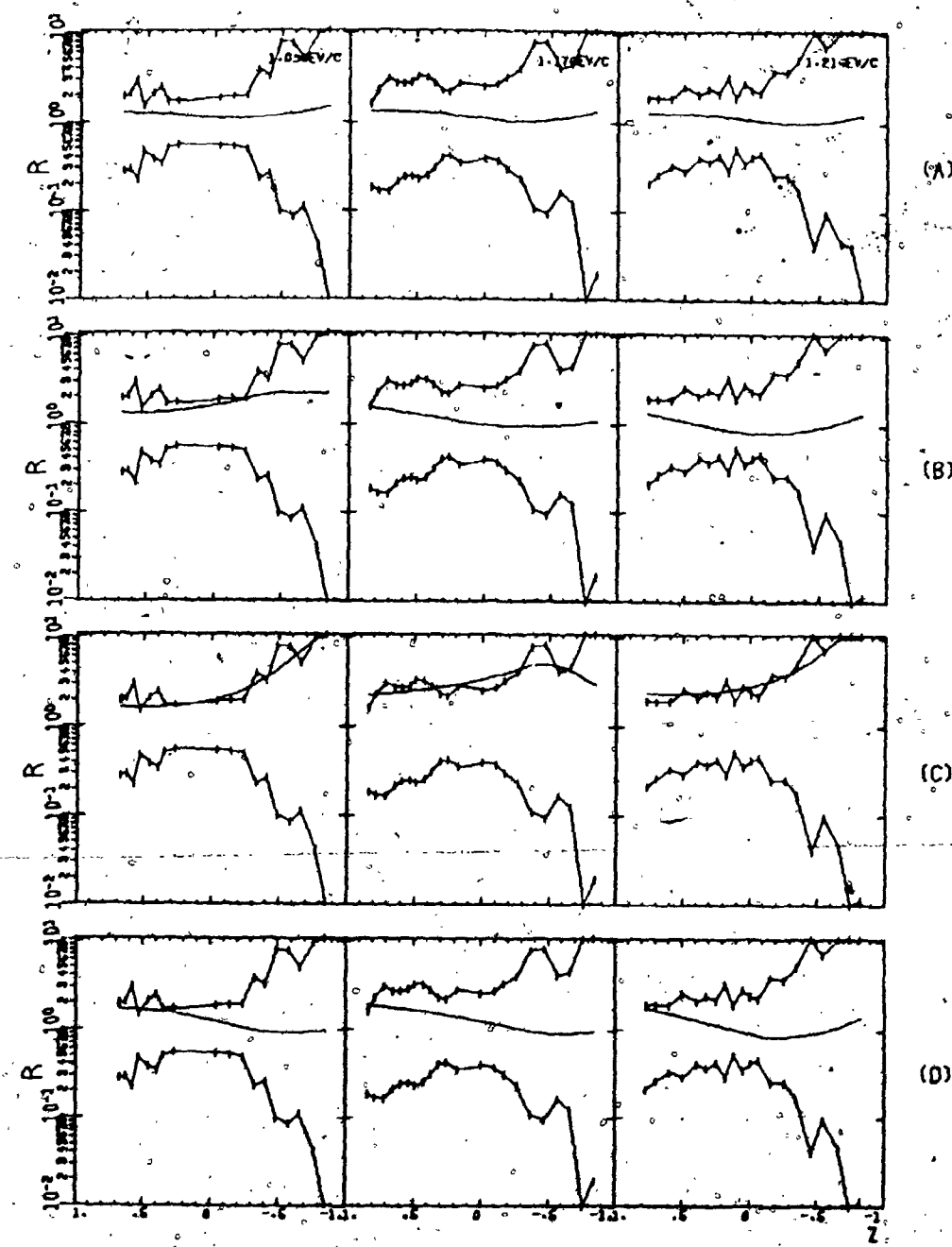


Figure 3.2. Comparison of the $K^+ p$ relative magnitude r with their bounds to test the inequalities (3.2.10a) and (3.2.10b). r are constructed from (A) Cutkosky phase shifts, (B) CERN α solutions, (C) CERN β solutions and, (D) CERN γ solutions and their upper and lower bound are found from P of Ref. 39 at $P_{lab} = 1.09$ Gev/c, 1.17 Gev/c and 1.21 Gev/c respectively. Experimental points are connected to guide the eye only.

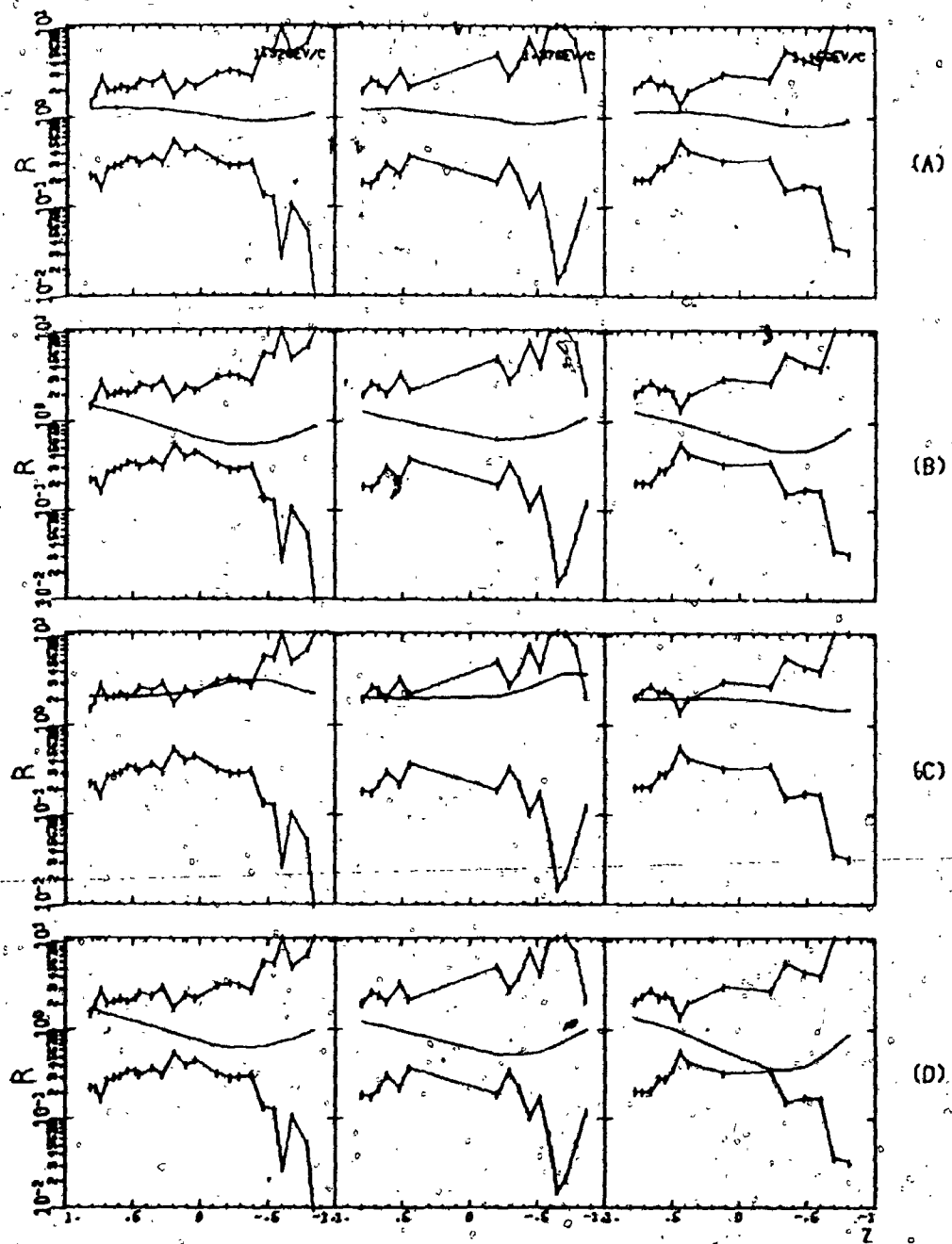


Figure 3.3. Comparison of the $K^+ p$ relative magnitude r with their bounds to test the inequalities (3.2.10a) and (3.2.10b). r are constructed from (A) Cutkosky phase shifts, (B) CERN γ solutions, (C) CERN β solutions and, (D) CERN γ solutions and their upper and lower bound are found from P of Ref. 39 at $P_{lab} = 1.32 \text{ Gev}/c$, $1.37 \text{ Gev}/c$ and $1.45 \text{ Gev}/c$ respectively. Experimental points are connected to guide the eye only.

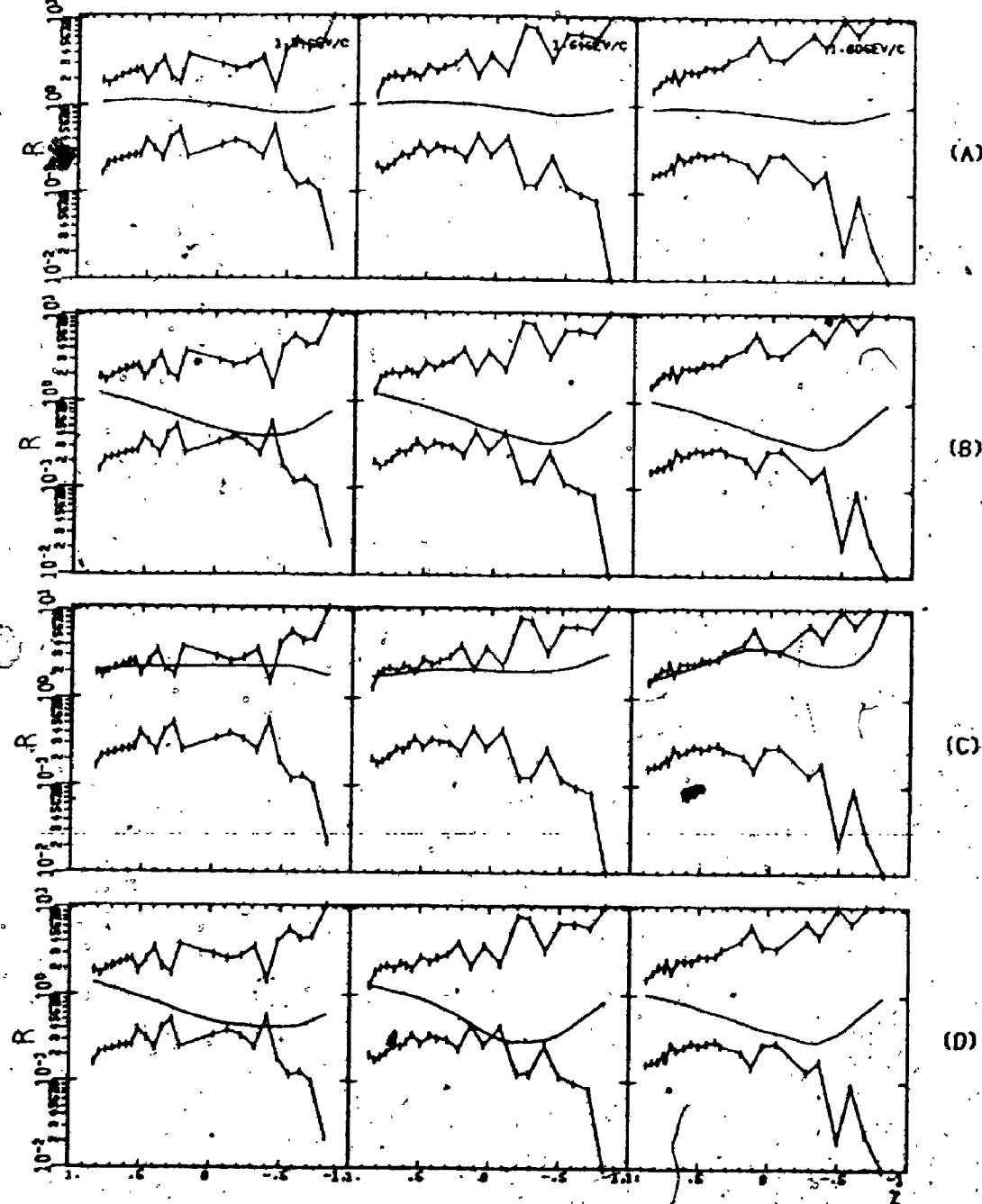


Figure 3.4. Comparison of the $K^+ p$ relative magnitude r with their bounds to test the inequalities (3.2.10a) and (3.2.10b). r are constructed from (A) Cutkosky phase shifts, (B) CERN α solutions, (C) CERN β solutions and, (D) CERN γ solutions and their upper and lower bound are found from P of Ref. 39 at $P_{\text{lab}} = 1.54 \text{ Gev}/c$, $1.64 \text{ Gev}/c$ and $1.80 \text{ Gev}/c$ respectively. Experimental points are connected to guide the eye only.

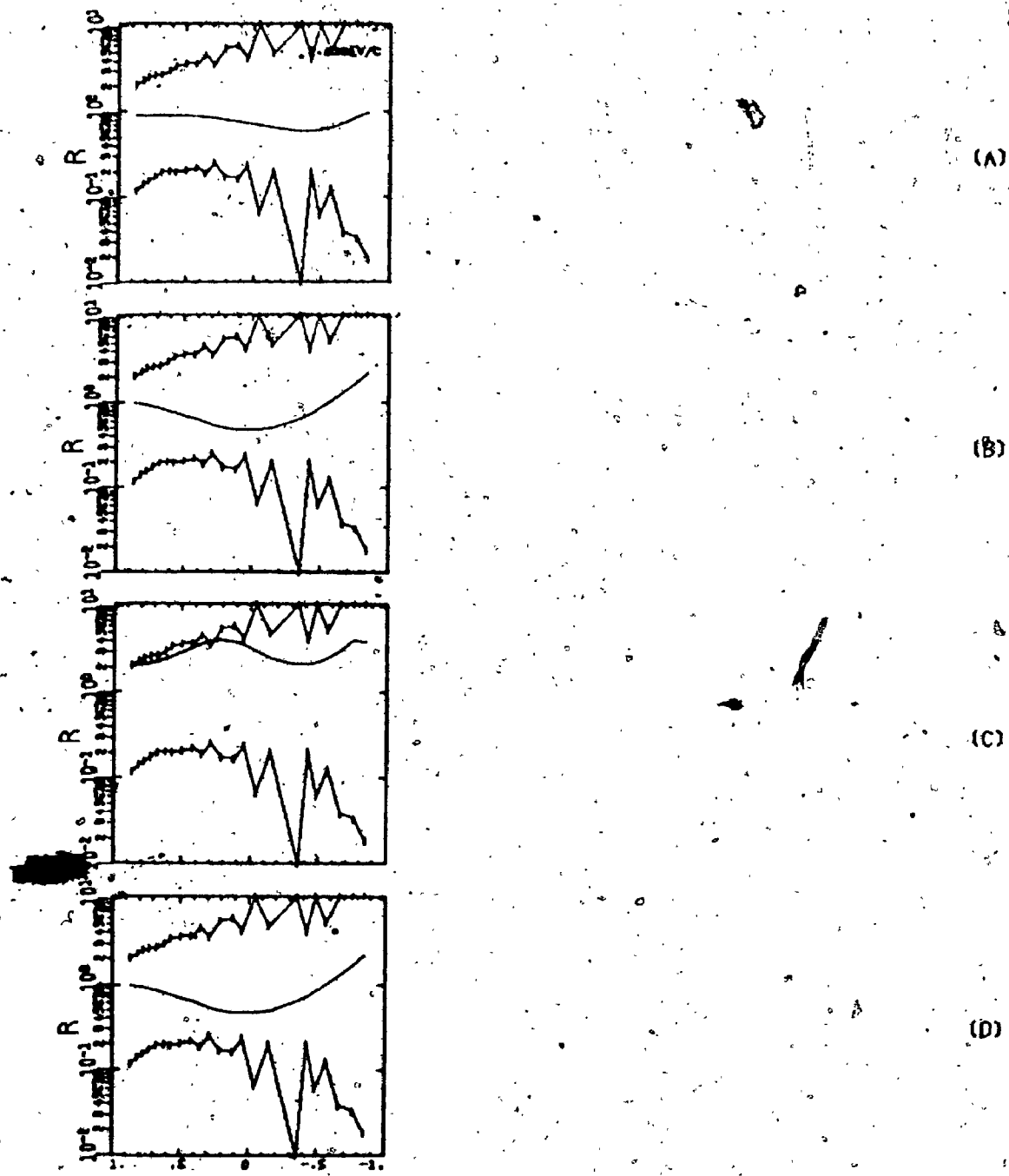


Figure 3.5. Comparison of the $K^+ p$ relative magnitude r with their bounds to test the inequalities (3.2.10a) and (3.2.10b). r are constructed from (A) Cutkosky phase shifts, (B) CERN α solutions, (C) CERN β solutions and, (D) CERN γ solutions and their upper and lower bound are found from F of Ref. 39 at $P_{lab} = 1.89$ Gev/c. Experimental points are connected to guide the eye only.

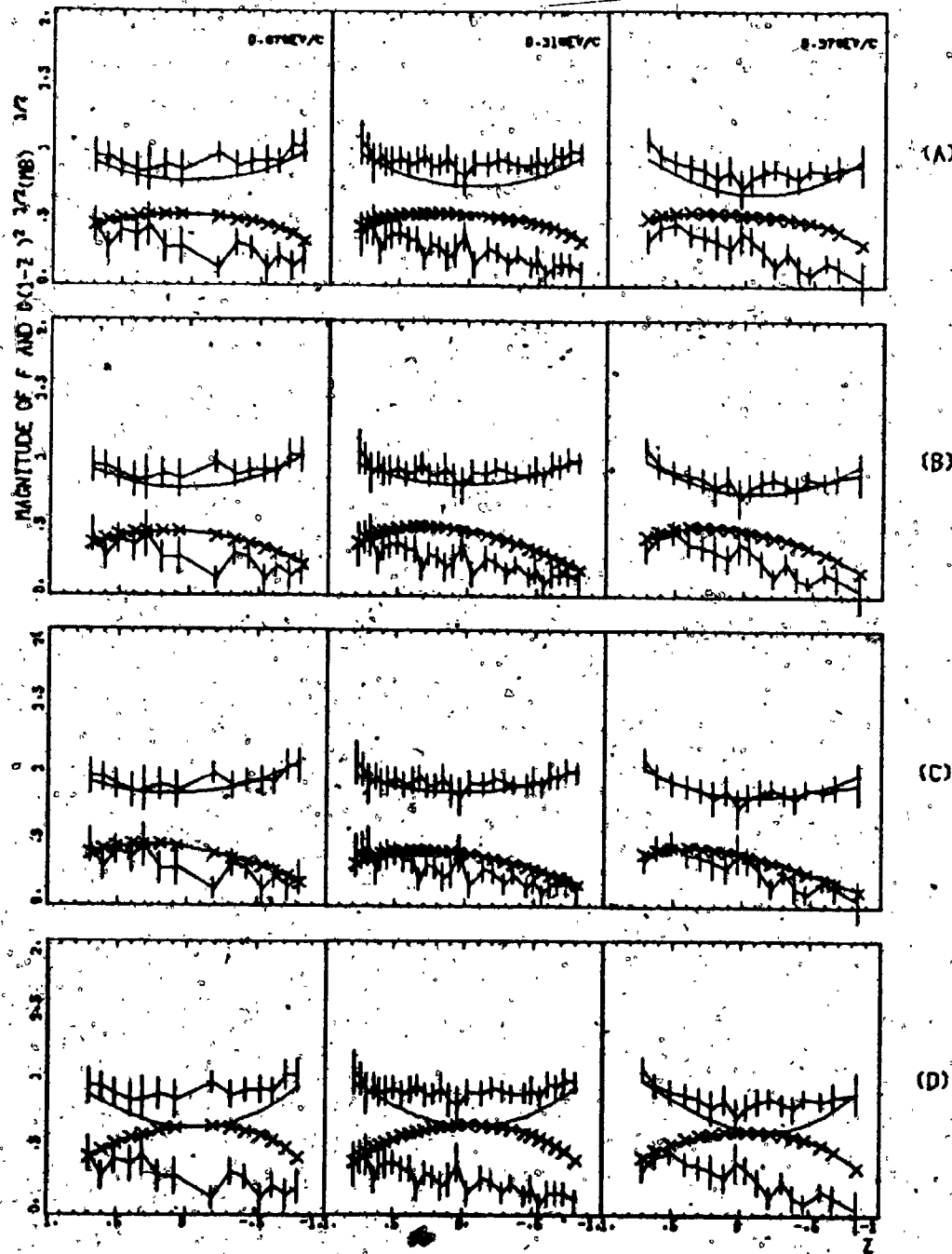


Figure 4.1. Comparison of the magnitudes of $K^+ p$ amplitudes f and $g \sin \theta$ with their bounds to test the inequalities (3.2.16a) and (3.2.16b). f and $g \sin \theta$ are constructed from (A) Cutkosky phase shifts, (B) CERN a solutions, (C) CERN B solutions and, (D) CERN γ solutions and their bounds are found from P and D of Ref. 39 at $P_{\text{lab}} = .87 \text{ Gev}/c$, $.91 \text{ Gev}/c$ and $.97 \text{ Gev}/c$ respectively. The line — and -X— represent $|f|$ and $|g \sin \theta|$ respectively. Here the bounds constructed from experimental data have error bars (Eq. 3.3.3). They are connected to guide the eye only.

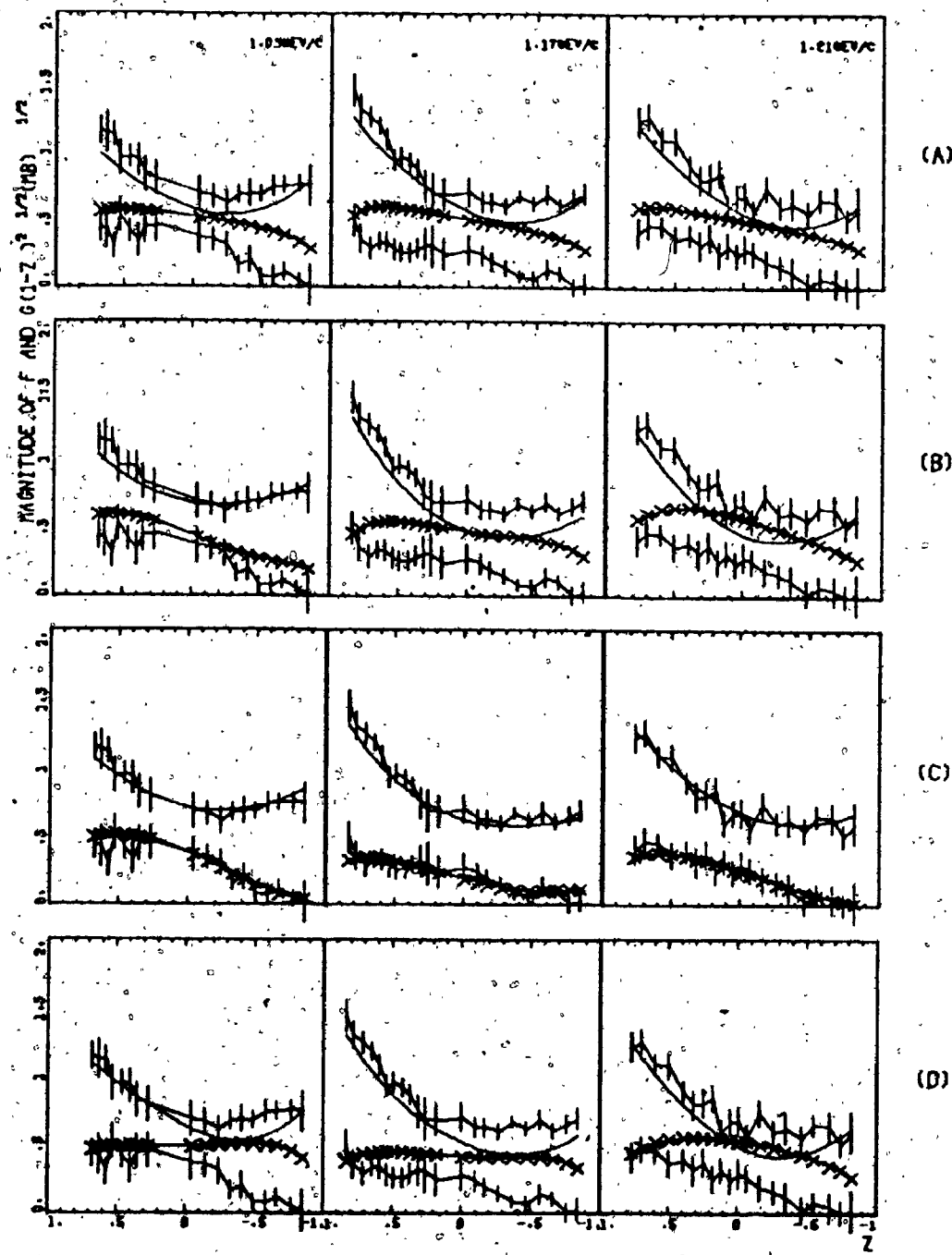


Figure 4.2. Comparison of the magnitudes of $K^+ p$ amplitudes f and $g \sin \theta$ with their bounds to test the inequalities (3.2.16a) and (3.2.16b). f and $g \sin \theta$ are constructed from (A) Cutkosky phase shifts, (B) CERN α solutions, (C) CERN β solutions and, (D) CERN γ solutions and their bounds are found from P and D of Ref. 39 at $P_{lab} = 1.09$ Gev/c, 1.17 Gev/c and 1.21 Gev/c respectively. The line — and —X— represent $|f|$ and $|g| \sin \theta$ respectively. Here the bounds constructed from experimental data have error bars (Eq. 3.3.3). They are connected to guide the eye only.

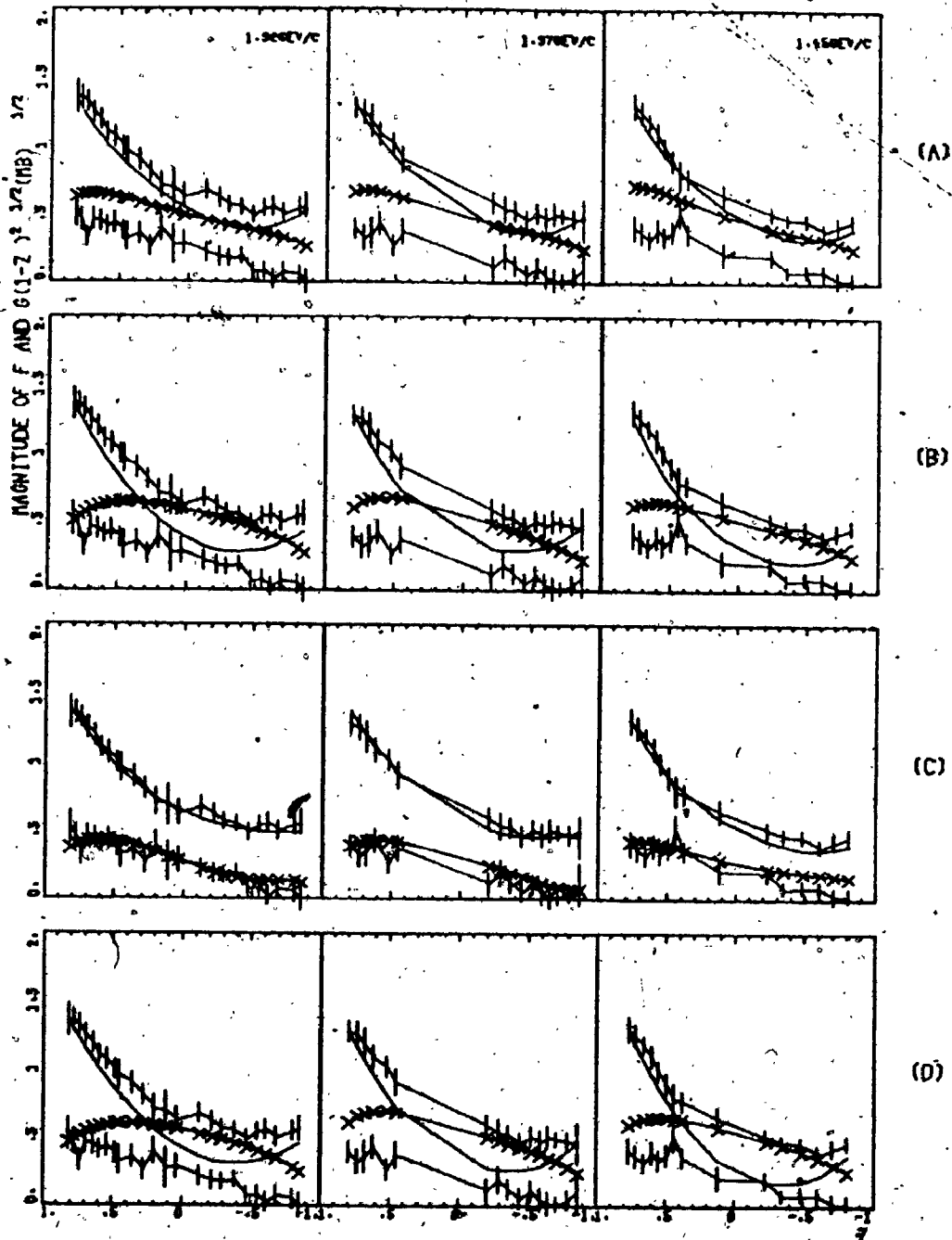


Figure 4.3. Comparison of the magnitudes of $K^+ p$ amplitudes f and $g \sin \theta$ with their bounds to test the inequalities (3.2.16a) and (3.2.16b). f and $g \sin \theta$ are constructed from (A) Cutkosky phase shifts, (B) CERN α solutions, (C) CERN β solutions and, (D) CERN γ solutions and their bounds are found from P and D of Ref. 39 at $P_{\text{lab.}} = 1.32 \text{ Gev}/c$, $1.37 \text{ Gev}/c$ and $1.45 \text{ Gev}/c$ respectively. The line --- and $\text{---} \times \text{---}$ represent $|f|$ and $|g| \sin \theta$ respectively. Here the bounds constructed from experimental data have error bars (Eq. 3.3.3). They are connected to guide the eye only.

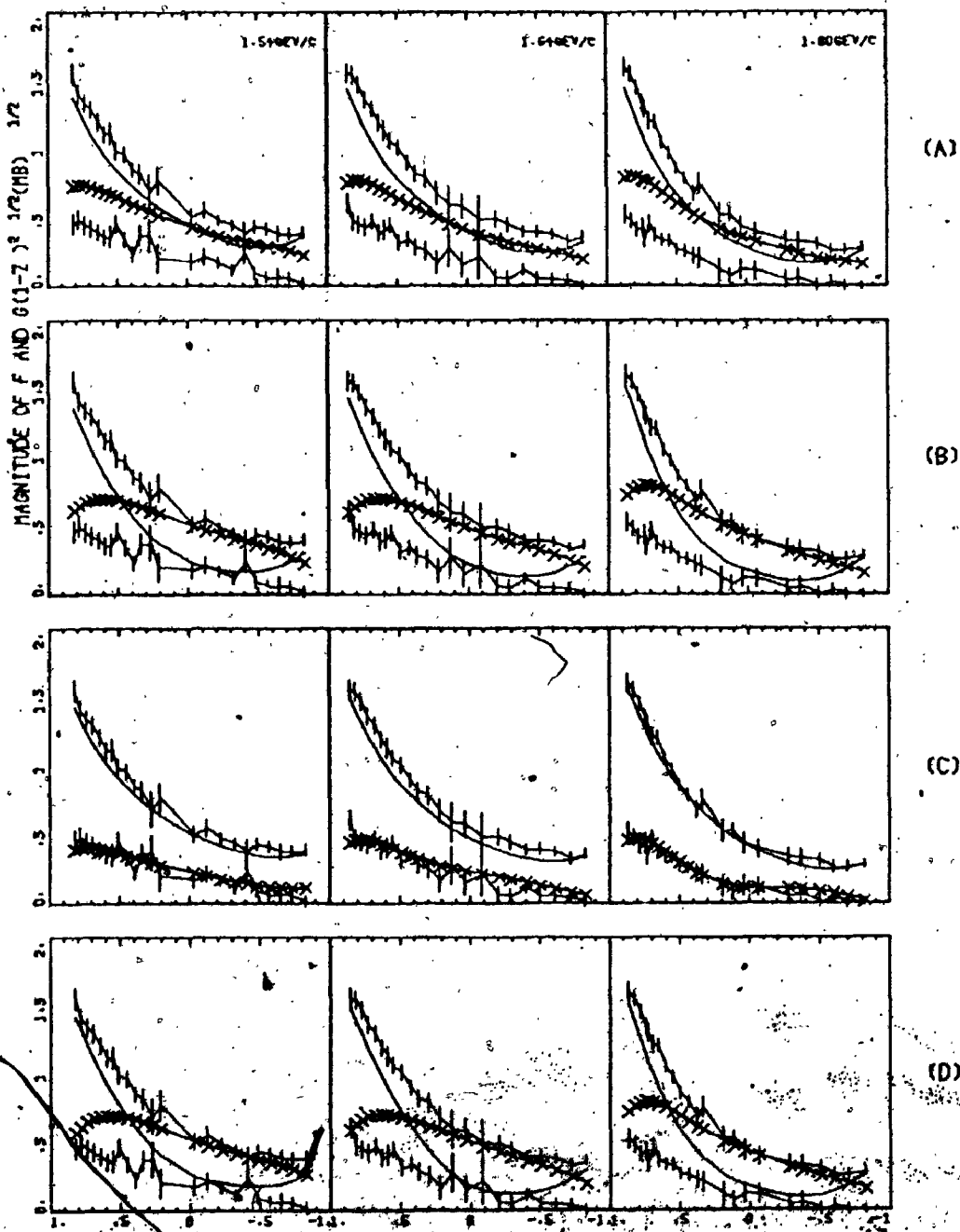


Figure 4.4. Comparison of the magnitudes of $K^+ p$ amplitudes f and $g \sin \theta$ with their bounds to test the inequalities (3.2.16a) and (3.2.16b). f and $g \sin \theta$ are constructed from (A) Cutkosky phase shifts, (B) CERN α solutions, (C) CERN β solutions and, (D) CERN γ solutions and their bounds are found from P and D of Ref. 39 at $P_{\text{lab}} = 1.54 \text{ Gev}/c$, $1.64 \text{ Gev}/c$ and $1.80 \text{ Gev}/c$ respectively. The line --- and $\text{—} \text{—}$ represent $|f|$ and $|g \sin \theta|$ respectively. Here the bounds constructed from experimental data have error bars (Eq. 3.3.3). They are connected to guide the eye only.

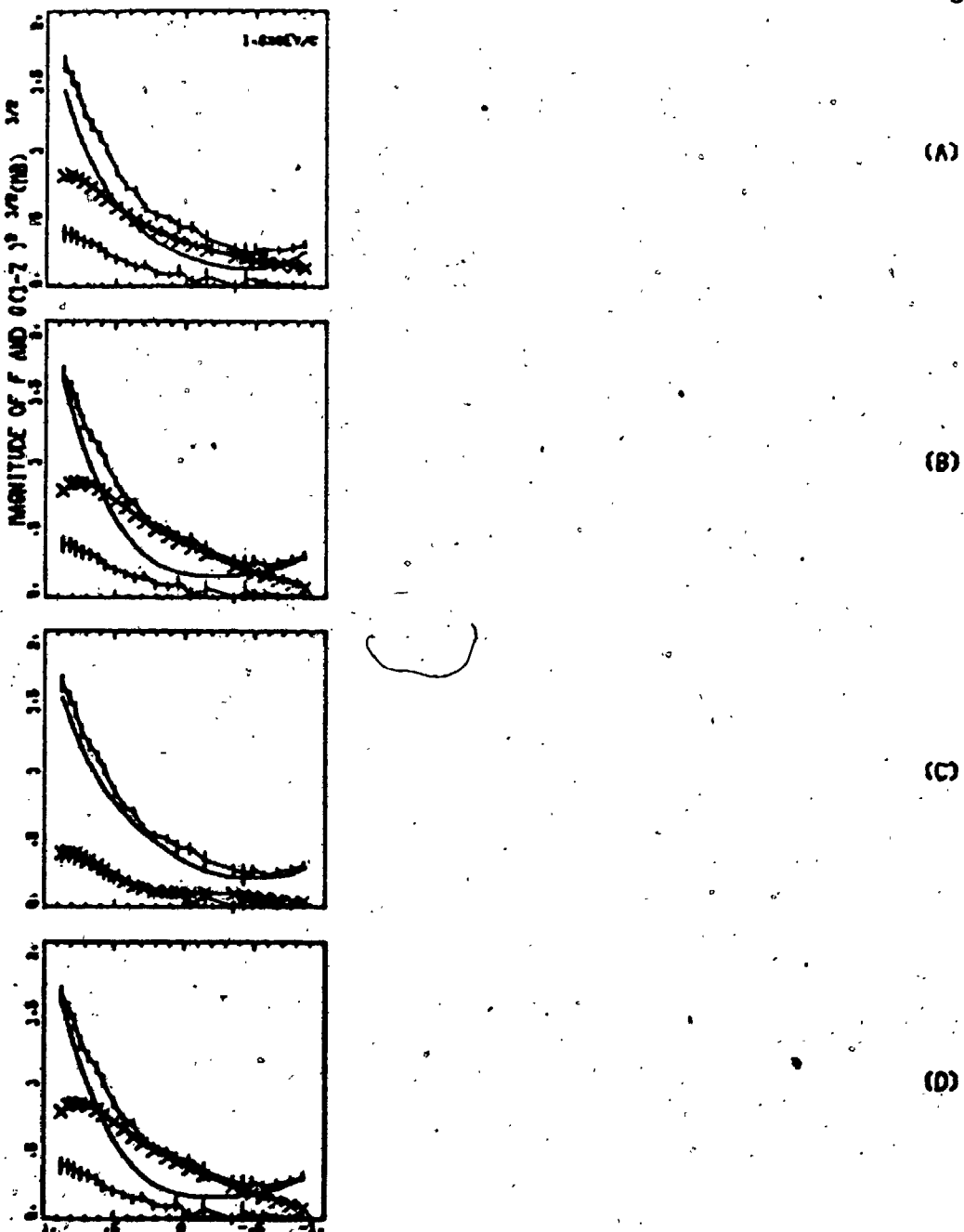


Figure 4.5. Comparison of the magnitudes of $K^- p$ amplitudes f and $g \sin \theta$ with their bounds to test the inequalities (3.2,16a) and (3.2,16b). f and $g \sin \theta$ are constructed from (A) Cutkosky phase shifts, (B) CERN α solutions, (C) CERN β solutions and, (D) CERN γ solutions and their bounds are found from P and D of Ref. 39 at $P_{lab} = 1.89$ Gev/c. The line — and — X — represent $|f|$ and $|g| \sin \theta$ respectively. Here the bounds constructed from experimental data have error bars (Eq. 3.3.3). They are connected to guide the eye only.

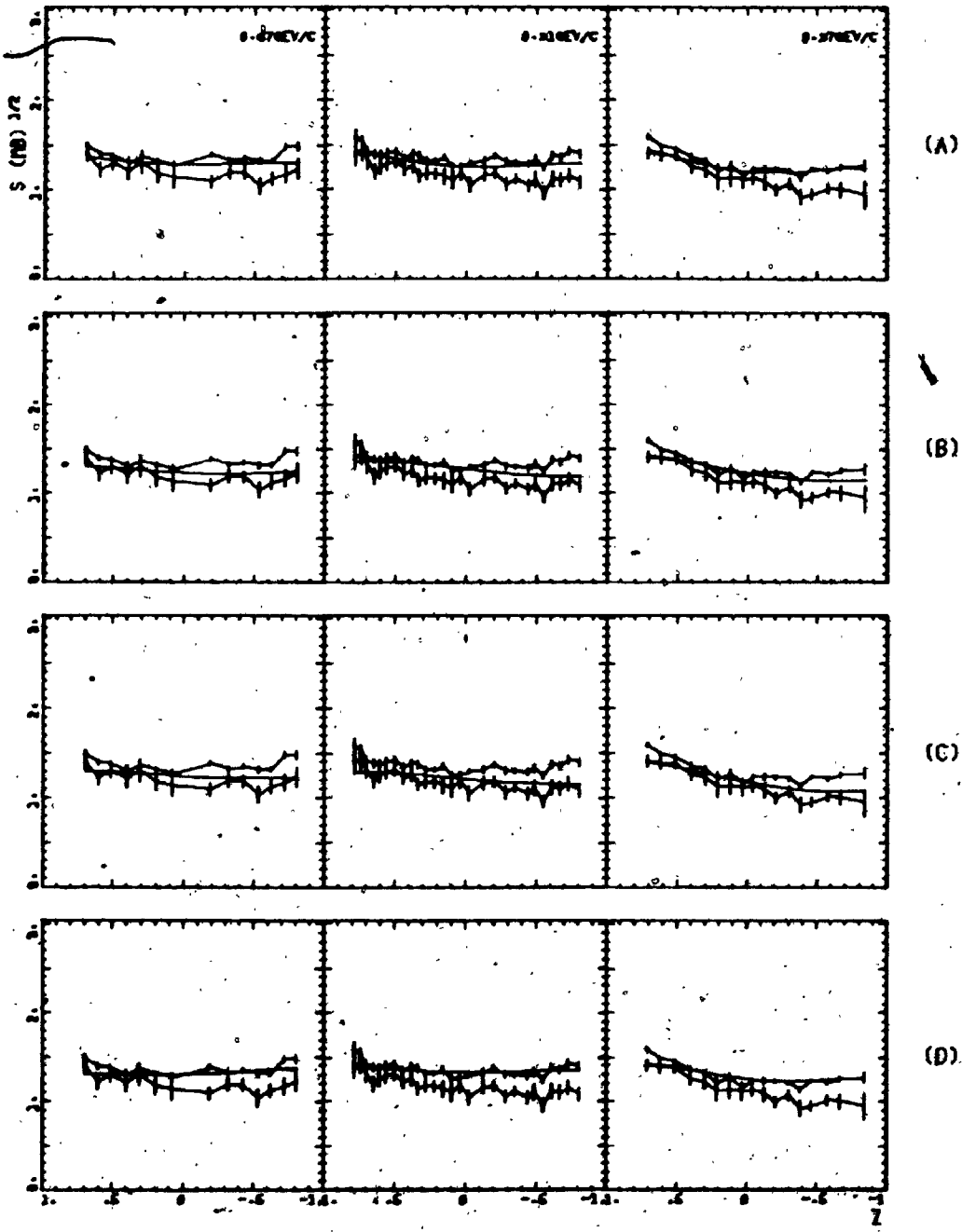


Figure 5.1. Comparison of the sum s of the moduli of the $K^+ p$ amplitudes with their bounds to test the inequalities (3.2.17a) and (3.2.17b). s are constructed from (A) Cutkosky phase shifts, (B) CERN α solutions, (C) CERN β solutions and, (D) CERN γ solutions and their bounds are found from P and D of Ref. 39 at $P_{\text{lab.}} = .87 \text{ Gev/c}$, $.91 \text{ Gev/c}$ and $.97 \text{ Gev/c}$ respectively. The bounds constructed from experimental data have error bars (Eq. 3.3.5). They are connected to guide the eye only.

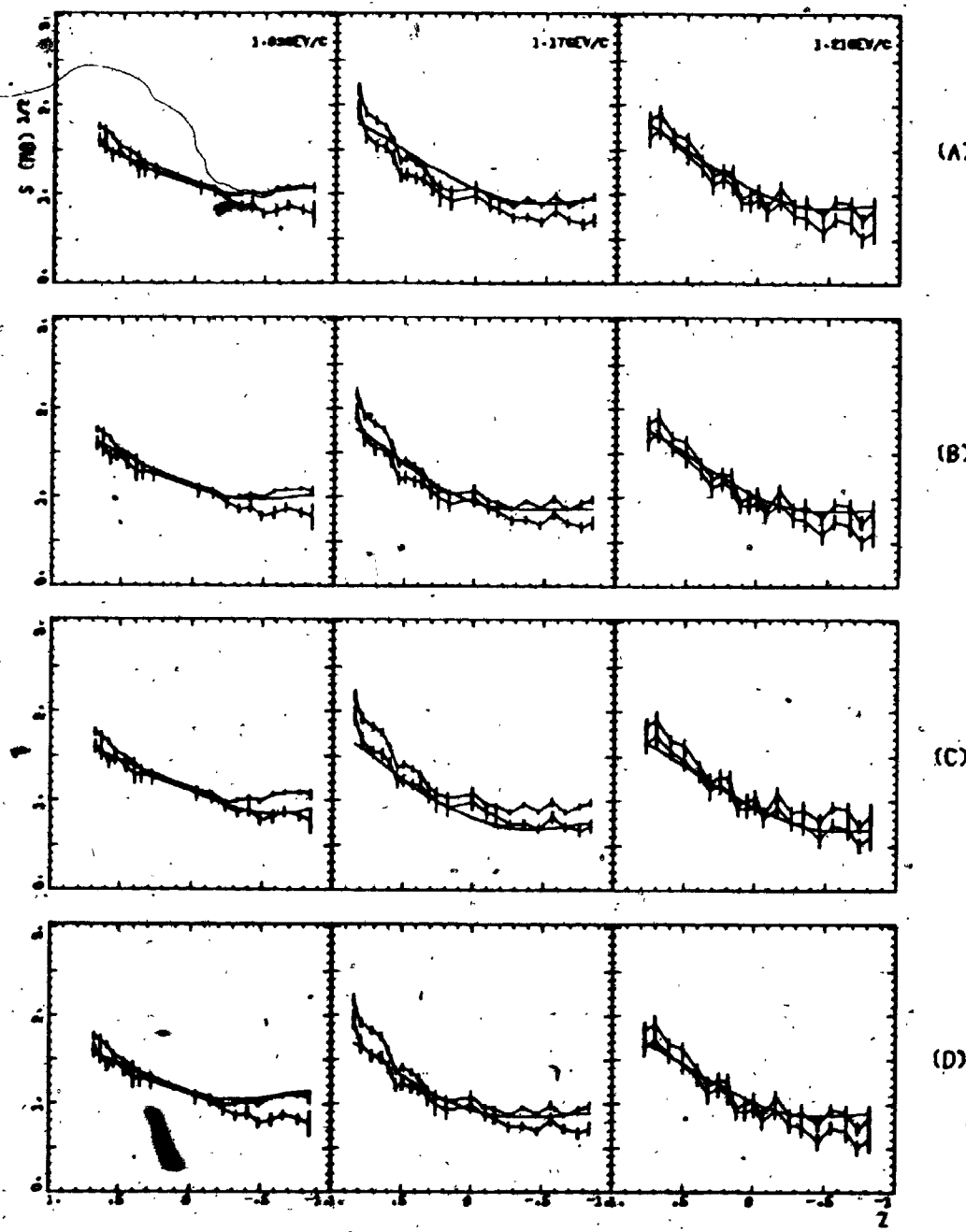


Figure 5.2. Comparison of the sum s of the moduli of the $K^+ p$ amplitudes with their bounds to test the inequalities (3.2.17a) and (3.2.17b). s are constructed from (A) Cutkosky phase shifts, (B) CERN α solutions, (C) CERN β solutions and, (D) CERN γ solutions and their bounds are found from P and D of Ref. 39 at $P_{lab} = 1.09 \text{ Gev}/c$, $1.17 \text{ Gev}/c$ and $1.21 \text{ Gev}/c$ respectively. The bounds constructed from experimental data have error bars (Eq. 3.3.5). They are connected to guide the eye only.

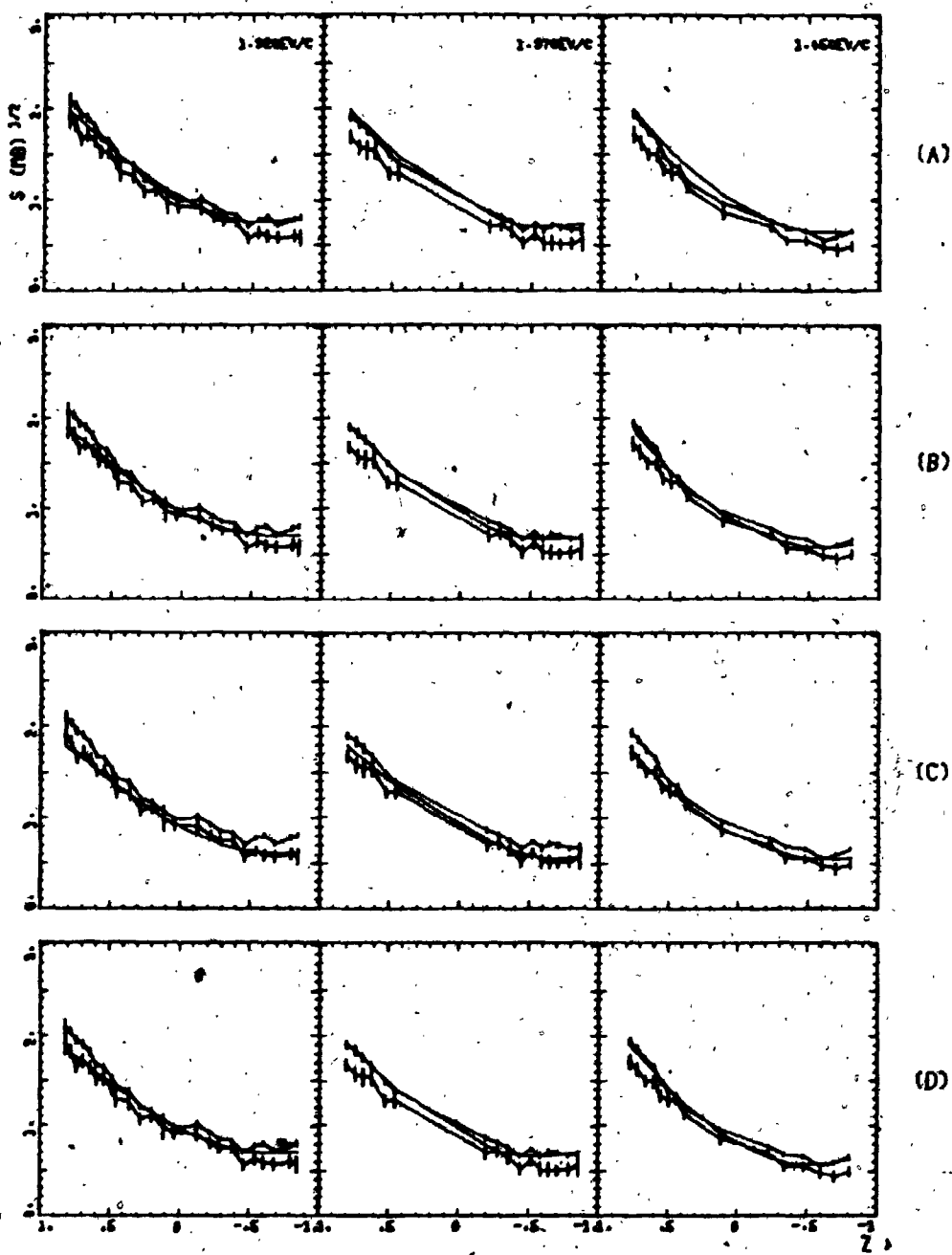


Figure 5.3. Comparison of the sum s of the moduli of the $K^+ p$ amplitudes with their bounds to test the inequalities (3.2.17a) and (3.2.17b). s are constructed from (A) Cutkosky phase shifts, (B) CERN α solutions, (C) CERN β solutions and, (D) CERN γ solutions and their bounds are found from P and D of Ref. 39 at $P_{\text{lab.}} = 1.32 \text{ Gev}/c$, $1.37 \text{ Gev}/c$ and $1.45 \text{ Gev}/c$ respectively. The bounds constructed from experimental data have error bars (Eq. 3.3.5). They are connected to guide the eye only.

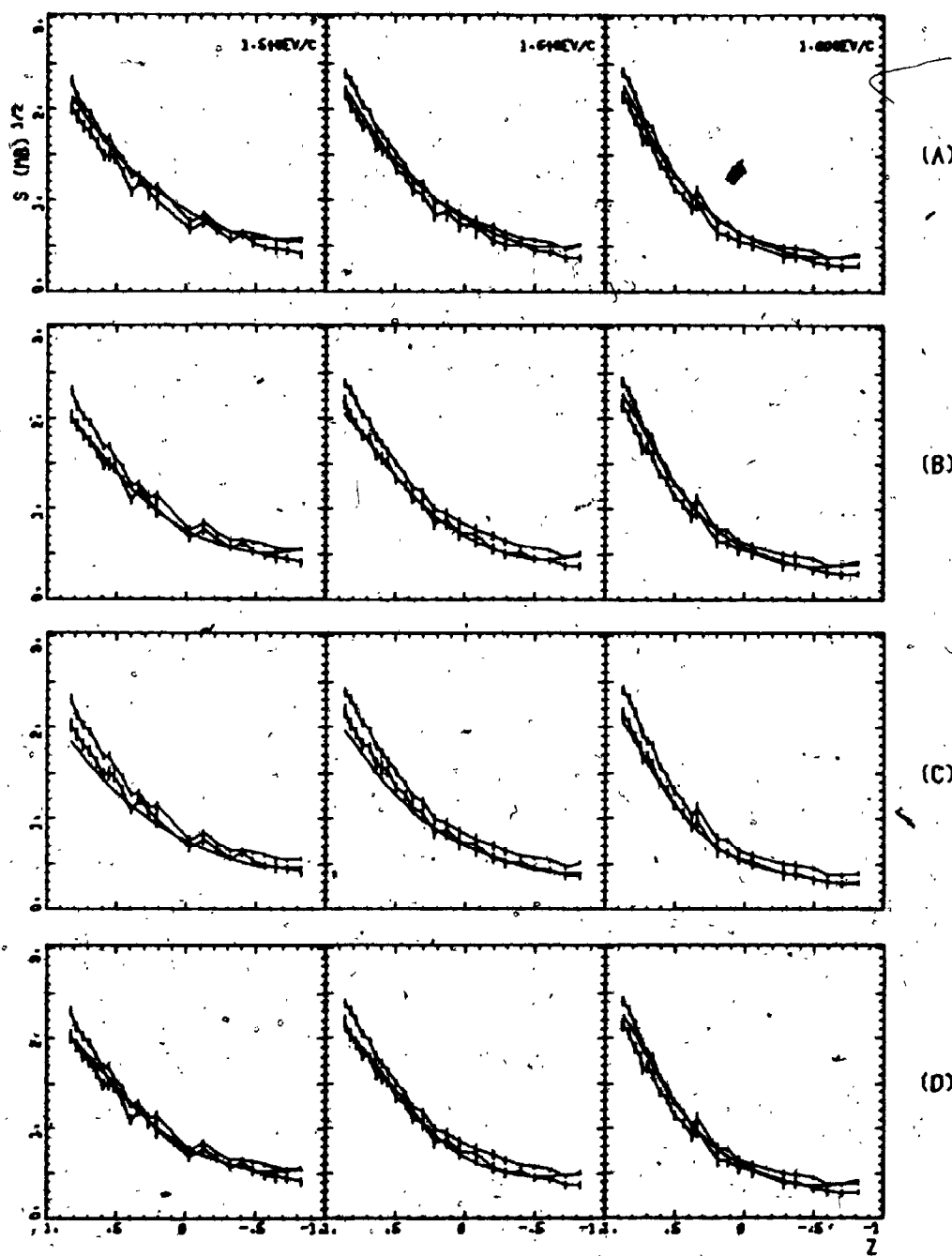


Figure 5.4. Comparison of the sum s of the moduli of the $K^+ p$ amplitudes with their bounds to test the inequalities (3.2.17a) and (3.2.17b). s are constructed from (A) Cutkosky phase shifts, (B) CERN α solutions, (C) CERN β solutions and, (D) CERN γ solution and their bounds are found from P and D of Ref. 39 at $P_{lab} = 1.54 \text{ GeV}/c$, $1.64 \text{ GeV}/c$ and $1.80 \text{ GeV}/c$ respectively. The bounds constructed from experimental data have error bars (Eq. 3.3.5). They are connected to guide the eye only.

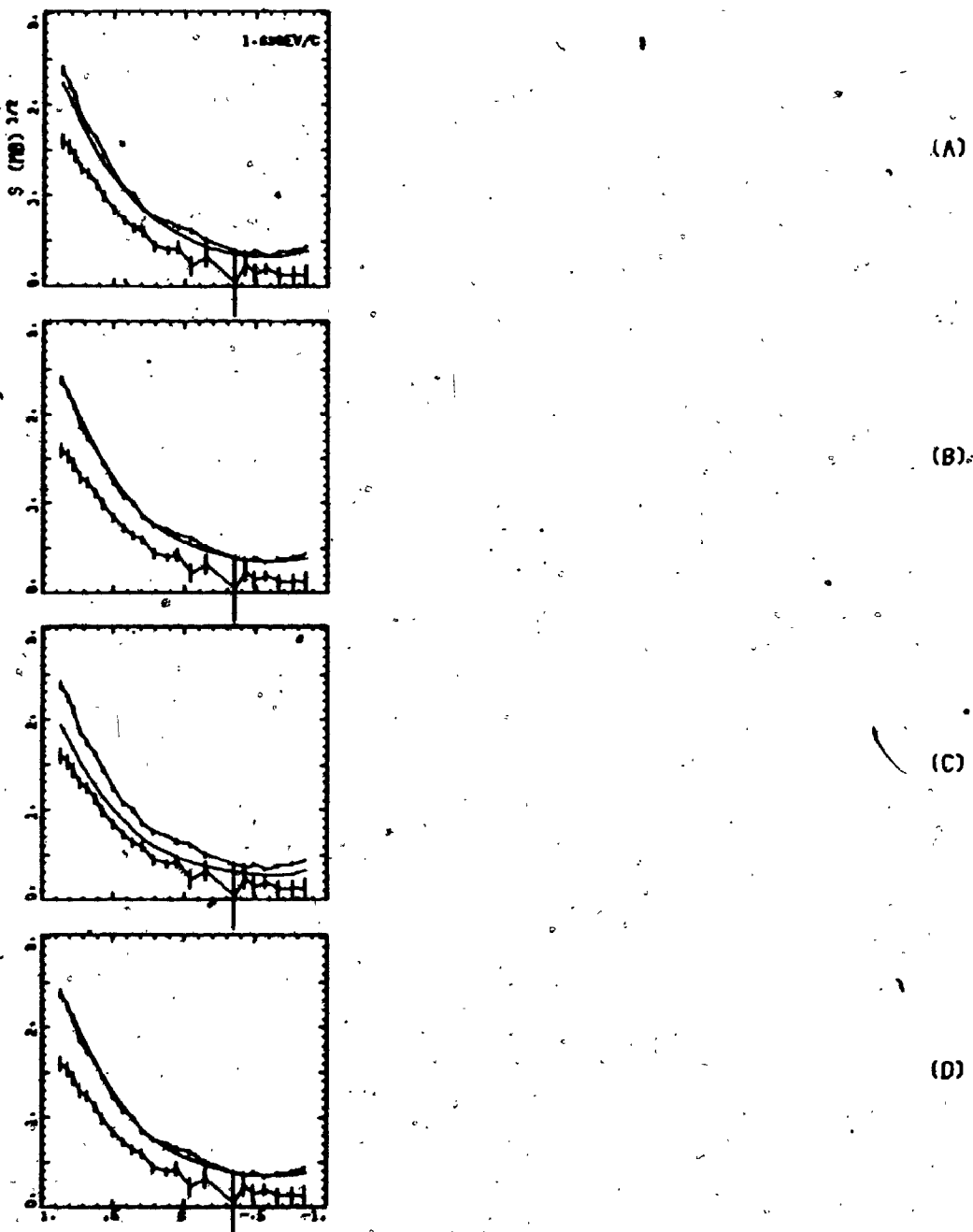


Figure 5.5. Comparison of the sum s of the moduli of the Kp amplitudes with their bounds to test the inequalities (3.2.17a) and (3.2.17b). s are constructed from (A) Cutkosky phase shifts, (B) CERN α solutions, (C) CERN β solutions and, (D) CERN γ solutions and their bounds are found from P and D of Ref. 39 at $P_{\text{lab.}} = 1.89 \text{ Gev}/c$. The bounds constructed from experimental data have error bars (Eq. 3.3.5). They are connected to guide the eye only.

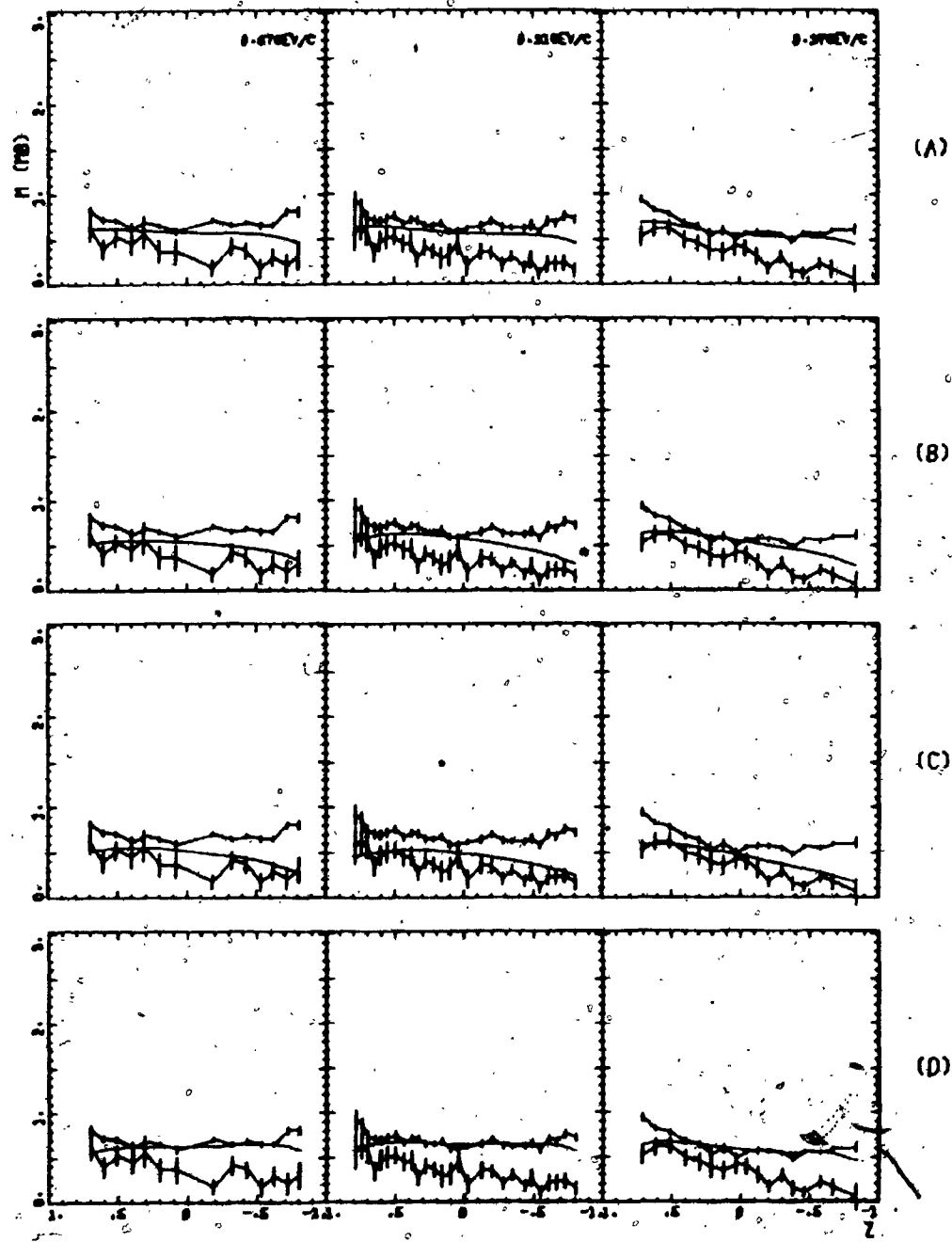


Figure 6.1. Comparison of the product m of the moduli for the $K^+ p$ amplitudes with their bounds to test the inequalities (3.2.16a) and (3.2.16b). m are constructed from (A) Cutkosky phase shifts, (B) CERN α solutions, (C) CERN β solutions and (D) CERN γ solutions and their bounds are found from P and D of Ref. 39 at $P_{\text{lab.}} = .87 \text{ Gev}/c$, $.91 \text{ Gev}/c$ and $.97 \text{ Gev}/c$ respectively. The bounds constructed from experimental data have error bars (Eq. 3.3.4). They are connected to guide the eye only.

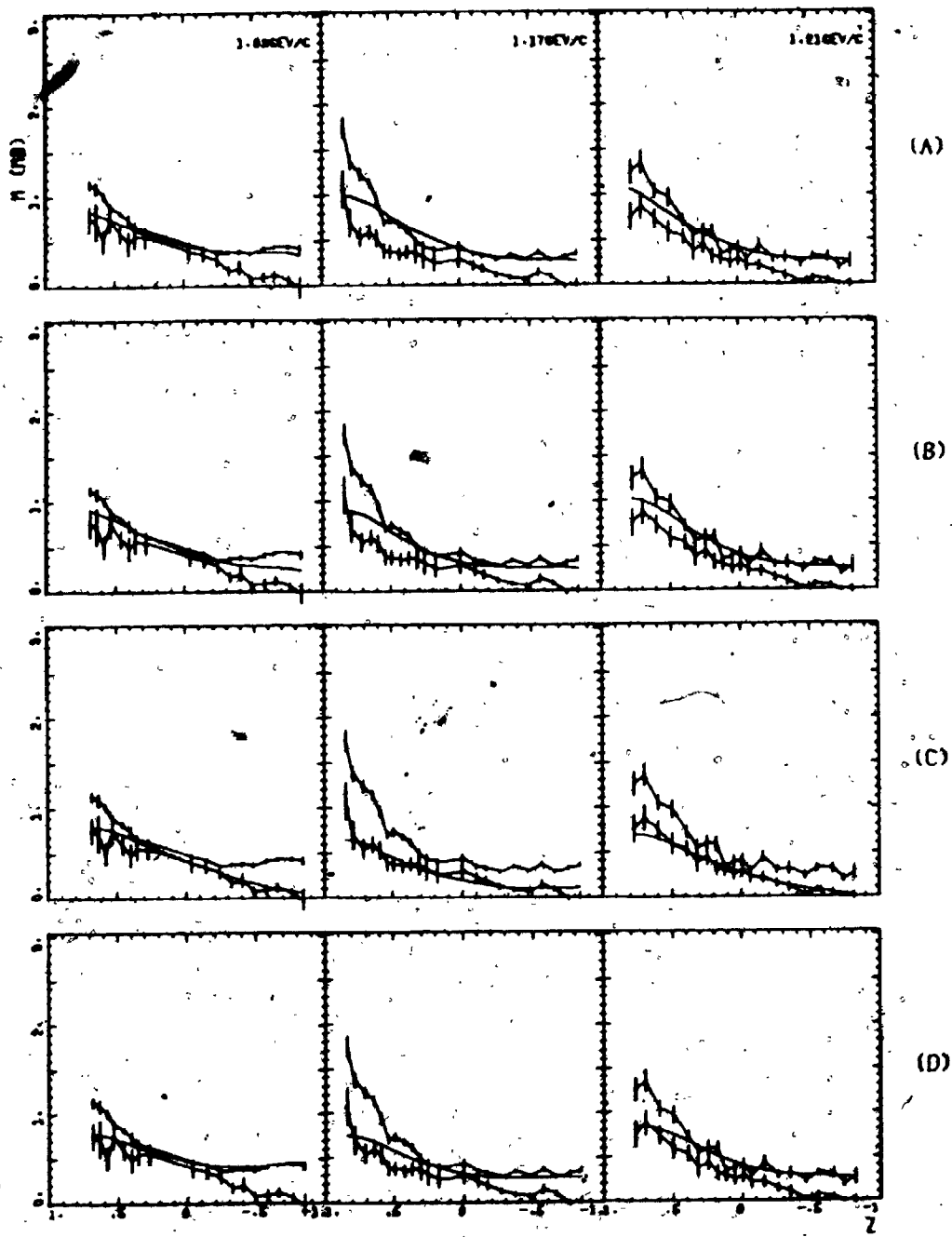


Figure 6.2. Comparison of the product m of the moduli for the $K^+ p$ amplitudes with their bounds to test the inequalities (3.2.16a) and (3.2.16b). m are constructed from (A) Cutkosky phase shifts; (B) CERN α solutions, (C) CERN β solutions and (D) CERN γ solutions and their bounds are found from P and D of Ref. 39 at $P_{\text{lab.}} = 1.09 \text{ Gev}/c$, $1.17 \text{ Gev}/c$ and $1.21 \text{ Gev}/c$ respectively. The bounds constructed from experimental data have error bars (Eq. 3.3.4). They are connected to guide the eye only.

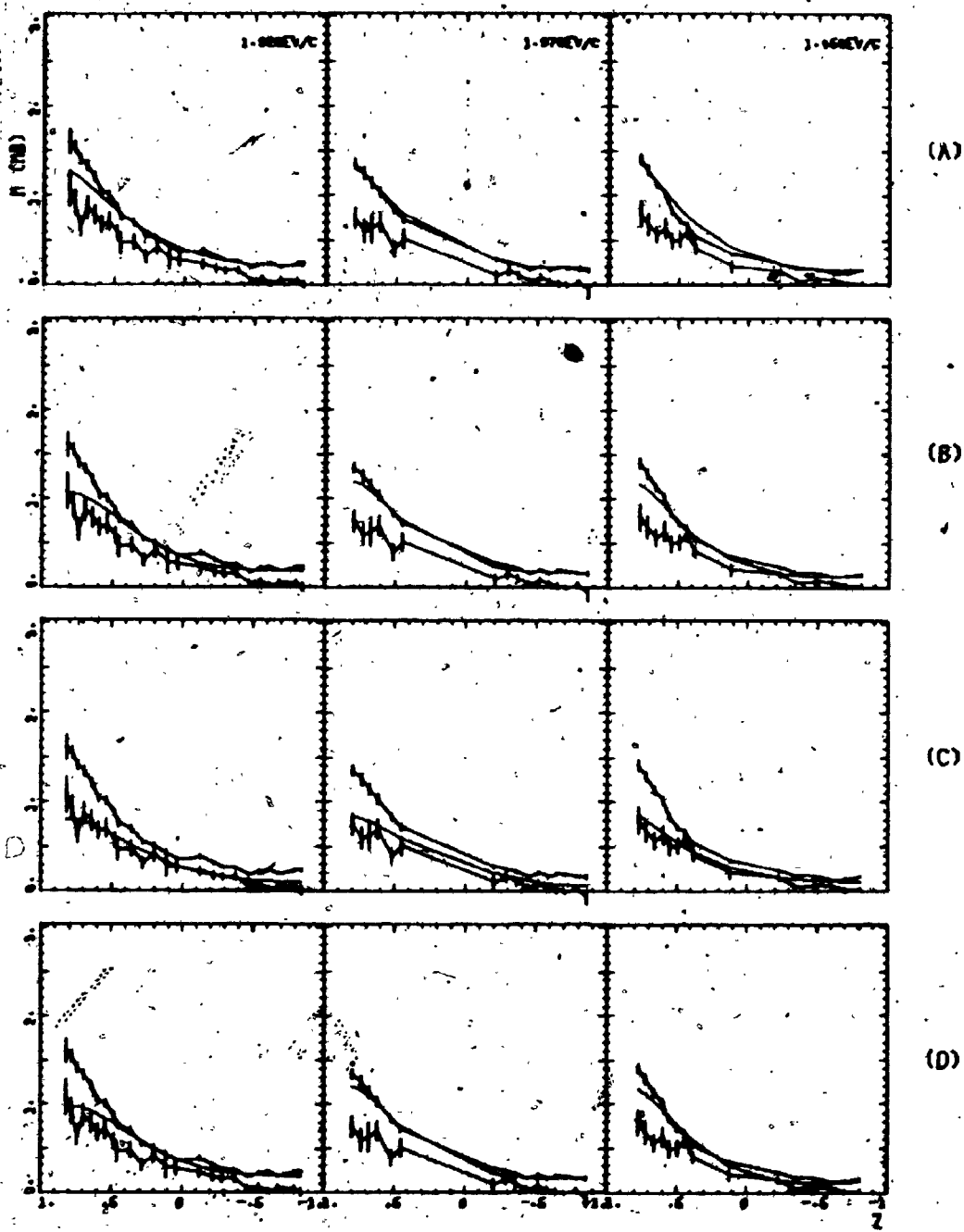


Figure 6.3. Comparison of the product m of the moduli for the $K^+ p$ amplitudes with their bounds to test the inequalities (3.2.16a) and (3.2.16b). m are constructed from (A) Cutkosky phase shifts, (B) CERN α solutions, (C) CERN β solutions and (D) CERN γ -solutions and their bounds are found from P and D of Ref. 39 at $P_{\text{lab}} = 1.32 \text{ Gev}/c$, $1.37 \text{ Gev}/c$ and $1.45 \text{ Gev}/c$ respectively. The bounds constructed from experimental data have error bars (Eq. 3.3.4). They are connected to guide the eye only.

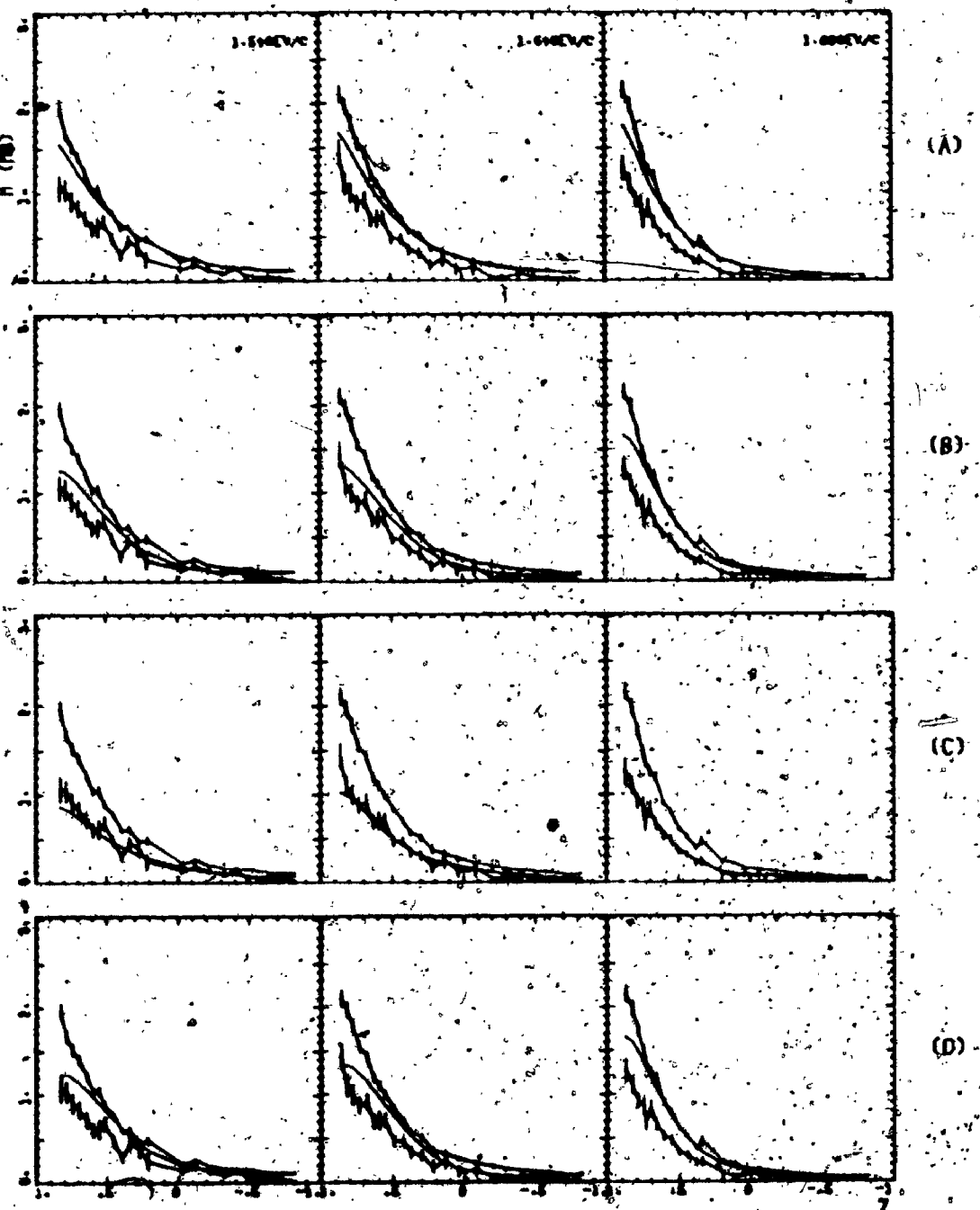


Figure 6.4. Comparison of the product m of the moduli for the $K^+ p$ amplitudes with their bounds to test the inequalities (3.2.16a) and (3.2.16b). m are constructed from (A) Cutkosky phase shifts, (B) CERN α solutions, (C) CERN β solutions and (D) CERN γ solutions, and their bounds are found from P and D of Ref. 39 at $p_{\text{lab}} = 1.54 \text{ Gev}/c$, $1.64 \text{ Gev}/c$ and $1.80 \text{ Gev}/c$ respectively. The bounds constructed from experimental data have error bars (Eq. 3.3.4). They are connected to guide the eye only.

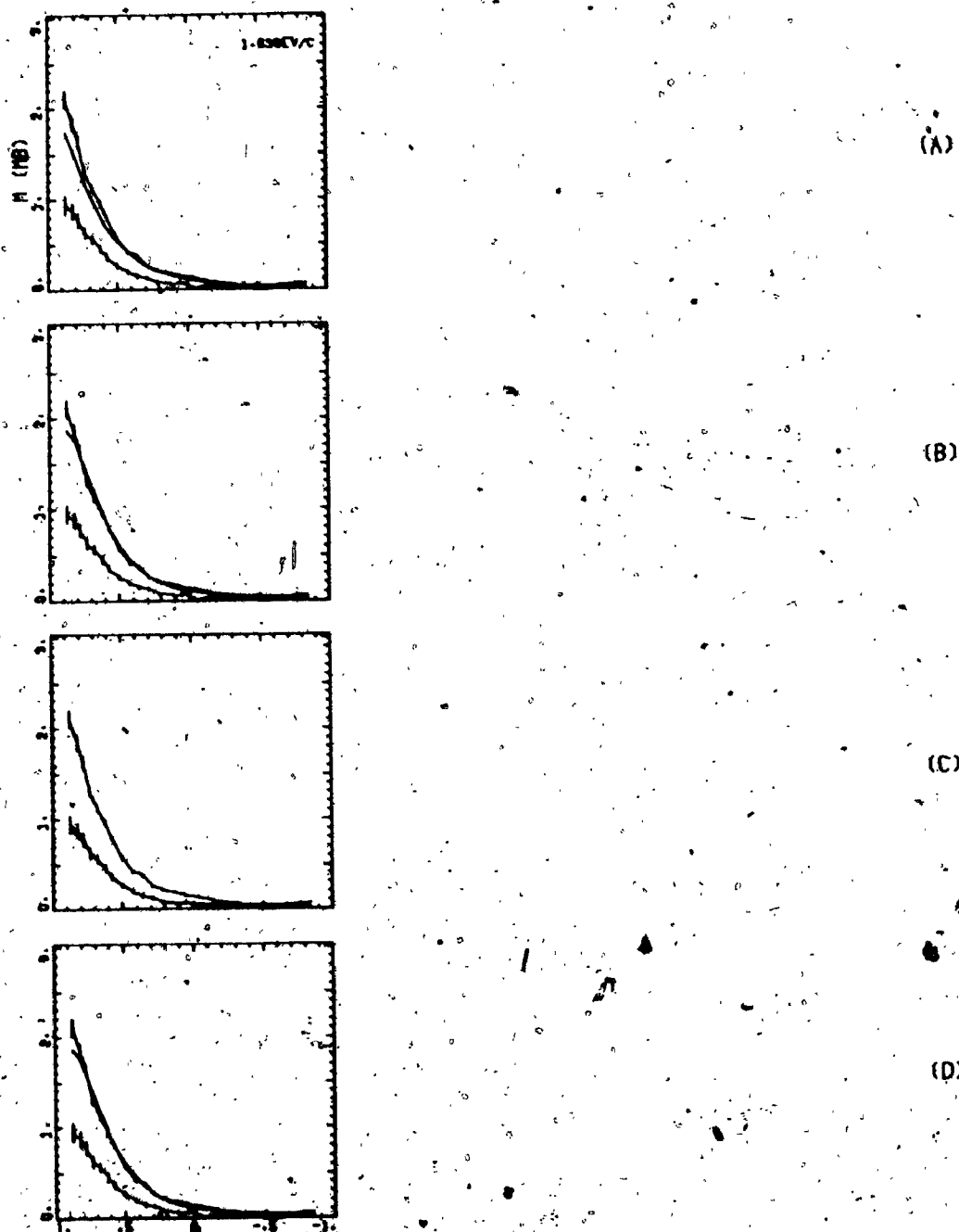


Figure 6.5. Comparison of the product m of the moduli for the $K^+ p$ amplitudes with their bounds to test the inequalities (3.2.16a) and (3.2.16b). m are constructed from (A) Cutkosky phase shifts, (B) CERN α solutions, (C) CERN β solutions and (D) CERN γ solutions and their bounds are found from P and D of Ref. 39 at $P_{lab} = 1.89$ Gev/c. The bounds constructed from experimental data have error bars (Eq. 3.3.4). They are connected to guide the eye only.

r)

r is right in the middle between upper and lower bounds at all energies.

$|f|, |g| \sin \theta$

At low energies $|f|$ and $|g| \sin \theta$ are close to their upper and lower bounds respectively. When the energy increases they move towards the middle region between the bounds, slightly crossing over each other at highest energies.

s)

s stays at all energies on or near the upper bounds, violating it in particular between 1.17 Gev/c and 1.45 Gev/c.

m)

m behaves very much like s, staying on or near upper bounds. It also shows the same violations between 1.17 Gev/c and 1.45 Gev/c.

CERN a solutions:

$\sin \alpha$)

For CERN a solution $\sin \alpha$ satisfies the bound staying at all energies.

above the polarization except at some odd experimental points. The behaviour of $\sin \alpha$ follows more or less P at low energies. Then beyond a certain energy (1.32 Gev/c) $\sin \alpha$ develops a hump in the middle angle region and has the same feature at the higher energies.

r)

At energies up to 1.09 Gev/c r is close to its upper bound. Above this energy it comes down. At high energies up to 1.80 Gev/c part of its backward section approaches the lower bound.

$|f|, |g| \sin \theta$

Up to 1.09 Gev/c this set is roughly similar to Cutkosky solution, both moduli staying more or less near their respective upper and lower bounds. Above this energy a strong cross over occurs, meaning that $|g| \sin \theta$ approaches now its upper bound whereas $|f|$ comes down to its lower bound.

s)

s stays within the limits at all energies in the entire scattering region.

m)

m behaves in general like s except that it has a tendency to fall

below the lower bound in the forward direction at certain energies.

CERN B solution:

$\sin \alpha$)

$\sin \alpha$ in this case behaves completely different. At most energies it stays close to one especially in the forward directions. In the backward direction it comes down rather abruptly at several energies. With such a large $\sin \alpha$ there is naturally not much possibility for violations.

Of all the solutions, this is the one which stays at all energies on or near the upper bound, violating it occasionally at different angles.

$|f|, |g| \sin \theta$)

The moduli in this case behave completely different from the other sets. At all energies $|f|$ stays on its upper bound, whereas $|g| \sin \theta$ stays on its lower bound which is not surprising if we remember the behaviour of r .

s)

s stays at all energies on or near the lower bound with bad violations at $P_{\text{lab.}} = 1.17 \text{ Gev/c}, 1.54 \text{ Gev/c}$ and 1.64 Gev/c .

m)

m stays close to or on the lower bound, violating it badly at some middle angles and the forward direction especially at 1.17 Gev/c , 1.54 Gev/c and 1.64 Gev/c .

CERN γ solution:

sin α)

For the γ solution $\sin \alpha$ behaves like the Cutkosky solution up to 1.32 Gev/c . That means it follows P closely sitting almost on top of it. Above 1.32 Gev/c it starts behaving like the CERN α -solution, developing the same hump in the middle region.

r)

At lower energies this set is close to Cutkosky solution. At high energies it is close to the α set.

$|f|, |g| \sin \theta$

Here again we have an entirely different behaviour. $|f|$ and $|g| \sin \theta$ are right in the middle between the upper and lower bounds up to 1.17 Gev/c. Above this energy a cross over occurs and $|g| \sin \theta$ approach its upper bound whereas $|f|$ comes down to its lower bound.

s)

s has the same behaviour as for a solution. It satisfies the bound at all energies in the entire scattering region.

m)

m shows, in general the same behaviour as s except the forward direction, where it tends to fall low. There are occasional local violations.

Rotation parameters:

With f and g being the spin non-flip and spin flip amplitudes, the following theoretical definitions can be introduced:

$$R = \frac{2 \operatorname{Re}(fg^*) \sin \theta}{|f|^2 + |g|^2 \sin^2 \theta}$$

$$A = \frac{|f|^2 - |g|^2 \sin^2 \theta}{|f|^2 + |g|^2 \sin^2 \theta}$$

Experimentalists use slightly different definitions, which are linear combinations of the above definition

$$^0\text{IR} = -(|f_{++}|^2 - |f_{+-}|^2)\cos \theta_p - 2 \operatorname{Re}(f_{++} f_{+-}^*) \sin \theta_p \quad (3.3.7)$$

$$\text{IA} = (|f_{++}|^2 - |f_{+-}|^2)\sin \theta_p - 2 \operatorname{Re}(f_{++} f_{+-}^*) \cos \theta_p \quad (3.3.8)$$

Here f_{++} and f_{+-} are helicity-nonflip and helicity-flip amplitudes and they are linear combinations of f and g . θ_p is the recoil proton angle measured in the laboratory frame. The relation between laboratory and C.M. angles is

$$\sin^2 \theta_p = \frac{1 + \cos \theta}{2 + (g^2/M^2)(1 - \cos \theta)}$$

where g is the meson C.M. momentum and M is the proton mass.

Using the definitions (3.3.7) and (3.3.8), we have constructed from Cutkosky phase shifts and CERN α , β , γ solutions the rotation parameters R and A . We present in figure 6A and 6B our results at three energies, namely at $P_{\text{lab}} = .91 \text{ Gev/c}$, 1.21 Gev/c and 1.64 Gev/c .

The R -parameter has more or less the same behaviour for the Cutkosky as well as for the CERN α and γ solutions. It is negative at all angles, except in the backward direction, where it goes $+1$.

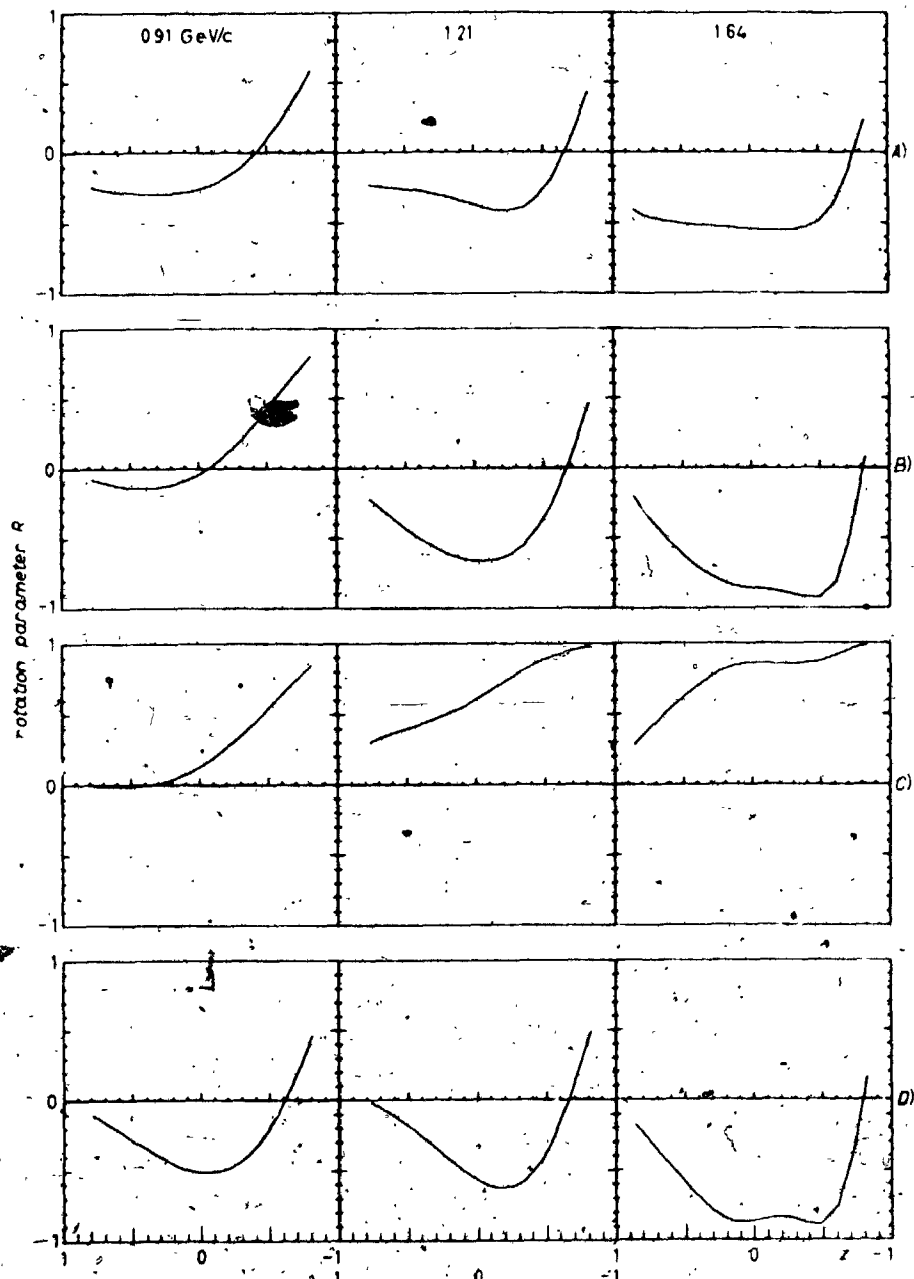


Figure 6A. The predictions for the rotation parameter R of the A) Cutkosky phase shifts, B) CERN α solutions, C) CERN β solutions and D) CERN γ solutions at $P_{\text{lab}} = 0.91 \text{ Gev}/c$, $1.21 \text{ Gev}/c$ and $1.64 \text{ Gev}/c$.

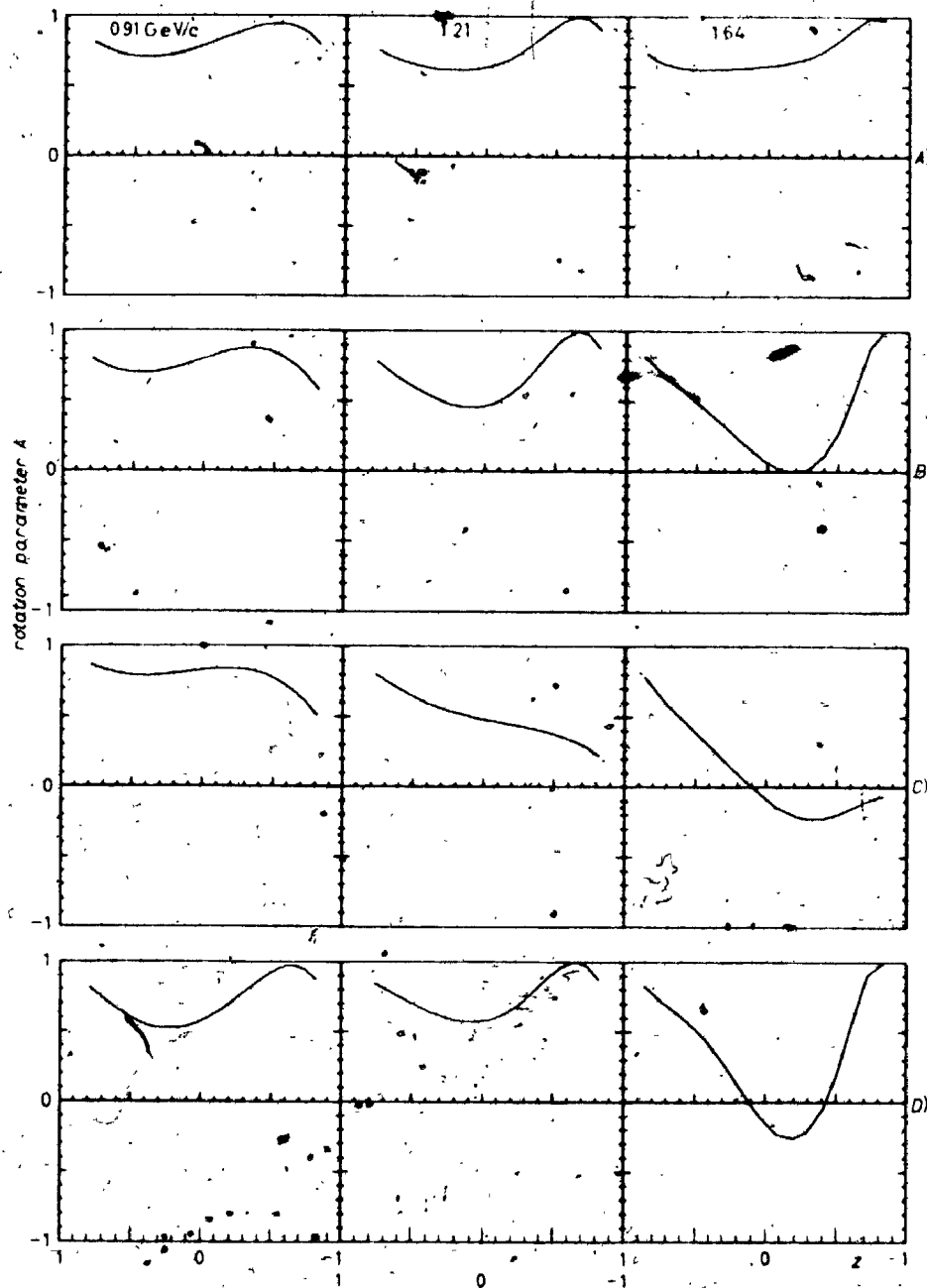


Figure 6B. The predictions for the rotation parameter A of the A) Cutkosky phase shifts, B) CERN α solutions, C) CERN β solutions and D) CERN γ solutions at $p_{\text{lab}} = .91 \text{ Gev/c}$, 1.21 Gev/c and 1.64 Gev/c .

In contrast, the CERN β solution predicts a R-parameter which is positive at all angles.

For the A-parameter, even though the Cutkosky and CERN α and γ solutions predict similar behaviours (positive at all angles) for the lower energies, at high energies the Cutkosky solution remains the same, whereas both α and γ solutions dip strongly, the γ solution becoming even negative.

The characteristic difference in the prediction of the CERN β solution is the lack of backward peak for the A-parameter. Here A stays small as one approaches the backward direction at high energies.

We note that inequalities for the relative magnitude and phase of the two independent amplitudes depend on experimental polarization only. They are sensitively effected by the error bar of polarization. The larger P is and smaller its error bar is, the better the bound are. The smaller P is and the larger its error bar is, the poorer the bound are. For example, if the error bar of the polarization crosses the z-axis (i.e. $P = 0$) r_+ has no limit and $r_- = 0$. This means that value of r can be any positive number (i.e. no bound at all) and the sign of $\sin \alpha$ is not determined since polarization can be positive or negative.

The bounds for $|f|$, $|g| \sin \theta$, m and s are determined by both polarization and differential cross section. Since the error of $|f|_+$, $|f|_-$, $|g|_+ \sin \theta$, $|g|_- \sin \theta$, m_+ , m_- , s_+ and s_- come from the combination of the errors in P and D. We expect larger errors in these

84

quantities.

Comparing α , β and γ solutions of CERN and Cutkosky solution with the bounds of P , r , $|f|$, $|g| \sin \theta$, m and s we find there are less violations in α and Cutkosky solutions. In our point of view the α and Cutkosky solutions are better than others. In the last case the only disagreements with the bounds occur between 1.17 Gev/c and 1.45 Gev/c. It seems that too large s and m with violations of the upper bounds at several angles indicate that the moduli of f or/and g could be lowered without violating the remaining bounds. As we remarked before, the bounds themselves do not tell where the physical quantities ought to be as long as they are between the limits. But they indicate what the peculiarities of the theoretical quantities are and those features of the quantities emerging from a comparison with the bounds may be of interest to the people who have obtained the phase shifts by fits to P and D . Thus one set leads to a relative phase ($\sin \alpha$) between f and g which is almost equal to P , its lower bound, whereas another set has $\sin \alpha$ equal to one, its upper bound. One set has a modulus for f equal to its upper bound with modulus of g equal to its lower bound whereas another set has a larger spin flip amplitude than f . Apparently we need badly good measurements of the rotation parameters.

Finally we would like to point out that the behaviour of the theoretical quantities could possibly be of help for dynamical models. Here we have tested different phase shifts against the rigorous bounds. A test of the different theoretical models like Regge pole model, direct channel resonance model etc. with these bounds would provide criteria to

choose among those models.

CHAPTER IV

THE BOUNDS ON THE IMAGINARY PARTS OF THE SCATTERING AMPLITUDES

4.1 The Unitarity Equation.

The conservation of probability leads to the unitarity equation of the S-matrix:

$$S^+ S = I \quad (4.1.1)$$

We define the T matrix by

$$S = I + iT$$

then

$$S^+ S = (I - iT^+) (I + iT) = I$$

$$-i(T - T^+) = T^+ T \quad (4.1.2)$$

The matrix elements between the states i and j as a sum over intermediate states are

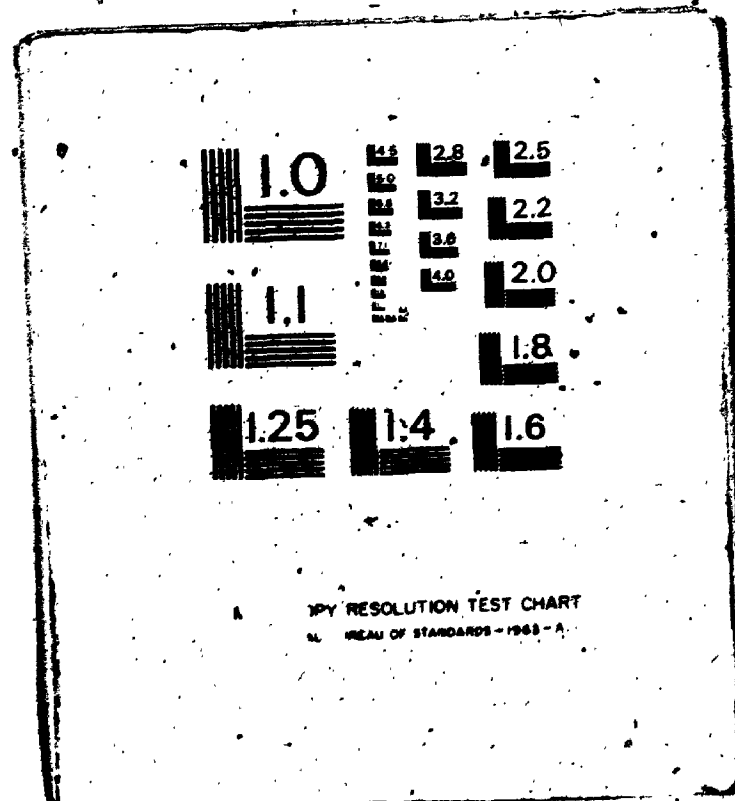
$$-i(T_{ij} - T_{ij}^*) = (T^+ T)_{ij} = \sum T_{ik}^+ T_{kj}$$

$$-i(T_{ij} - T_{ji}^*) = \sum T_{ki}^* T_{kj}$$

2

3

OF/DE



For the scattering under time reversal and rotation invariance T matrix is symmetric

$$T_{ij} = T_{ji}$$

We have

$$-i(T_{ij} - T_{ij}^*) = \sum_k T_{ik}^* T_{kj} \quad (4.1.3)$$

This means

$$2 \operatorname{Im} T_{ij} = \sum_k T_{ik}^* T_{kj} \quad (4.1.4)$$

The left hand side is a real quantity but the right hand side is in general a complex quantity. Hence the imaginary part of the right hand side must vanish. So the equation (4.1.4) is actually two real equations:

$$2 \operatorname{Im} T_{ij} = \operatorname{Re} \sum_k T_{ik}^* T_{kj} \quad (4.1.5a)$$

$$0 = \operatorname{Im} \sum_k T_{ik}^* T_{kj} \quad (4.1.5b)$$

For the elastic scattering the states differ only by orientation of the momentum vector. Thus summation over all states is a integration over all directions.

$$\operatorname{Im} F(z) = \frac{q \text{C.M.}}{4\pi} \int F^*(z'') F(z') dz'' d\psi'' \quad (4.1.6)$$

The factor $\frac{q_{C.M.}}{4\pi}$ on the right hand side gives the correct dimensionality and will be derived below. Where $q_{C.M.}$ is the C.M. momentum of the scattering particle, Z is the cosine of the angle between the initial and the final state ($\cos \theta$), Z'' is the cosine of the angle between the initial and the intermediate state ($\cos \theta''$), Z' is the cosine of the angle between the intermediate state and the final state ($\cos \theta'$). These angles and vectors are shown in figure 7

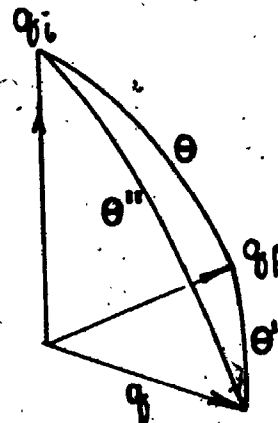


Figure 7. C.M. momentum of the initial, intermediate and final states.

The angles θ , θ' and θ'' are not independent. They have the relation

$$\cos \theta' = \cos \theta \cos \theta'' + \sin \theta \sin \theta'' \cos \psi''$$

$$\text{or } Z' = Z \cdot Z'' + \sqrt{1 - Z^2} \sqrt{1 - Z''^2} \cos \psi'' \quad (4.1.7)$$

When we change the integral variable from θ'' and ψ'' to Z'' and Z' then the integral becomes

$$\text{Im } F(Z) = \frac{q_{C.M.}}{2\pi} \int \frac{F^*(Z'')F(Z')}{\sqrt{k}} \theta(k) dz'' dz' \quad (4.1.8)$$

where $k = 1 - z^2 - z'^2 - z''^2 + 2z z' z''$. $\theta(k)$ is a step function.

It guarantees that the integration is over the inside of the unitarity ellipse

$$1 - z^2 - z'^2 - z''^2 + 2z z' z'' = 0 \quad (4.1.9)$$

with the semi-axis:

$$R = \sqrt{1+z} \quad \text{and} \quad r = \sqrt{1-z}$$

as in figure 8.

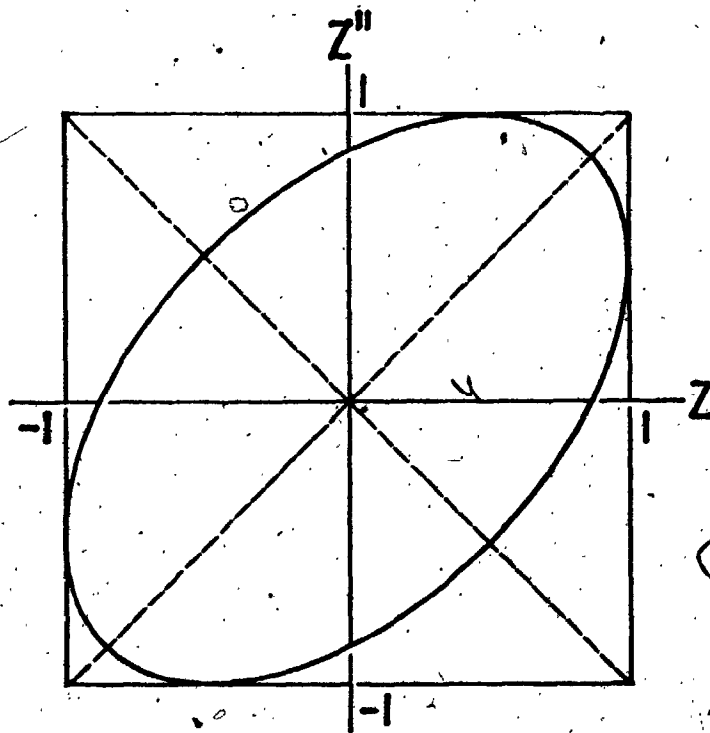


Figure 8. The unitarity ellipse.

This means

$$\text{Im } F(Z) = \frac{q_{\text{C.M.}}}{2\pi} \int_{-1}^1 dz' \int_{z_-}^{z_+} dz'' \frac{F^*(z'')F(z')}{\sqrt{k}} \quad (4.1.10)$$

and $F(Z)$ is the scattering amplitude.

In scalar-scalar scattering case (for example, the $\pi\pi$ scattering) $F(Z)$ is a scalar. In $0^- \frac{1}{2}^+ \rightarrow 0^- \frac{1}{2}^+$ case (for example, πN and KN scattering) it is a 2×2 matrix. And in $\frac{1}{2}^+ \frac{1}{2}^+ \rightarrow \frac{1}{2}^+ \frac{1}{2}^+$ scattering (for example, NN scattering) it is a tensor with rank two.

a) scalar particle scattering

$F(Z)$ is a scalar and the normalization is such that

$$D = \frac{d\sigma(Z)}{d\Omega} = |F(Z)|^2 \quad (4.1.11)$$

The equations (4.1.6) and (4.1.8) are the general optical theorem. When it is forward scattering (i.e. $\theta = 0$) then $\theta' = \theta''$. The equation (4.1.6) leads to the particular (forward direction) optical theorem

$$\text{Im } F(\theta = 0) = \frac{q_{\text{C.M.}}}{4\pi} \int F^*(Z'')F(Z')dz''d\psi''$$

$$= \frac{q_{\text{C.M.}}}{4\pi} \int \frac{d\sigma}{d\Omega} dz'' d\psi''$$

$$= \frac{q_{\text{C.M.}}}{4\pi} \sigma_{\text{Tot.}} \quad (4.1.12)$$

b) $0^- \frac{1+}{2} \rightarrow 0^- \frac{1+}{2}$ scattering

$F(Z)$ is no longer a scalar but a 2×2 matrix. The most general form of the scattering matrix in the two-component spin space is a linear combination of I , the unit 2×2 matrix and the Pauli spin matrix $\vec{\sigma}$. The T matrix is

$$T_{if} = \langle \vec{n}_f, \frac{1}{2}, v' | T | \vec{n}_i, \frac{1}{2}, v \rangle = (u_1 \frac{1}{2}, v', (A + i\vec{\sigma} \cdot \vec{B}) u_1 \frac{1}{2}, v) \quad (4.1.13)$$

where $|\vec{n}_f, \frac{1}{2}, v'\rangle$ is the final state with unit momentum vector \vec{n}_f , spin $\frac{1}{2}$ and spin orientation v' , $|\vec{n}_i, \frac{1}{2}, v\rangle$ is the initial state with unit momentum vector \vec{n}_i , spin $\frac{1}{2}$ and spin orientation v , $u_1 \frac{1}{2}, v'$ and $u_1 \frac{1}{2}, v$ are the spin eigenfunctions of the final and initial states respectively.

Here, since T is invariant under rotations $A = A(\vec{n}_f \cdot \vec{n}_i)$ must be a function of $\vec{n}_f \cdot \vec{n}_i$ (and of course the energy), while B will be of the form

$$\vec{B} = b_1 \vec{n}_i + b_2 \vec{n}_f + b_3 \vec{n}_i \times \vec{n}_f \quad (4.1.14)$$

where b_1 , b_2 and b_3 are functions of $\vec{n}_f \cdot \vec{n}_i$ (and the total energy).

Under the time reversal operation we have

$$\langle \vec{n}_f, \frac{1}{2}, v' | T | \vec{n}_i, \frac{1}{2}, v \rangle = (-1)^{\frac{1}{2} + v - \frac{1}{2} - v'} \times$$

$$\times \langle -\vec{n}_i, \frac{1}{2}, -v | T | -\vec{n}_f, \frac{1}{2}, -v' \rangle \quad (4.1.15)$$

Let

$$A + i\vec{\sigma} \cdot \vec{B} = T(\vec{n}_f, \vec{n}_i, \vec{\sigma}) \quad (4.1.16)$$

Since

$$i\sigma_2 \frac{u_1^*}{\frac{1}{2}, v} = (-1)^{\frac{1}{2} + v} u_1 \frac{1}{2}, -v \quad (4.1.17)$$

then we may write the right hand side of (4.1.15) as

$$\begin{aligned} & (i\sigma_2 \frac{u_1^*}{\frac{1}{2}, v}, T(-\vec{n}_i, -\vec{n}_f, \vec{\sigma}) i\sigma_2 \frac{u_1^*}{\frac{1}{2}, v'}) \\ &= (T^*(-\vec{n}_i, -\vec{n}_f, \vec{\sigma}) \sigma_2 \frac{u_1^*}{\frac{1}{2}, v'}, \sigma_2 \frac{u_1^*}{\frac{1}{2}, v'}) \\ &= (u_1 \frac{1}{2}, v', \sigma_2 T(-\vec{n}_i, -\vec{n}_f, \tilde{\vec{\sigma}}) \sigma_2 \frac{u_1^*}{\frac{1}{2}, v'}) \\ &= (u_1 \frac{1}{2}, v', T(-\vec{n}_i, -\vec{n}_f, -\tilde{\vec{\sigma}}) \frac{u_1^*}{\frac{1}{2}, v'}) \end{aligned} \quad (4.1.18)$$

where $\tilde{\vec{\sigma}}$ is the transpose of $\vec{\sigma}$ and we have used $\sigma_2^* = \sigma_2$, $\sigma_2 \cdot \sigma_2 = I$ and $\sigma_2 \tilde{\vec{\sigma}} \sigma_2 = -\tilde{\vec{\sigma}}$.

From (4.1.15) and (4.1.16) the time reversal invariance requires

$$T(\vec{n}_f, \vec{n}_i, \vec{\sigma}) = T(-\vec{n}_i, -\vec{n}_f, -\vec{\sigma}) \quad (4.1.19)$$

Comparing (4.1.16) and (4.1.19) and inserting (4.1.14) into latter we find that

$$\begin{aligned} A(\vec{n}_f \cdot \vec{n}_i) + i\vec{\sigma} \cdot [b_1 \vec{n}_i + b_2 \vec{n}_f + b_3 (\vec{n}_i \times \vec{n}_f)] \\ = A(\vec{n}_f \cdot \vec{n}_i) - i\vec{\sigma} \cdot [-b_1 \vec{n}_f - b_2 \vec{n}_i + b_3 (\vec{n}_f \times \vec{n}_i)]. \end{aligned} \quad (4.1.20)$$

This is true only when $b_1 = b_2$. So the general form of T matrix consistent with invariance under rotations and time reversal is

$$\begin{aligned} \langle \vec{n}_f, \frac{1}{2}, v' | T | \vec{n}_i, \frac{1}{2}, v \rangle &= (u_{\frac{1}{2}, v'}, [A + ib_1 \vec{\sigma} \cdot (\vec{n}_i + \vec{n}_f) \\ &\quad + ib_3 \vec{\sigma} \cdot (\vec{n}_i \times \vec{n}_f)] u_{\frac{1}{2}, v}) \end{aligned} \quad (4.1.21)$$

Next we impose the parity conservation in the T matrix. Parity conservation is $P T P^{-1} = T$ where P is parity operator. Since $P x_{n, s, v}^{\pm} = x_{-n, s, v}^{\mp}$ where $x_{n, s, v}^{\pm}$ is the eigenfunction of the state with momentum \vec{n} , spin s and spin orientation v , therefore we have

$$\begin{aligned} \langle \vec{n}_f, \frac{1}{2}, v' | T | \vec{n}_i, \frac{1}{2}, v \rangle &= (x_{\vec{n}_f, \frac{1}{2}, v'}^{\pm}, T(\vec{n}_f, \vec{n}_i, \vec{\sigma}) x_{\vec{n}_i, \frac{1}{2}, v}^{\pm}) \\ &= (x_{\vec{n}_f, \frac{1}{2}, v'}^{\pm}, P^{-1} T(\vec{n}_f, \vec{n}_i, \vec{\sigma}) P x_{\vec{n}_i, \frac{1}{2}, v}^{\pm}) \end{aligned}$$

$$= (\chi_{-\vec{n}_f, \frac{1}{2}, v}^{\rightarrow}, T(\vec{n}_f, \vec{n}_i, \vec{\sigma}) \chi_{-\vec{n}_i, \frac{1}{2}, v}^{\rightarrow})$$

$$= (\chi_{\vec{n}_f, \frac{1}{2}, v}^{\rightarrow}, T(-\vec{n}_f, -\vec{n}_i, \vec{\sigma}) \chi_{\vec{n}_i, \frac{1}{2}, v}^{\rightarrow})$$

(4.1.22)

This implies

$$T(\vec{n}_f, \vec{n}_i, \vec{\sigma}) = T(-\vec{n}_f, -\vec{n}_i, \vec{\sigma}) \quad (4.1.23)$$

and then

$$\begin{aligned} & A(\vec{n}_f \cdot \vec{n}_i) + i b_1 \vec{\sigma} \cdot (\vec{n}_i + \vec{n}_f) + i b_3 \vec{\sigma} [(\vec{n}_i \times \vec{n}_f) \\ & = A(\vec{n}_f \cdot \vec{n}_i) - i b_1 \vec{\sigma} (\vec{n}_i + \vec{n}_f) + i b_3 \vec{\sigma} (\vec{n}_i \times \vec{n}_f) \end{aligned} \quad (4.1.24)$$

This is true only if b_1 vanishes. So the general form of the scattering amplitude consistent with time reversal and rotation invariance and with parity conservation is

$$F(Z) = f(Z) + i g(Z) \vec{\sigma} \cdot (\vec{n}_i \times \vec{n}_f) \quad (4.1.25)$$

If we choose \vec{n}_i to be in Z direction and \vec{n}_f in $x - z$ plane (i.e. the scattering plane is in $x - z$ plane) as figure 9

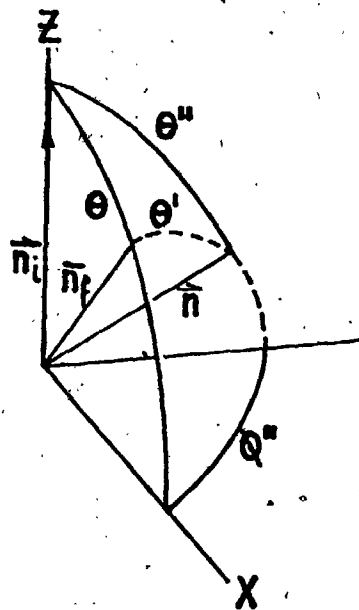


Figure 9. Unit vectors in the direction of momenta.

$$\vec{n}_i = (0, 0, 1)$$

$$\vec{n}_f = (\sin \theta, 0, \cos \theta)$$

$$\vec{n} = (\sin \theta'' \cos \phi'', \sin \theta'' \sin \phi'', \cos \theta'')$$

$$\vec{n}_i \times \vec{n}_f = (0, \sin \theta, 0)$$

$$\vec{n} \times \vec{n}_f = (\cos \theta \sin \theta'' \sin \phi'', -\sin \theta'' \cos \theta \cos \phi''$$

$$+ \sin \theta \cos \theta'', -\sin \theta \sin \theta'' \cos \phi'')$$

$$\vec{n}_i \times \vec{n} = (-\sin \theta'' \sin \phi'', \sin \theta'' \cos \phi'', 0)$$

$$\vec{\sigma} \cdot (\vec{n}_i \times \vec{n}_f) = \begin{pmatrix} 0 & -i \sin \theta \\ i \sin \theta & 0 \end{pmatrix}$$

$$\vec{\sigma} \cdot (\vec{n}_i \times \vec{n}) = \begin{pmatrix} 0 & -\sin \theta'' \sin \phi'' - i \sin \theta'' \cos \phi'' \\ -\sin \theta'' \sin \phi'' + i \sin \theta'' \cos \phi'' & 0 \end{pmatrix}$$

$$\vec{\sigma} \cdot (\vec{n} \times \vec{n}_f) = \begin{pmatrix} -\sin \theta \sin \theta'' \sin \phi'' & \cos \theta \sin \theta'' \sin \phi'' \\ \cos \theta \sin \theta'' \sin \phi'' & +i(\sin \theta'' \cos \theta \cos \phi'' - \sin \theta \cos \theta'') \\ -i(\sin \theta'' \cos \theta \cos \phi'' - \sin \theta \cos \theta'') & \sin \theta \sin \theta'' \sin \phi'' \end{pmatrix}$$

So

$$F(\theta) = \begin{pmatrix} f(\theta) & g(\theta) \sin \theta \\ -g(\theta) \sin \theta & f(\theta) \end{pmatrix}$$

$$F(\theta'') = \begin{pmatrix} m_{11} & m_{12} \\ m_{21} & m_{22} \end{pmatrix}$$

$$F(\theta') = \begin{pmatrix} N_{11} & N_{12} \\ N_{21} & N_{22} \end{pmatrix}$$

where

$$m_{11} = m_{22} = f(\theta'')$$

$$m_{12} = g(\theta'') \sin \theta'' \cos \phi'' - i g(\theta'') \sin \theta'' \sin \phi''$$

$$m_{21} = -g(\theta'') \sin \theta'' \cos \phi'' - i g(\theta'') \sin \theta'' \sin \phi''$$

$$N_{11} = f(\theta') - i g(\theta') \sin \theta \sin \theta'' \sin \phi''$$

(4.1.26)

$$N_{12} = -g(\theta')(\sin\theta''\cos\theta\cos\phi'' - \sin\theta\cos\theta'') + i g(\theta')\cos\theta\sin\theta''\sin\phi'' \quad (4.1.27)$$

$$N_{21} = g(\theta')(\sin\theta''\cos\theta\cos\phi'' - \sin\theta\cos\theta'') + i g(\theta')\cos\theta\sin\theta''\sin\phi'' \quad (4.1.28)$$

$$N_{22} = f(\theta') + i g(\theta')\sin\theta\sin\theta''\sin\phi'' \quad (4.1.29)$$

The unitarity equation (4.1.3) becomes

$$\begin{aligned} & -i[(f(\theta) - f^*(\theta)) + i(g(\theta) - g^*(\theta))\vec{\sigma} \cdot (\vec{n}_i \times \vec{n}_f)] \\ &= \frac{q_{C.M.}}{2\pi} \int d\vec{n} [f^*(\theta'') + i g^*(\theta'')\vec{\sigma} \cdot (\vec{n}_i \times \vec{n})] \\ & \quad \times [f(\theta') + i g(\theta')\vec{\sigma} \cdot (\vec{n} \times \vec{n}_f)] \end{aligned} \quad (4.1.30)$$

Here we have used the facts

$$\vec{\sigma}^+ = \vec{\sigma}$$

$$\vec{n}_i \times \vec{n}_f \rightarrow \vec{n}_f \times \vec{n}_i = -(\vec{n}_i \times \vec{n}_f) \quad \text{when } T_{if} \rightarrow T_{fi}$$

$$\text{and } [i(\vec{n}_i \times \vec{n}_f) \cdot \vec{\sigma}]^+ = i(\vec{n}_i \times \vec{n}_f) \cdot \vec{\sigma}$$

then

$$\begin{aligned} \text{Im} & \begin{pmatrix} f(\theta) & g(\theta)\sin\theta \\ -g(\theta)\sin\theta & f(\theta) \end{pmatrix} \\ & = \frac{q_{C.M.}}{4\pi} \int d\vec{n} \begin{pmatrix} M_{11} & M_{12} \\ M_{21} & M_{22} \end{pmatrix} \begin{pmatrix} N_{11} & N_{12} \\ N_{21} & N_{22} \end{pmatrix} \quad (4.1.31) \end{aligned}$$

where N_{11} , N_{12} , N_{21} and N_{22} are defined in (4.1.26), (4.1.27), (4.1.28) and (4.1.29) respectively

$$M_{11}^* = M_{22}^* = f^*(\theta'') \quad (4.1.32)$$

$$M_{12}^* = g^*(\theta'') (\sin\theta''\cos\phi'' - i\sin\theta''\sin\phi'') \quad (4.1.33)$$

$$M_{21}^* = -g^*(\theta'') (\sin\theta''\cos\phi'' + i\sin\theta''\sin\phi'') \quad (4.1.34)$$

After some simplification (see appendix 5) we get two coupled equations:

$$\text{Im } f(\theta) = \frac{q_{C.M.}}{4\pi} \int dz'' d\psi'' [f^*(\theta'') f(\theta') + g^*(\theta'') g(\theta') (z'' - z' z'')] \quad (4.1.35)$$

$$\begin{aligned} \text{Im } g(\theta) \sin\theta &= \frac{q_{C.M.}}{4\pi} \int dz'' d\psi'' [f^*(\theta'') g(\theta') \frac{z'' - z z'}{\sqrt{1 - z^2}} \\ &+ f(\theta') g^*(\theta'') \frac{z' - z z''}{\sqrt{1 - z^2}} \\ &+ g^*(\theta'') g(\theta') \frac{1 - z^2 - z'^2 - z''^2 + 2zz'z''}{\sqrt{1 - z^2}}] \quad (4.1.36a) \end{aligned}$$

OR

$$\begin{aligned} \text{Im } g(\theta) = & \frac{q_{\text{C.M.}}}{4\pi} \int dz'' d\psi'' [f^*(\theta'')g(\theta') \frac{z'' - zz'}{1 - z^2} \\ & + f(\theta')g^*(\theta'') \frac{z' - zz''}{1 - z^2}] \\ & + g^*(\theta'')g(\theta') \frac{1 - z^2 - z'^2 - z''^2 + 2zz'z''}{1 - z^2} \quad (4.1.36b) \end{aligned}$$

For the forward scattering case $\theta' = \theta''$ and $z = 1$. Then (4.1.35) leads to the optical theorem

$$\text{Im } f(z) = \frac{q_{\text{C.M.}}}{4\pi} \sigma_{\text{Tot.}}$$

and both sides of the equation (4.1.36a) vanish.

In fact each of these coupled equations contains two equations since the right hand sides of the equations are in general the complex quantities. The real parts of these quantities should equal the left hand side and the imaginary parts should be zero. They are

$$\begin{aligned} \text{Im } f(z) = & \frac{q_{\text{C.M.}}}{4\pi} \int dz'' d\psi'' [|f(z'')| |f(z')| \cos[\phi_f(z') - \phi_f(z'')] \\ & + |g(z'')| |g(z')| (z - z' z'') \cos[\phi_g(z') - \phi_g(z'')]] \quad (4.1.37a) \end{aligned}$$

$$\begin{aligned}
 \text{Im } g(z) = & \frac{q_{\text{C.M.}}}{4\pi} \int dz'' d\psi'' \{ |f(z'')| |g(z')| \frac{z'' - zz'}{1 - z^2} \\
 & \times \cos[\phi_g(z') - \phi_f(z'')] \\
 & + |f(z')| |g(z'')| \frac{z' - zz''}{1 - z^2} \cos[\phi_f(z') - \phi_g(z'')] \\
 & + |g(z'')| |g(z')| \frac{1 - z^2 - z'^2 - z''^2 + 2zz'z''}{1 - z^2} \\
 & \times \cos[\phi_g(z') - \phi_g(z'')] \} \quad (4.1.37b)
 \end{aligned}$$

$$\begin{aligned}
 0 = & \frac{q_{\text{C.M.}}}{4\pi} \int dz'' d\psi'' \{ |f(z'')| |f(z')| \sin[\phi_f(z') - \phi_f(z'')] \\
 & + |g(z'')| |g(z')| (z - z'z'') \sin[\phi_g(z') - \phi_g(z'')] \} \quad (4.1.38a)
 \end{aligned}$$

$$\begin{aligned}
 0 = & \frac{q_{\text{C.M.}}}{4\pi} \int dz'' d\psi'' \{ |f(z'')| |g(z')| \frac{z'' - zz'}{1 - z^2} \sin[\phi_g(z') - \phi_f(z'')] \\
 & + |f(z')| |g(z'')| \frac{z' - zz''}{1 - z^2} \sin[\phi_f(z') - \phi_g(z'')] \\
 & + |g(z')| |g(z'')| \frac{1 - z^2 - z'^2 - z''^2 + 2zz'z''}{1 - z^2} \\
 & \times \sin[\phi_g(z') - \phi_g(z'')] \} \quad (4.1.38b)
 \end{aligned}$$

where ϕ_f and ϕ_g are the phase of the spin non-flip amplitude and spin flip amplitude respectively.

We focus now on the equations (4.1.37a), and (4.1.37b). Unlike the scalar particle scattering the $|f|$ and $|g|$ in the integral equation

(4.1.37a) and (4.1.37b) cannot be written in terms of the differential cross section, polarization and their combination. We only have the bounds of them in terms of the differential cross section and polarization as in (3.2.15a) and (3.2.15b).

4.2 The Bound on the Imaginary Part of the Non-Spin Flip Amplitude.

We majorize the integral in the right hand side of equation (4.1.37a) in different ways.

a)

Consider first the unitarity equation (4.1.37a)

$$\text{Im } f(z) = \frac{q_{\text{C.M.}}}{4\pi} \int \int dz'' d\psi'' [f^*(z'')f(z') + (z - z'z'')g^*(z'')g(z')] \quad (4.1.37a)$$

We change the integral variables from z'' and ψ'' to z'' and z' and write the real part of right hand side

$$\begin{aligned} \text{Im } f(z) &= \frac{q_{\text{C.M.}}}{2\pi} \int \int dz'' dz' \frac{\theta(K)}{\sqrt{K}} (|f(z'')||f(z')|\cos[\phi_f(z')] \\ &\quad - \phi_f(z'')] + |g(z'')||g(z')|(z - z'z'')\cos[\phi_g(z')] \\ &\quad - \phi_g(z'')]) \end{aligned} \quad (4.2.1)$$

$\theta(K)$ ensures that the integration is over the ellipse defined by

$K = 0$ where $K = 1 - z^2 - z'^2 - z''^2 + 2zz'z''$. We use the relation

(2.2.15a); $|f|$, $|g|\sin\theta$ are bounded by $\sqrt{\frac{1}{2} D[1 + \sqrt{1 - P^2}]}$

$$|f|, |g|\sin\theta \leq \sqrt{\frac{1}{2} D(1 + \sqrt{1 - P^2})} \quad (2.2.15a)$$

We majorize

$$|f(z'')|, |f(z')|, |g(z'')|\sqrt{1 - z''^2} \text{ and } |g(z')|\sqrt{1 - z'^2}$$

by taking the largest value sup. of $\sqrt{\frac{1}{2} D(1 + \sqrt{1 - P^2})}$ in the entire angle region with the understanding that each term under the integral will be majorized by positive quantities:

$$\begin{aligned} \operatorname{Im} f(z) &\leq \frac{C.M.}{2\pi} \left[\frac{1}{2} D(1 + \sqrt{1 - P^2}) \right] \sup. \int \int dz'' dz' \frac{\theta(K)}{\sqrt{K}} \\ &\times \{ \cos[\phi_f(z') - \phi_f(z'')] + \frac{z - z' z''}{\sqrt{1 - z'^2} \sqrt{1 - z''^2}} \\ &\times \cos[\phi_g(z') - \phi_g(z'')] \} \end{aligned} \quad (4.2.2)$$

We note that the spin flip amplitude $g(z)$ appearing in the unitarity equation contains a $\sin\theta$ factor implicitly. This means that the differential cross section is expressed in terms of $|f|$ and $|g|$ as

$$D(z) = |f(z)|^2 + |g(z)|^2(1 - z^2)$$

The extremum of

$$\frac{z - z'z''}{\sqrt{1 - z'^2} \sqrt{1 - z''^2}} = \chi(z', z'') \quad (z = \text{fixed})$$

is on the ellipse (see Figure 8). The maximum value of χ is one when

$$z' = -z'' = \sqrt{\frac{1-z}{2}} \quad \text{and the minimum is minus one when } z' = z'' = \sqrt{\frac{1+z}{2}}.$$

(We remember $\sqrt{1+z}$ and $\sqrt{1-z}$ are the semi-axis of the ellipse.) For this case $|\chi|_{\max} = 1$. Majorizing now cosine terms by one, we find

$$\operatorname{Im} f(z) \leq \frac{q_{\text{C.M.}}}{2\pi} \left[\frac{1}{2} D(1 + \sqrt{1 - P^2}) \right] \sup_{\text{sup.}} \int \int dz'' dz' \frac{\theta(K)}{\sqrt{K}} \quad (4.2.3)$$

with $\frac{\theta(K)}{\sqrt{K}} = \frac{\pi}{2} \sum_{\ell=0}^{\infty} (2\ell + 1) P_{\ell}(z) P_{\ell}(z') P_{\ell}(z'')$

the integral becomes

$$\int \int dz'' dz' \frac{\theta(K)}{\sqrt{K}} = \int \frac{\pi}{2} \sum_{\ell=0}^{\infty} (2\ell + 1) \frac{2}{2\ell + 1} \delta_{\ell 0} P_{\ell}(z) P_{\ell}(z') dz' \\ = 2\pi$$

Hence

$$\operatorname{Im} f(z) \leq 2 q_{\text{C.M.}} \left[\frac{1}{2} D(1 + \sqrt{1 - P^2}) \right] \sup. \quad (4.2.4)$$

The noteworthy aspect of this result is the explicit $q_{\text{C.M.}}$ dependent as opposed to

$$\operatorname{Im} f(z) \leq \sqrt{D(z)} \quad \text{or} \quad \sqrt{\frac{1}{2} D(1 + \sqrt{1 - P^2})}$$

We also remark that the full experimental information is not used in the sense that the only piece of data used is the sup. of $\sqrt{\frac{1}{2} D(1 + \sqrt{1 - P^2})}$ in the entire angle region.

b)

We try to improve this bound by latter majorizations. Using only D and P cannot improve $|f|$ or $|g|$. Therefore, the implication is clear: we must improve the phase factors. There is the relation between sine of the relative phase α of f and g and the polarization

$$\frac{\sin \alpha}{P} \geq 1 \quad (3.2.29)$$

where

$$\alpha = \phi_f - \phi_g$$

Since $|f(z)|_{\max} = |g(z)|_{\max} \sin \theta$ we write now $\operatorname{Im} f(z)$ in the form

$$\operatorname{Im} f(z) \leq \frac{q_{C.M.}}{2\pi} \int \int dz'' dz' \frac{\theta(K)}{\sqrt{K}} |f(z')|_{\max} |f(z'')|_{\max}$$

$$\times [\cos(\Delta\alpha + \beta) + \frac{z - z' z''}{\sqrt{1 - z'^2} \sqrt{1 - z''^2}} \cos \beta] \quad (4.2.5)$$

where

$$\begin{aligned}\Delta\alpha &= [\phi_f(z') - \phi_g(z')] - [\phi_f(z'') - \phi_g(z'')] \\ &= \alpha(z') - \alpha(z'')\end{aligned}\quad (4.2.6)$$

$$\beta = \phi_g(z') - \phi_g(z'') \quad (4.2.7)$$

The largest value of

$$\frac{z - z'z''}{\sqrt{1 - z'^2} \sqrt{1 - z''^2}}$$

is one. The above majorization is justified only if each term in the bracket is positive. We now find the maximum of the bracket for a fixed $\Delta\alpha$ as a function of β .

Call

$$F(\beta) = |\cos(\Delta\alpha + \beta)| + |\cos \beta| \quad (4.2.8)$$

$$\frac{dF(\beta)}{d\beta} = 0$$

it means $-\sin(\Delta\alpha + \beta) \pm \sin \beta = 0$

gives

$$\tan \beta = \frac{\sin \Delta\alpha}{\pm 1 - \cos \Delta\alpha} \quad (4.2.9)$$

with this value of β , $F(\beta)$ becomes (Appendix 6)

$$F(\beta) = \sqrt{2(1 \pm \cos \Delta\alpha)} \quad (4.2.10a)$$

$F(\beta)$ will be larger of the two cases. It is

$$F(\beta) = \sqrt{2(1 + |\cos \Delta\alpha|)} \quad (4.2.10b)$$

If in relation (4.2.5)

$$\left| \frac{z - z'z''}{\sqrt{1 - z'^2} \sqrt{1 - z''^2}} \right| = a$$

is kept rather than majorized by 1, one has to find the maximum of an expression such as

$$|\cos(\Delta\alpha + \beta)| + a|\cos \beta|$$

where a is positive and less than one.

In this case further possibilities arise depending on whether a is larger or smaller than $|\cos \Delta\alpha|$. The result here is (see appendix 7).

$$|F(\beta)| = \sqrt{1 + a^2 + 2a|\cos \Delta\alpha|} \quad (4.2.11)$$

(4.2.10a) is the limit of (4.2.11) when a is one.

Now the imaginary part of f satisfies

$$\operatorname{Im} f(z) \leq \frac{q_{\text{C.M.}}}{2\pi} \iint dz'' dz' \frac{\theta(K)}{\sqrt{K}} |f(z')|_{\max} |f(z')|_{\max} \times \sqrt{1 + a^2 + 2a|\cos \Delta\alpha|} \quad (4.2.12)$$

We now write $\cos \Delta\alpha$ in the following form:

$$\cos(\alpha(z') - \alpha(z'')) = \cos \alpha(z') \cos \alpha(z'') + \sin \alpha(z') \sin \alpha(z'') \quad (4.2.13)$$

We would hope to use the inequality (3.2.9)

$$\frac{\sin \alpha}{P} \geq 1 \quad (3.2.9)$$

in the majorization of the expression (4.2.12). However, the inequality (3.2.9) is in opposite sense. That is, $|P|$ is not an upper bound for $|\sin \alpha|$ but a lower bound. Still there is information in the inequality (3.2.9) which can be used in the following manner.

First of all, (3.2.9) tells us that $\sin \alpha$ and P have the same sign. Hence a knowledge of experimental P gives us the sign of the second term in (4.2.13). When $\sin \alpha(z') \sin \alpha(z'')$ has the same sign as the first term for a pair of points z' , z'' we majorize $\cos \Delta\alpha$ by one.

When it has opposite sign we write (4.2.13) in the following form

$$\cos(\alpha(z') - \alpha(z'')) = \sqrt{1 - \sin^2 \alpha(z')} \sqrt{1 - \sin^2 \alpha(z'')} \\ - |\sin \alpha(z')| |\sin \alpha(z'')| \quad (4.2.14)$$

To determine the relative sign of the two terms in (4.2.13) one either needs the sign of the rotation parameter R since the inequality (3.2.21)

$$\frac{\cos \alpha}{R} \geq 1 \quad (3.2.21)$$

indicates that $\cos \alpha$ has the same sign as R, or cases where P = 1. Obviously we have to know where R (or $\cos \alpha$) changes its sign. From continuity arguments $\cos \alpha$ cannot change its sign unless $\sin \alpha = 1$. But at places where $\sin \alpha = 1$, P must be one as can be seen from (3.2.9).

We shall study the situation below more in detail. Let us consider (4.2.14), when its two terms have opposite signs. To majorize this we see that in the first term $\sin \alpha$ must be replaced by its smallest value. Similarly the second term must be made as small as possible. Thus we find

$$\cos \Delta\alpha \leq \sqrt{1 - P^2(z')} \sqrt{1 - P^2(z'')} - |P(z')| |P(z'')| \quad (4.2.15)$$

Here inequality (3.2.9) has been used in the form

$$|\sin \alpha| \geq |P|$$

30,46

Consider now a typical experimental polarization measurement 47,48,49 (Even though the references are for inelastic cases our purpose here is just the discussion on how the unitarity ellipse is divided into different sections. We will not use the inelastic data in our calculations.). Suppose the polarization changes sign twice at point x_1 and x_2 and equals -1 at x_3 . (Figure 10) (cases where P changes its sign less or more than twice are analyzed in a similar manner. See in particular the $K^- p$ and $\pi^- p$ data for the case where P changes its sign three times.)

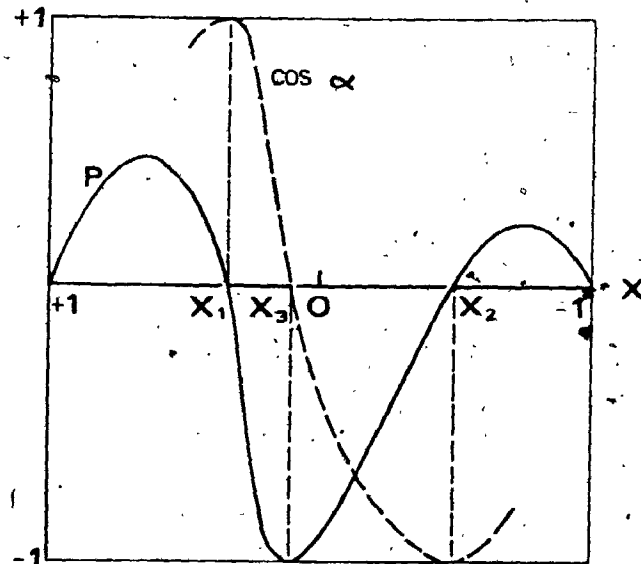


Figure 10. An example for the polarization curve and the behaviour of $\cos \alpha$.

Since we are interested only in the sign of $\cos \alpha(z') \cos \alpha(z'')$ it does not matter which one of cosine is (+) or (-). For the sake of illustration we choose an arbitrary sign for it and draw $\cos \alpha$ as in Figure 10. (We are also not considering the case where $\cos \alpha$ may be

tangent to the Z-axis at the point where $\sin \alpha = \pm 1$.) Also it does not matter what the value of $\cos \alpha$ is in any region, as long as it does not change sign. $\cos \alpha$ cannot do this without making $\sin \alpha = \pm 1$. However, even though we can conclude from $|P| = 1$ that $|\sin \alpha| = 1$, the reverse is not true and we may lack information about such points where $|P| < 1$, $|\sin \alpha| = 1$ on whether $\cos \alpha$ changes sign or not. But even with this limited knowledge and possible experimental knowledge on the sign of R we can do the following.

Let us divide the unitarity ellipse with a knowledge of the zeros of the experimental polarization into the domains shown in Figure 11. Next we divide the same ellipse according to partial or complete knowledge of the zero of R (or $\cos \alpha$). We may not know the sign of all domains in this second case. But for the regions in which the signs are known we can combine Figure 11 with Figure 12 and find the domains in which the signs are opposite. In those domains we majorize $\cos \Delta\alpha$ by

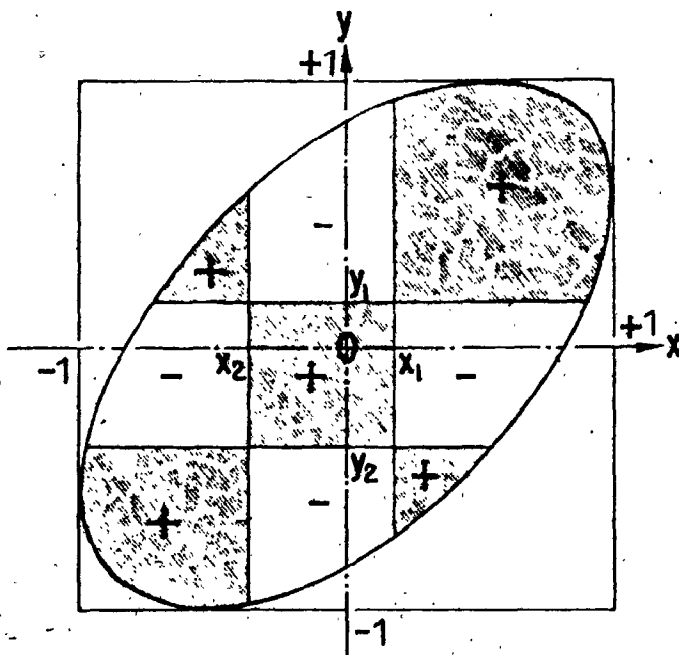


Figure 11. Separation of the unitarity ellipse into domains of different

signs for the term $\sin \alpha(y) \sin \alpha(x)$.

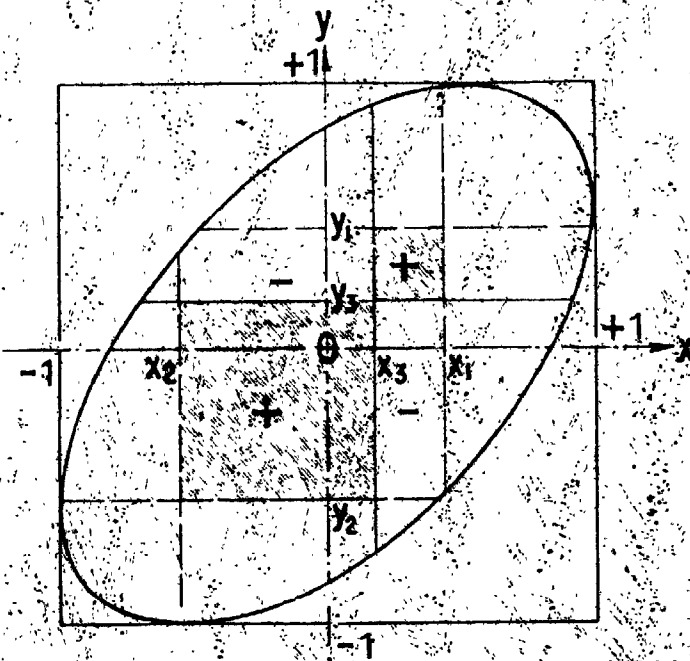


Figure 12. Separation of the unitarity ellipse into domains of different signs for the term $\cos \alpha(y) \cos \alpha(x)$.

(4.2.15); in all other domains we majorize it by one. The results depend on the values of P as well as on the size of the domains which are determined by the zeros of the polarization and $\cos \alpha$. Here Z plays the role of a fixed parameter and when Z is changed the shape of the ellipse as well as the size of the domains change.

Now we write the inequality (4.2.12) explicitly as

$$\text{Im } f(Z) \leq \frac{q_{\text{C.M.}}}{2\pi} \int \int dz' dz'' \frac{\theta(K)}{\sqrt{K}} \sqrt{\frac{1}{2} D(z') [1 + \sqrt{1 - P^2(z')}]} \\ \times \sqrt{\frac{1}{2} D(z'') [1 + \sqrt{1 - P^2(z'')}]} \sqrt{1 + a_z^2 + 2a_z \cos \Delta \alpha} \quad (4.2.16)$$

When we do the numerical calculation here it is understood that

$|\cos \Delta\alpha|$ is majorized by either one or expression (4.2.15) depending on whether the product of the signs in the domains of the unitarity ellipse (+) or (-)

c)

In the above majorization we consider $|f|$ and $|g|\sin \theta$ inside the integral individually. $|f|$ and $|g|\sin \theta$ are majorized by their upper bounds. In fact, $|f|$ and $|g|\sin \theta$ are not completely free. They have the relation

$$D = \frac{d\sigma}{d\Omega} = |f|^2 + |g|^2 \sin^2 \theta \quad (3.2.7)$$

They cannot reach their maximum values simultaneously. Under this constraint we majorize the function

$$F = |f(z')||f(z'')|\cos(\Delta\alpha + \beta) \cdot \frac{|z - z'z''|}{\sqrt{1 - z'^2}\sqrt{1 - z''^2}} \times |g(z')|\sin \theta |g(z'')|\sin \theta'' \cos \beta \quad (4.2.17)$$

first we replace $\cos(\Delta\alpha + \beta)$ and $\cos \beta$ by one and keep

$$\frac{|z - z'z''|}{\sqrt{1 - z'^2}\sqrt{1 - z''^2}} \leq 1$$

We define

$$x = |f(z')|/\sqrt{D}$$

$$y = |f(z'')|/\sqrt{E}$$

where $D = D(z')$ and $E = E(z'')$;

and the regions of x and y are

$$0 \leq x \leq 1$$

$$0 \leq y \leq 1$$

then

$$F = \sqrt{DE} [xy + a\sqrt{1-x^2}\sqrt{1-y^2}] \quad (4.2.18)$$

From appendix 8 we know this function has no local maximum or minimum point and it has only a saddle point in $x = 0$ and $y = 0$. Furthermore when we search the maximum of F with fixed y we find it is at

$$x = \sqrt{\frac{y^2}{y^2(1-a^2) + a^2}} \geq y \quad (4.2.19)$$

in our domain. So the maximum of F with fixed y is

$$\sqrt{DE} \sqrt{y^2(1-a^2) + a^2}$$

This function is an increasing function with respect to y . Its maximum is \sqrt{DE} at the end point $y = 1$. Hence

$$F_{\max} = \sqrt{DE} = \sqrt{D(Z')} \sqrt{D(Z'')} \quad (4.2.20)$$

with this result the inequality (4.2.16) is replaced by

$$\operatorname{Im} f(z) \leq \frac{q_{C.M.}}{2\pi} \int \int dz' dz'' \frac{\theta(K)}{\sqrt{K}} \sqrt{D(Z')} \sqrt{D(Z'')} \quad (4.2.21)$$

Similarly inequality (4.2.4) is improved by almost a factor of two

$$\operatorname{Im} f(z) \leq q_{C.M.} D_{\sup}. \quad (4.2.22)$$

However $|f|$ and $|g|\sin \theta$ are bounded by their upper and lower bounds (3.2.15a) and (3.2.15b). Hence we should maximize (4.2.17) subject to constraints

$$\sqrt{\frac{D}{2} [1 - \sqrt{1 - P^2}]} \leq |f|, \quad |g|\sin \theta \leq \sqrt{\frac{D}{2} [1 + \sqrt{1 - P^2}]}$$

We have shown that there is no local maximum and minimum in the range $0 \leq x \leq 1$ and $0 \leq y \leq 1$ as it is in the domain

$$x_L = \sqrt{\frac{1}{2} [1 - \sqrt{1 - P^2}]} \leq x \leq \sqrt{\frac{1}{2} [1 + \sqrt{1 - P^2}]} = x_u \quad (4.2.23)$$

$$y_L = \sqrt{\frac{1}{2} [1 - \sqrt{1 - P^2}]} \leq y \leq \sqrt{\frac{1}{2} [1 + \sqrt{1 - P^2}]} = y_u$$

Here $P = P(Z')$ $P' = P(Z'')$

Therefore, the largest value of F must be on the borders. It depends not only on \sqrt{D} and \sqrt{E} but on P and P' too.

Since the maximum of the function G

$$G = xy + a\sqrt{1 - x^2} \sqrt{1 - y^2} \quad (4.2.24)$$

with fixed y is at

$$x = \sqrt{\frac{y^2}{y^2(1 - a^2) + a^2}}$$

This curve is shown in Figure 13. (curve I).

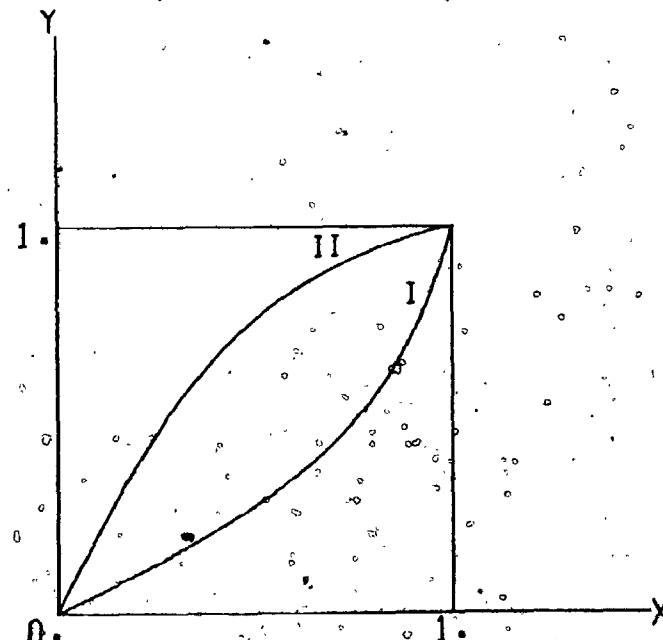


Figure 13. The curves for the maximum value of G (4.2.24) with fixed x and y respectively.

And the value is

$$y = \sqrt{x^2(1-a^2) + a^2}$$

This is an increasing function of y .

Because this function is symmetric with respect to x and y , the maximum point with fixed x is at

$$y = \sqrt{x^2(1-a^2) + a^2}$$

as shown in curve II of figure 13.

One can prove

$$\sqrt{y^2} \text{ and } \sqrt{x^2(1-a^2) + a^2}$$

Since $y^2(1-a^2) + a^2$ is an increasing function with respect to y ,

$$a^2 \leq y^2(1-a^2) + a^2 \leq 1$$

$$\text{Also } y^2(1-a^2) + a^2 = a^2(1-y^2) + y^2$$

is an increasing function with respect to a . Then

$$y^2 \leq a^2(1-y^2) + y^2 \leq 1$$

combining these results we find

$$y^2(1 - a^2) + a^2 \leq 1$$

Hence

$$\frac{y^2}{1-a^2} + a^2 = 1$$

Similarly

$$\frac{x^2}{1-a^2} + a^2 = 1$$

In our domain there is no local maximum and minimum then the largest value of F must be in the border. There are five cases. The discussion is following.

Case 1:

If $x_u < u$

$$\frac{y^2}{1-a^2} + a^2 = 1$$

(4.2.25)

as shown in figure 14.

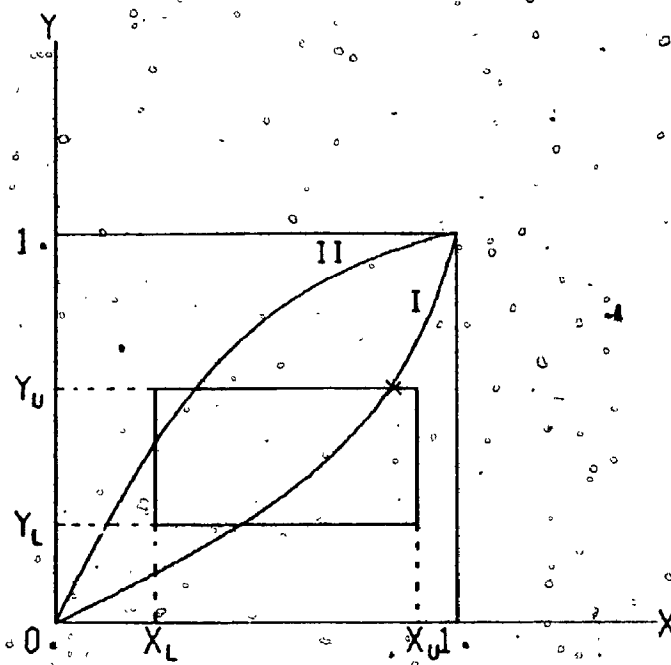


Figure 14. The maximum point of G (4.2.24) in case 1.

The largest value of G (equation (4.2.24)) should be the intersection of $y = y_u$ and the curve I of maximum point with fixed y (i.e. $x =$

$\sqrt{\frac{y_u^2}{y_u^2(1 - a^2) + a^2}}$, since the G is an increasing function.

Hence the maximum point is at

$$x = \sqrt{\frac{y_u^2}{y_u^2(1 - a^2) + a^2}} \quad \text{and} \quad y = y_u$$

and

$$\begin{aligned} G_{\max} &= y_u \sqrt{\frac{y_u^2}{y_u^2(1 - a^2) + a^2} + a \sqrt{1 - \frac{y_u^2}{y_u^2(1 - a^2) + a^2}}} \sqrt{1 - \frac{y_u^2}{y_u^2(1 - a^2) + a^2}} \\ &= \sqrt{y_u^2(1 - a^2) + a^2} \leq 1 \end{aligned}$$

then

$$F_{\max} = \sqrt{D + E} \sqrt{\frac{y_u^2(1 - a^2)}{1 - y_u^2(1 - a^2)} + a^2} \quad (4.2.26)$$

Case 2:

$$\sqrt{\frac{a^2 y_u^2}{1 - y_u^2(1 - a^2)}} < x_u < \sqrt{\frac{y_u^2}{y_u^2(1 - a^2) + a^2}} \quad (4.2.27)$$

as shown in figure 15.

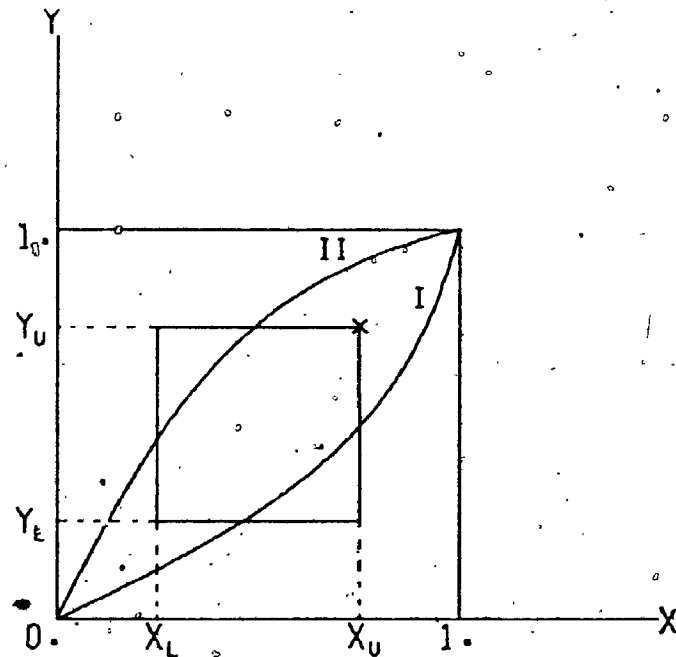


Figure 15. The maximum point of G (4.2.24) in case 2.

where curve I is

$$x = \sqrt{\frac{y^2}{y^2(1 - a^2) + a^2}}$$

and curve II is

$$y = \sqrt{\frac{x^2}{x^2(1-a^2) + a^2}} \quad \text{or} \quad x = \sqrt{\frac{a^2 y^2}{1-y^2(1-a^2)}}$$

It means the corner of x_u, y_u is between curves I and II. The largest value of G is at the corner $x = x_u$ and $y = y_u$ since on the line $x = x_u$ it is an increasing function from $y = 0$ to the point where it intersects the curve II. Also it is an increasing function on the line $y = y_u$ from $x = 0$ to the point where it intersects the curve I.

Hence

$$G_{\max} = x_u y_u + a \sqrt{1-x_u^2} \sqrt{1-y_u^2}$$

$$= x_u y_u + a x_L y_L \leq 1$$

then

$$F_{\max} = \sqrt{D+E} [x_u y_u + a x_L y_L] \quad (4.2.28)$$

Case 3:

$$x_L \geq \sqrt{\frac{y_u^2}{y_u^2(1-a^2) + a^2}} \quad (4.2.29)$$

as shown in figure 16.

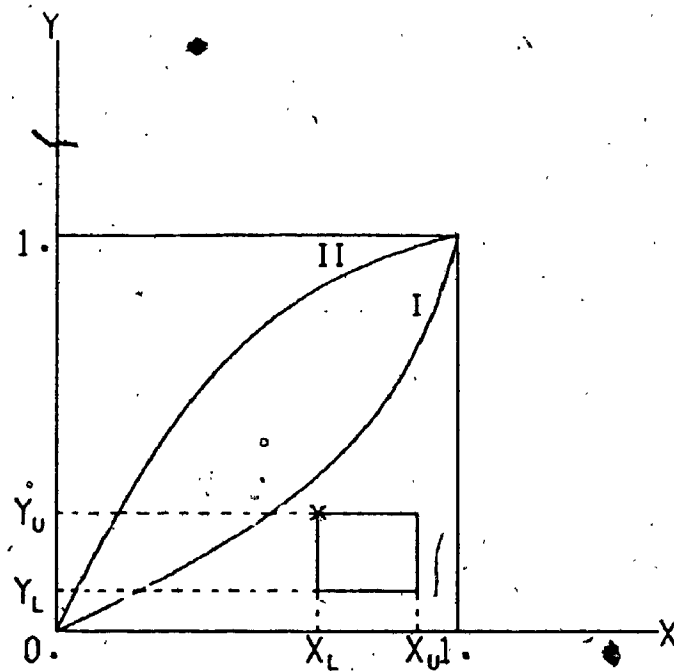


Figure 16. The maximum point of G (4.2.24) in case 3,

The largest value of G is at the left upper corner $x = x_L$ and $y = y_u$ since G is an increasing function on the line $x = x_L$ from $y = 0$ to the point where it intersects the curve II and a decreasing function on the line $y = y_u$ from the point of intersection with the curve I to $x = 1$.

Hence

$$\begin{aligned} G_{\max} &= x_L y_u + a \sqrt{1 - x_L^2} \sqrt{1 - y_u^2} \\ &= x_L y_u + a x_u y_L \end{aligned}$$

then

$$F_{\max} = \sqrt{D + E} [x_L y_u + a x_u y_L] \quad (4.2.30)$$

Case 4:

$$y_L \geq \sqrt{\frac{x_u^2}{x_u^2(1-a^2) + a^2}} \quad \text{or} \quad x_u \leq \sqrt{\frac{a^2 y_L^2}{1-y_L^2(1-a^2)}} \quad (4.2.31)$$

as shown in figure 17.

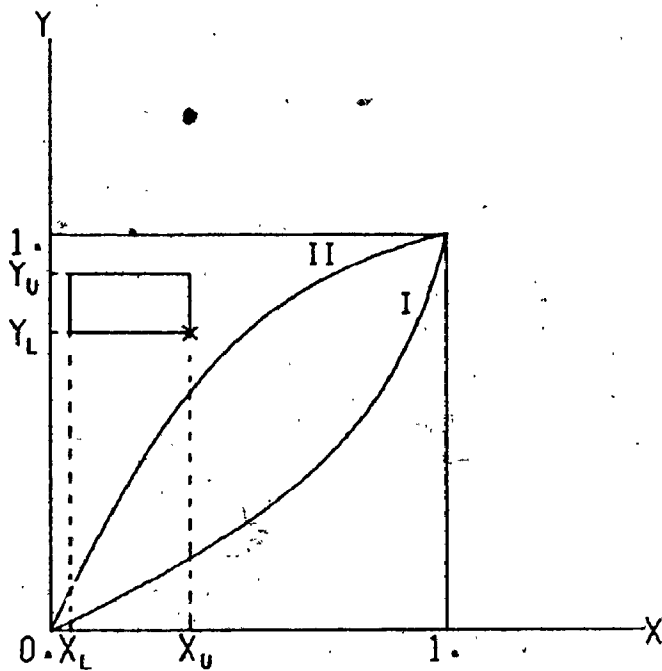


Figure 17. The maximum point of G (4.2.24) in case 4.

Since G is symmetric with respect to x and y, this case is similar to case 3. The largest value of G is at $x = x_u$ and $y = y_L$ and

$$G_{\max} = x_u y_L + a x_L y_u$$

then

$$F_{\max} = \sqrt{D \cdot E} (x_u y_L + a x_L y_u) \quad (4.2.32)$$

Case 5:

$$y_u \geq \sqrt{\frac{x_u^2}{x_u^2(1-a^2) + a^2}} > y_L \quad (4.2.33)$$

or

$$\sqrt{\frac{a^2 y_L^2}{1 - y_L^2(1 - a^2)}} < x_u \leq \sqrt{\frac{a^2 y_u^2}{1 - y_u^2(1 - a^2)}}$$

as shown in figure 18.

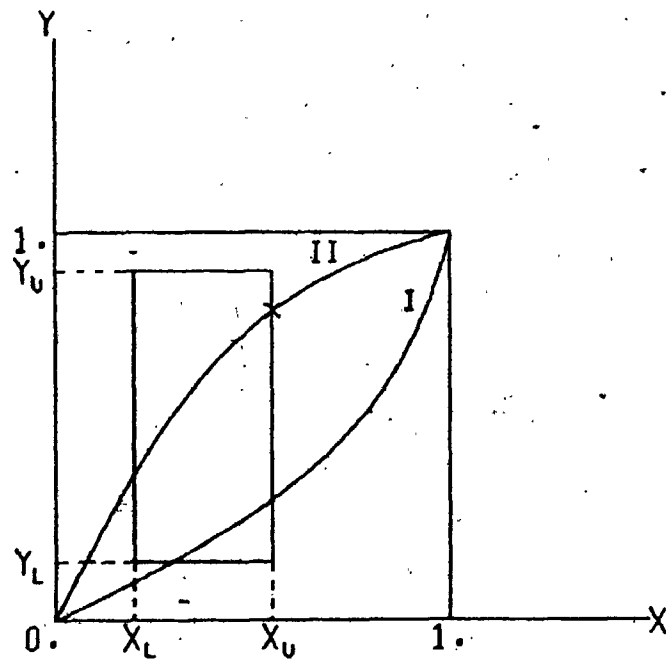


Figure 18. The maximum point of G (4.2.24) in case 5.

Again it is similar to case 1. The largest value of G is at $x = x_u$

and

$$y = \sqrt{\frac{x_u^2}{x_u^2(1-a^2) + a^2}}$$

Hence

$$G_{\max} = \sqrt{x_u^2(1 - a^2) + a^2}$$

then

$$F_{\max} = \sqrt{D + E} \sqrt{x_u^2(1 - a^2) + a^2} \quad (4.2.34)$$

4.3 The Bound on the Imaginary Part of the Spin-Flip Amplitude.

We now turn to the spin-flip amplitude. The elastic unitarity condition (4.1.37b) is

$$\begin{aligned} \text{Im } g(z) &= \frac{q_{\text{C.M.}}}{4\pi} \int \int dz'' d\psi'' \{ |f(z'')| |g(z')| \frac{z'' - zz'}{1 - z^2} \\ &\quad \times \cos[\phi_g(z') - \phi_f(z'')] + |f(z')| |g(z'')| \frac{z' - zz''}{1 - z^2} \\ &\quad \times \cos[\phi_f(z') - \phi_g(z'')] + |g(z')| |g(z'')| \\ &\quad \times \frac{1 - z^2 - z'^2 - z''^2 + 2zz'z''}{1 - z^2} \cos[\phi_g(z') - \phi_g(z'')] \} \end{aligned} \quad (4.1.17b)$$

Since we shall majorize $|f|$ and $|g|\sin\theta$ we write out the sin factors explicitly. We also change the integral variable from z'' and ψ'' to z' and z'' .

$$\text{Im } g(z) \sqrt{1 - z^2} = \frac{q_{\text{C.M.}}}{2\pi} \int \int dz'' dz' \frac{\theta(K)}{\sqrt{K}} \frac{1}{\sqrt{1 - z^2}}$$

$$\begin{aligned}
 & \times \left\{ \frac{K|g(z')|^2 |g(z'')| \sqrt{1-z'^2} \sqrt{1-z''^2}}{\sqrt{1-z'^2} \sqrt{1-z''^2}} \cos[\phi_g(z') - \phi_g(z'')] \right. \\
 & + (z' - zz'') \frac{|f(z')||g(z'')| \sqrt{1-z''^2}}{\sqrt{1-z'^2}} \cos[\phi_f(z') - \phi_g(z'')] \\
 & \left. + (z'' - zz') \frac{|f(z'')||g(z')| \sqrt{1-z'^2}}{\sqrt{1-z''^2}} \cos[\phi_g(z') - \phi_f(z'')] \right\} \quad (4.3.1)
 \end{aligned}$$

Defining again

$$\phi_f(z') - \phi_g(z') = \alpha(z') \quad \phi_g(z') - \phi_g(z'') = \beta(z', z'')$$

this becomes

$$\begin{aligned}
 \operatorname{Im} g(z) \sqrt{1-z^2} & \leq \frac{Q_{C.M.}}{2\pi} \int \int dz' dz'' \frac{\theta(K)}{\sqrt{K}} \frac{1}{\sqrt{1-z^2}} \\
 & \times \sqrt{D(z')[1 + 1 - P^2(z')]} \sqrt{D(z'')[1 + 1 - P^2(z'')]} \quad (4.3.2)
 \end{aligned}$$

where

$$A = \frac{K|\cos \beta|}{\sqrt{1-z'^2} \sqrt{1-z''^2}} + \left[\frac{|z'' - zz'|}{\sqrt{1-z'^2}} |\cos(\beta - \alpha(z''))| \right]$$

$$+ \frac{|z' - zz''|}{\sqrt{1 - z''^2}} |\cos(\alpha(z') + \beta)| \quad (4.3.3)$$

The moduli of the amplitudes are majorized and taken outside of the bracket with the understanding that the multiplying factors will be majorized by positive quantities.

We can combine the second and third terms of (4.3.3) as twice of either one of them because of the symmetry of the integrand with respect to z' and z'' in the second and third terms of (4.3.1) and the symmetry of the area of the integral range with respect to z' and z'' (unitarity ellipse). Thus we obtain

$$\begin{aligned} A &= \frac{K}{\sqrt{1 - z'^2} \sqrt{1 - z''^2}} |\cos \beta(z', z'')| \\ &+ 2 \frac{|z' - zz''|}{\sqrt{1 - z''^2}} |\cos(\beta(z', z'') - \alpha(z'))| \end{aligned} \quad (4.3.4)$$

Majorizing the cosine by one we have

$$A = \frac{K}{\sqrt{1 - z'^2} \sqrt{1 - z''^2}} + 2 \frac{|z' - zz''|}{\sqrt{1 - z''^2}} \quad (4.3.5)$$

We now apply the consideration used for the non-spin flip amplitude also to $g(z)\sqrt{1 - z^2}$; namely the $|f|$ and $|g|\sqrt{1 - z^2}$ cannot have their maximum simultaneously. Keeping the symmetry of the second and third terms the integrand of (4.3.1) becomes

$$\begin{aligned}
 F = & \frac{K}{\sqrt{1 - z'^2} \sqrt{1 - z''^2}} |g(z')| \sqrt{1 - z'^2} |g(z'')| \sqrt{1 - z''^2} \\
 & \times \cos[\phi_g(z') - \phi_g(z'')] + 2 \frac{|z' - zz''|}{\sqrt{1 - z''^2}} \\
 & \times |f(z')| |g(z'')| \sqrt{1 - z''^2} \cos[\phi_g(z') - \phi_f(z'')] \quad (4.3.6)
 \end{aligned}$$

we define as before

$$|f(z')| = \sqrt{Dx} \quad \text{then} \quad |g(z')| \sqrt{1 - z'^2} = \sqrt{D} \sqrt{1 - x^2}$$

$$|f(z'')| = \sqrt{Ey} \quad \text{then} \quad |g(z'')| \sqrt{1 - z''^2} = \sqrt{E} \sqrt{1 - y^2}$$

$$\text{and } D = D(z')$$

$$E = D(z'')$$

also we define

$$a' = \frac{K}{\sqrt{1 - z'^2} \sqrt{1 - z''^2}}$$

$$a'' = 2 \frac{|z' - zz''|}{\sqrt{1 - z''^2}}$$

we replace cosines by one. Then

$$F = \sqrt{DE} [a' \sqrt{1 - x^2} \sqrt{1 - y^2} + a'' x \sqrt{1 - y^2}] \quad (4.3.7)$$

We now consider

$$G = a' \sqrt{1 - x^2} \sqrt{1 - y^2} + a'' x \sqrt{1 - y^2} \quad (4.3.8)$$

where $0 \leq x \leq 1$ and $0 \leq y \leq 1$

We majorized the function G

$$\frac{\partial G}{\partial x} = \sqrt{1 - y^2} \left[-\frac{a'x}{1 - x^2} + a'' \right]$$

Solve

$$\frac{\partial G}{\partial x} = 0$$

for x then the solution is

$$x = \sqrt{\frac{a''^2}{a'^2 + a''^2}} = x_0$$

$$\frac{\partial^2 G}{\partial x^2} = -a'(1 - y^2)^{\frac{1}{2}}(1 - x^2)^{-\frac{3}{2}} < 0$$

This means $x = x_0$ is the line on which the function G is maximum (with fixed y).

Also

$$\frac{\partial G}{\partial y} = [a' \sqrt{1 - x^2} + a'' x] \frac{-y}{1 - y^2}$$

solve

$$\frac{\partial G}{\partial y} = 0$$

for y then $y = 0$ is the solution

$$\frac{\partial^2 G}{\partial y^2} = -[a' \sqrt{1-x^2} + a''x] \frac{1}{(1-y^2)^{3/2}} < 0$$

Again $y = 0$ is the line on which G is a maximum (with fixed x).

Calculate

$$\frac{\partial^2 G}{\partial x \partial y} = \left[-\frac{a'x_0}{\sqrt{1-x_0^2}} + a'' \right] \frac{-y}{\sqrt{1-y^2}}$$

Since

$$\frac{\partial^2 G}{\partial x^2} = \frac{\partial^2 G}{\partial y^2} = \left(\frac{\partial^2 G}{\partial x \partial y} \right)_x = x_0 = \frac{(a'^2 + a''^2)^2}{a'^2} > 0$$

So there is a relative maximum at $x = x_0$, $y = 0$. Actually this point is the absolute maximum point for G . It can be seen in Figure 19.

Curve I is the line on which G is maximum with fixed y value. Curve II is the line on which G is maximum with fixed x . Here $x_0 = \sqrt{\frac{a'^2}{a'^2 + a''^2}}$

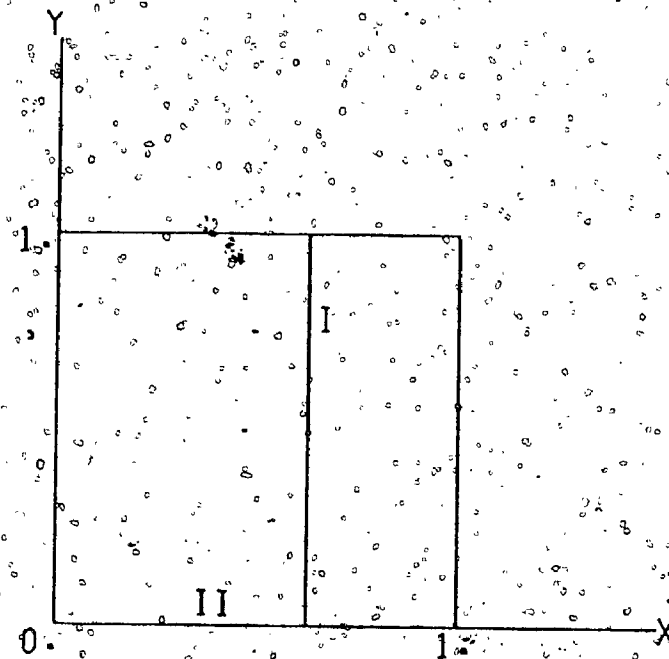


Figure 19. The curves for the maximum value of G (4.3.8) with fixed x and y respectively.

The largest value of G is

$$G_{\max} = \sqrt{a'^2 + a''^2} \quad (4.3.9)$$

when

$$x = x_0 = \frac{a''^2}{a'^2 + a''^2} \quad \text{and} \quad y = 0$$

Since $|f(z)|$ and $|g(z)|\sqrt{1-z^2}$ are bounded by their upper and lower bounds. Then

$$x_L \leq x \leq x_U$$

$$y_L \leq y \leq y_u$$

where

$$x_u = \sqrt{\frac{1}{2} [1 + \sqrt{1 - p^2}]}$$

$$x_L = \sqrt{\frac{1}{2} [1 - \sqrt{1 - p^2}]}$$

$$y_u = \sqrt{\frac{1}{2} [1 + \sqrt{1 - p'^2}]}$$

$$y_L = \sqrt{\frac{1}{2} [1 - \sqrt{1 - p'^2}]}$$

p and p' are defined as before $p = P(z')$ and $p' = P(z'')$. We discuss the largest value of G in different cases.

Case 1:

$$x_u \geq \sqrt{\frac{a''^2}{a''^2 + a'^2}} = x_0 \quad \text{and} \quad x_L \leq \sqrt{\frac{a''^2}{a''^2 + a'^2}} = x_0$$

as shown in figure 20.

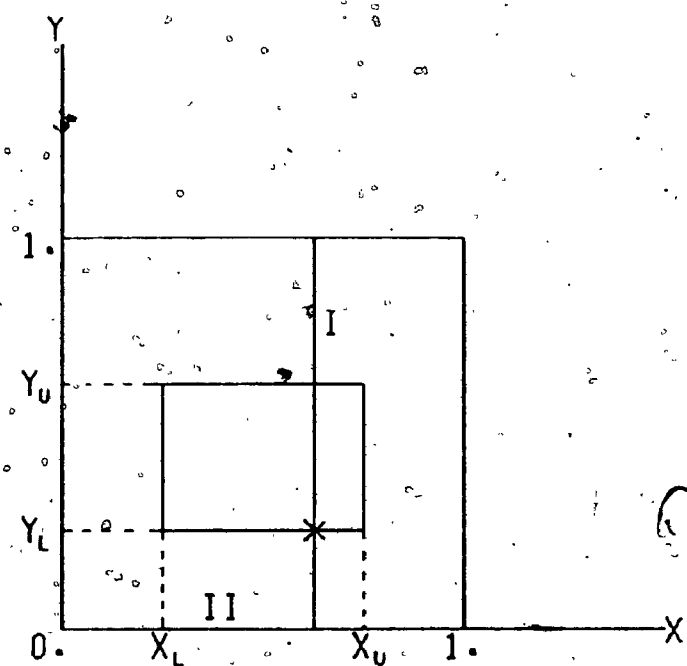


Figure 20. The maximum point of G (4.3.8) in case 1.

The largest value of G is at $x = x_0$ and $y = y_L$

$$G_{\max} = \sqrt{D + a''^2} y_u$$

and

$$F_{\max} = \sqrt{D + E} \sqrt{a'^2 + a''^2} y_u \quad (4.3.10)$$

Case 2:

$$x_L \geq x_0$$

as shown in figure 21.

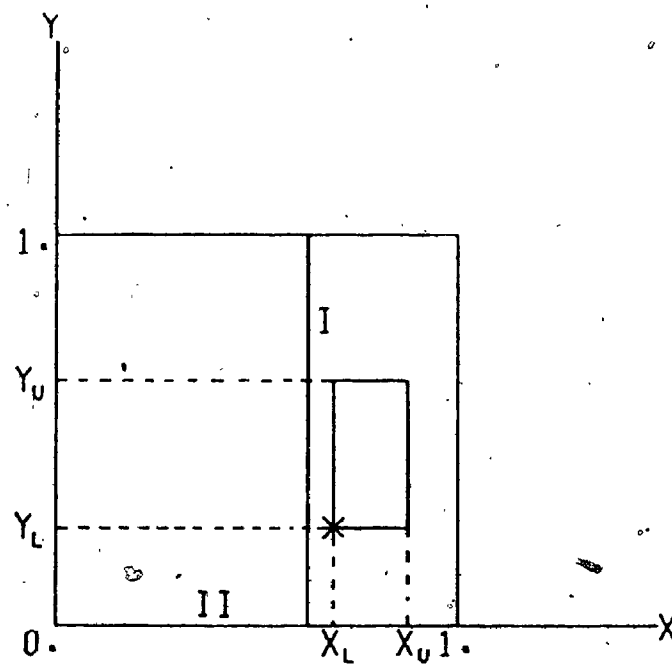


Figure 21. The maximum point of G (4.3.8) in case 2.

The maximum point is at the left lower corner $x = x_L$ and $y = y_L$.

$$\begin{aligned} G_{\max} &= a' \sqrt{1 - x_L^2} \sqrt{1 - y_L^2} + a'' x_L \sqrt{1 - y_L^2} \\ &= a' x_u y_u + a'' x_L y_L \end{aligned}$$

and

$$F_{\max} = \sqrt{D + E} [a' x_u y_u + a'' x_L y_L] \quad (4.3.11)$$

Case 3:

$$x_u \leq x_0$$

as shown in figure 22.

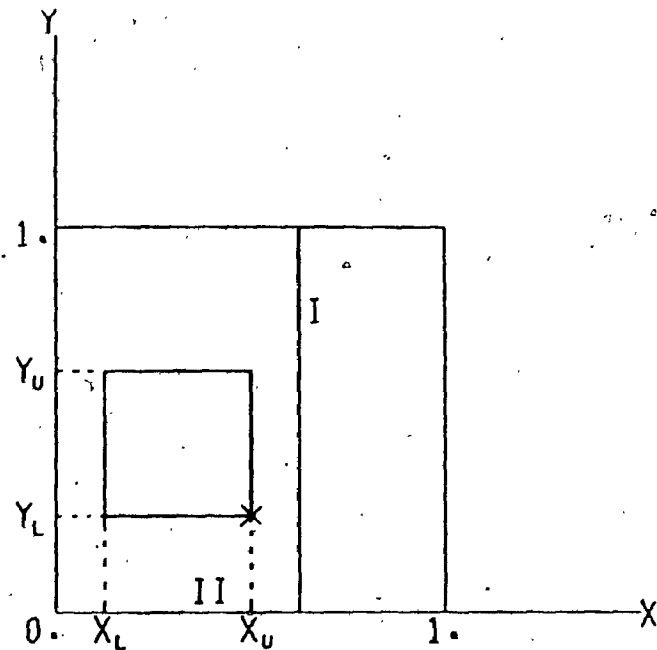


Figure 22. The maximum point of G (4.3.8) in case 3.

The maximum point is at the right lower corner $x = x_u$ and $y = y_L$.

Hence

$$\begin{aligned} G_{\max} &= a' \sqrt{1 - x_u^2} \sqrt{1 - y_L^2} + a'' x_u \sqrt{1 - y_L^2} \\ &= a' x_L y_u + a'' x_u y_u \end{aligned}$$

then

$$F_{\max} = \sqrt{D \cdot E} [a' x_L y_u + a'' x_u y_u] \quad (4.3.12)$$

In order to compare these results with (4.3.2) and (4.3.5) we write the integrand of (4.3.2) with (4.3.5) in the following form

$$F = \sqrt{D \cdot E} [a' x_u y_u + a'' x_u y_u] \quad (4.3.13)$$

There is no doubt the results in case 2 and case 3, (4.3.11) and (4.3.12) are better than (4.3.13). But it is not clear about which one is better than case 1.

On the other hand the second and third terms of the expression (4.3.3) are symmetric with respect to Z' and Z'' . This can be seen from

$$\beta(Z', Z'') = \phi_g(Z') - \phi_g(Z'') = -\beta(Z'', Z')$$

and

$$\cos[-\beta(Z'Z'') - \alpha(Z')] = \cos[\beta(Z', Z'') + \alpha(Z')]$$

Thus an interchange $Z' \leftrightarrow Z''$ takes the second term of (4.3.3) to the third term and third term to second term. Let us call the second and third terms of (4.3.3) $\xi(Z', Z'')$. Since $\xi(Z', Z'')$ is symmetric in Z' and Z'' its extremum is at $Z' = Z''$

$$\begin{aligned} \xi(Z', Z') &= \frac{|Z' - ZZ'|}{\sqrt{1 - Z'^2}} |\cos[\beta(Z', Z') - \alpha(Z')]| \\ &\quad + \frac{|Z' - ZZ'|}{\sqrt{1 - Z'^2}} |\cos[\alpha(Z') + \beta(Z', Z')]| \end{aligned} \quad (4.3.14)$$

Because $\beta(Z', Z') = 0$ and cosine function is an even function we find

$$\xi = 2 \frac{|z'|}{\sqrt{1 - z'^2}} (1 - z) |\cos \alpha(z')| \quad (4.3.15)$$

We can find that the largest value of

$$\frac{|z'|}{\sqrt{1 - z'^2}}$$

is on or in the unitarity ellipse (for the time being $\cos \alpha(z')$ is majorized by one). As a larger z' increases the numerator and decreases the denominator, z' must be as large as possible, consistent with the condition to be in or on the ellipse. Since at the largest value $z' = z''$ it must be on the ellipse. Hence

$$1 - z^2 - z'^2 - z''^2 + 2zz'z'' = 0$$

when $z' = z''$ then it is

$$1 - z^2 - zz'^2 + 2zz'^2 = 0$$

It gives

$$z' = \pm \sqrt{\frac{1+z}{2}}$$

and

$$\frac{|z'|}{\sqrt{1 - z'^2}} = \sqrt{\frac{1+z}{1-z}}$$

$$\xi_{\max} = 2 \sqrt{1 - z^2} \quad (4.3.16)$$

Again except for the reasons of simplicity we do not have to use the largest value of $z' \sqrt{1 - z'^2}$ since it can be explicitly evaluated.

The bound (4.3.16) can be improved if we replace in relation

(4.3.15)

$$\cos \alpha(z') = \sqrt{1 - \sin^2 \alpha(z')}$$

and majorize this by

$$\cos \alpha(z') \leq \sqrt{1 - P^2(z')}$$

Then A becomes

$$A = \frac{K}{\sqrt{1 - z'^2} \sqrt{1 - z''^2}} + 2 \frac{|z'|}{\sqrt{1 - z'^2}} (1 - z) \sqrt{1 - P^2(z')} \quad (4.3.17)$$

When integrating inequality (4.3.2) with (4.3.17) we should remember that the largest value of $|z'|$ is $\sqrt{(1+z)/2}$. Hence for

$$\sqrt{\frac{1+z}{2}} \leq z' \leq 1 \quad \text{and} \quad -\sqrt{\frac{1+z}{2}} \geq z' \geq -1$$

We should take $P(z') = 0$.

4.4 The Numerical Calculation in πp and $K^+ p$ Scattering Processes.

A)

In relation (4.2.22) q is the centre-of-mass projectile momentum in $\text{mb}^{-\frac{1}{2}}$. The conversion from Mev/c is achieved by multiplying the momentum with .0016

$$q(\text{mb}^{-\frac{1}{2}}) = 0.0016 q(\text{Mev}/c)$$

As an example we take π^+ data at $q_{\text{C.M.}} = 91.4 \text{ Mev}/c$ (Ref. 47 and 48). With negligible polarization at this energy and $D_{\text{sup.}} = 1.56 \text{ mb}$ relation (4.2.22) gives

$$q_{\text{C.M.}}^{-\frac{1}{2}} = .0016 \times 91.4 = 0.146 \text{ mb}^{-\frac{1}{2}}$$

$$\text{Im } f(z) \leq .146 \times 1.58 = .231 \text{ mb}^{-\frac{1}{2}}$$

This compares with $\text{Im } f(z) \leq \sqrt{D(z)}$ as given by the following examples.

$$\text{At } z = -.9062 \quad D = 1.58 \text{ mb} \quad \sqrt{D} = 1.257 \text{ mb}^{-\frac{1}{2}}$$

$$z = -.5446 \quad D = 1.13 \text{ mb} \quad \sqrt{D} = 1.063 \text{ mb}^{-\frac{1}{2}}$$

$$z = .6018 \quad D = 1.30 \text{ mb} \quad \sqrt{D} = .361 \text{ mb}^{-\frac{1}{2}}$$

We see that at this energy the bound (4.2.22) is better than \sqrt{D} even for the smallest differential cross section. The goodness of inequality (4.2.22) depends on the test

$$q D_{\text{sup}} \leq \sqrt{D(z)}$$

$$\text{or } q \leq \frac{\sqrt{D(z)}}{D_{\text{sup}}}$$

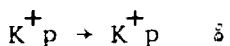
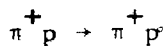
which is satisfied at 91.4 Mev/c.

B)

For $\text{Im } f(z)$ we evaluated both (4.2.16) and (4.2.21). In calculating (4.2.16) $|\cos \Delta\alpha|$ is majorized by either one or expression (4.2.15). As it turns out (4.2.21) is better than (4.2.16). We also calculated the right hand side of the unitarity inequality with the integrand F (4.2.25), (4.2.27), (4.2.29), (4.2.31) and (4.2.33) in different cases. It shows that the improvement is not much since the polarization is small in most of our cases, (less than .4). But from the relations indicate that much better results can be obtained when the polarization is large.

For $\text{Im } g(z) \sin \theta$ we used the inequality (4.3.2) with (4.3.5) and (4.3.17). Also we calculated the right hand side of relation with the integral F (4.3.10), (4.3.11) and (4.3.12) in different cases. We can see this improvement is much better than the relation (4.3.2) with (4.3.5).

All these inequalities are tested for the processes



below the inelastic threshold. In evaluation of these integrals the computer Cyber 73 of the University of Western Ontario was used. We choose the Gauss-Legendre method to calculate these integrals since these integrands are smooth functions. For $\pi^+ p$ and $\pi^- p$ the data were taken from phase shifts of Almehed and Lovelace⁴⁹. For $K^+ p$ the data were taken from the α phase shifts of Albrow et al.³⁹. In fact in our calculations the only necessary input are the differential cross sections and polarizations in the entire scattering region. The use of the phase shifts is for convenience only. The unitarity condition is given for pure isospin states. For $\pi^- p$ case we form the proper combination of the different isospin states. In general the lower the energy the better are our bounds as compared to \sqrt{D} on the upper bound of $|f|$ and $|g| \sin \theta$. But when energy increases the results are not as good as at lower energies. The bound at some scattering angles are larger than \sqrt{D} . In the $\pi^+ p$ and $\pi^- p$ cases our bound for $\text{Im } f$ and $\text{Im } g \sin \theta$ in the entire scattering region are better than \sqrt{D} up to the $P_{\text{lab.}} = .14 \text{ Gev/c}$ (halfway to inelastic threshold). Near the inelastic threshold the bounds of $\text{Im } g \sin \theta$ are better than \sqrt{D} only in the forward direction. The results are shown in tables 2 and 3. In the $K^+ p$ case all our bounds

for the $\text{Im } f$ and $\text{Im } g \sin \theta$ are better than \sqrt{D} in the entire angle region below the inelastic threshold. We present all our results below the inelastic threshold in table 4.

Also we compare our bounds with the imaginary parts of non-spin-flip and spin flip amplitudes constructed from phase shifts directly in the typical cases. These comparisons are included in the tables 2.4, 2.7, 3.4, 3.7 and 4.7.

TABLE 2.1 PIP PLUS-P SCATTERING
 $P_{LAB} = .0800 \text{ GEV/C}$ $PCM = .0680 \text{ GEV/C}$

SF	SFIP	SDCS	UF	SG1	SGIP	SG2
.90	.024	.102	.100	.036	.032	.017
.80	.024	.134	.132	.037	.032	.022
.70	.023	.168	.167	.037	.032	.025
.60	.023	.204	.203	.037	.032	.028
.50	.022	.22	.241	.037	.031	.029
.40	.022	.22	.279	.037	.031	.030
.30	.021	.021	.317	.036	.031	.031
.20	.021	.021	.355	.036	.030	.032
.10	.020	.020	.393	.035	.029	.032
.00	.020	.020	.431	.034	.029	.032
-.10	.019	.019	.469	.033	.028	.032
-.20	.019	.019	.507	.032	.027	.032
-.30	.018	.018	.545	.031	.026	.032
-.40	.018	.018	.584	.030	.025	.032
-.50	.017	.017	.622	.029	.025	.031
-.60	.017	.017	.660	.028	.024	.031
-.70	.016	.016	.698	.026	.023	.030
-.80	.016	.016	.736	.025	.021	.030
-.90	.015	.015	.775	.023	.020	.030

2. -COSINE OF THE SCATTERING ANGLE:

SF - THE RIGHT HAND SIDE OF EQ. (4.2.21).

SFIP - THE RIGHT HAND SIDE OF EQ. (4.2.1) WITH THE INTEGRAND (4.2.17) MAJORIZED BY (4.2.25), (4.2.27), (4.2.29), (4.2.31) AND (4.2.33) FOR DIFFERENT CASES.

SDCS - SQUARE ROOT OF THE DIFFERENTIAL CROSS SECTION.

UF - THE UPPER BOUND OF THE MODULI OF THE SPIN-NON-FLIP AMPLITUDE CALCULATED FROM EQ. (3.2.15A).

SG1 - THE RIGHT HAND SIDE OF EQ. (4.3.2) WITH (4.3.5).

SG2 - THE RIGHT HAND SIDE OF EQ. (4.3.2) WITH (4.3.17).

SGIP - THE RIGHT HAND SIDE OF EQ. (4.3.1) WITH THE INTEGRAND (4.3.6) MAJORIZED BY (4.3.10), (4.3.11) AND (4.3.12) FOR DIFFERENT CASES.

TABLE 2.2 PIPLUS-P SCATTERING
 $P_{LAB} = 1000 \text{ GEV}/c$ $PCM_0 = .0850 \text{ GEV}/c$

Z	SFIP	SDCS	UF	SGI	SGIP	SG2
.90	.057	.185	.179	.083	.074	.038
.80	.056	.231	.225	.086	.075	.050
.70	.055	.277	.272	.087	.075	.058
.60	.054	.323	.320	.088	.075	.064
.50	.053	.370	.367	.088	.074	.068
.40	.052	.452	.416	.087	.074	.071
.30	.051	.463	.461	.087	.073	.073
.20	.050	.505	.510	.085	.072	.075
.10	.049	.649	.556	.084	.070	.077
.00	.048	.648	.603	.083	.069	.078
.10	.047	.647	.649	.081	.068	.078
.20	.046	.646	.696	.079	.066	.079
.30	.045	.645	.743	.077	.065	.079
.40	.044	.644	.789	.074	.063	.078
.50	.043	.643	.836	.072	.061	.078
.60	.042	.642	.882	.069	.059	.078
.70	.041	.641	.929	.066	.057	.077
.80	.041	.640	.975	.062	.055	.077
.90	.040	.639	1.022	.058	.052	.076

Z - COSINE OF THE SCATTERING ANGLE.

SF - THE RIGHT HAND SIDE OF EQ. (4.2.21).

SFIP - THE RIGHT-HAND SIDE OF EQ. (4.2.1) WITH THE INTEGRAND (4.2.17) MAJORIZED BY (4.2.25), (4.2.27), (4.2.29), (4.2.31) AND (4.2.33) FOR DIFFERENT CASES.

SDCS - SQUARE ROOT OF THE DIFFERENTIAL CROSS SECTION.

UF - THE UPPER BOUND OF THE MODULI OF THE SPIN-NON-FLIP AMPLITUDE CALCULATED FROM EQ. (3.2.15A).

SG1 - THE RIGHT HAND SIDE OF EQ. (4.3.2) WITH (4.3.5).

SG2 - THE RIGHT HAND SIDE OF EQ. (4.3.2) WITH (4.3.17).

SGIP - THE RIGHT HAND SIDE OF EQ. (4.3.1) WITH THE INTEGRAND (4.3.6) MAJORIZED BY (4.3.10), (4.3.11) AND (4.3.12) FOR DIFFERENT CASES.

TABLE 2.3 PIP PLUS-P SCATTERING
 $P_{LAB} = 1150 \text{ GEV/C}$ $P_{CM} = 9700 \text{ GEV/C}$

Z	SF	SFIP	SDCS	UF	SG1	SG2
.90	.010	.010	.040	.039	.015	.007
.80	.010	.010	.040	.039	.015	.009
.70	.010	.010	.041	.041	.016	.011
.60	.010	.010	.044	.043	.016	.012
.50	.009	.010	.047	.047	.016	.012
.40	.009	.009	.051	.051	.016	.013
.30	.009	.009	.056	.056	.016	.013
.20	.009	.009	.061	.061	.016	.013
.10	.009	.009	.066	.066	.015	.013
.00	.009	.009	.072	.072	.015	.013
-.10	.009	.009	.078	.078	.015	.014
-.20	.009	.009	.084	.084	.015	.015
-.30	.008	.008	.090	.090	.014	.015
-.40	.008	.008	.096	.096	.014	.015
-.50	.008	.008	.103	.103	.014	.012
-.60	.008	.008	.109	.109	.013	.011
-.70	.008	.008	.116	.115	.013	.011
-.80	.008	.008	.122	.122	.012	.011
-.90	.008	.008	.129	.129	.011	.010

2. -COSINE OF THE SCATTERING ANGLE:

SF -THE RIGHT HAND SIDE OF EQ. (4.2.21).
 SFIP -THE RIGHT HAND SIDE OF EQ. (4.2.1) WITH THE INTEGRAND (4.2.17) MAJORIZED BY (4.2.25), (4.2.27), (4.2.29), (4.2.31) AND (4.2.33) FOR DIFFERENT CASES.

SDCS -SQUARE ROOT OF THE DIFFERENTIAL CROSS SECTION.
 UF -THE UPPER BOUND OF THE MODULI OF THE SPIN-NON-FLIP AMPLITUDE CALCULATED FROM EQ. (3.2.15A).

SG1 -THE RIGHT HAND SIDE OF EQ. (4.3.2) WITH (4.3.5);
 SG2 -THE RIGHT HAND SIDE OF EQ. (4.3.2) WITH (4.3.17).
 SGIP -THE RIGHT HAND SIDE OF EQ. (4.3.1) WITH THE INTEGRAND (4.3.6) MAJORIZED BY (4.3.10), (4.3.11) AND (4.3.12) FOR DIFFERENT CASES.

TABLE 2.4: PIPLUS-P SCATTERING

Z	IMF	SF ¹	SFIP	SDCS	UF	SG1	SGIP	SG2	IMG
.90	.207	.216	.215	.720	.717	.316	.283	.150	.037
.80	.189	.213	.213	.695	.689	.329	.288	.196	.051
.70	.171	.211	.210	.682	.674	.336	.291	.227	.061
.60	.154	.208	.208	.683	.673	.341	.292	.248	.068
.50	.136	.206	.205	.697	.687	.342	.292	.265	.073
.40	.118	.204	.203	.724	.714	.343	.292	.278	.078
.30	.101	.202	.201	.761	.753	.344	.292	.289	.081
.20	.083	.200	.199	.809	.802	.342	.290	.298	.083
.10	.066	.198	.197	.864	.859	.340	.288	.306	.084
-.00	.048	.196	.195	.927	.923	.339	.286	.314	.085
-.10	.030	.194	.193	.994	.991	.334	.283	.320	.084
-.20	.013	.192	.191	1.067	1.065	.330	.279	.327	.083
-.30	-.005	.191	.189	1.143	1.142	.325	.276	.333	.081
-.40	-.023	.189	.188	1.223	1.222	.319	.271	.339	.078
-.50	-.040	.187	.186	1.305	1.305	.312	.266	.345	.073
-.60	-.058	.186	.185	1.390	1.390	.304	.262	.350	.068
-.70	-.078	.184	.183	1.477	1.477	.295	.255	.365	.061
-.80	-.093	.183	.182	1.566	1.566	.282	.248	.358	.051
-.90	-.111	.181	.181	1.656	1.656	.265	.238	.360	.037

Z -COSINE OF THE SCATTERING ANGLE.

IMF -THE IMAGINARY PART OF SPIN NON-FLIP AMPLITUDE CALCULATED FROM THE PHASE SHIFTS DIRECTLY.

SF² -THE RIGHT HAND SIDE OF EQ. (4.2.21).

SFIP -THE RIGHT HAND SIDE OF EQ. (4.2.1) WITH THE INTEGRAND (4.2.17) MAJORIZED BY (4.2.25), (4.2.27), (4.2.29), (4.2.31) AND (4.2.33) FOR DIFFERENT CASES.

SDCS -SQUARE ROOT OF THE DIFFERENTIAL CROSS SECTION.

UF -THE UPPER BOUND OF THE MODULI OF THE SPIN-NON-FLIP AMPLITUDE CALCULATED FROM EQ. (3.2.15A).

SG1 -THE RIGHT HAND SIDE OF EQ. (4.3.2) WITH (4.3.5).

SG2 -THE RIGHT HAND SIDE OF EQ. (4.3.2) WITH (4.3.17).

SGIP -THE RIGHT HAND SIDE OF EQ. (4.3.1) WITH THE INTEGRAND (4.3.6) MAJORIZED BY (4.3.10), (4.3.11) AND (4.3.12) FOR DIFFERENT CASES.

IMG -THE IMAGINARY PART OF SPIN FLIP AMPLITUDE CALCULATED FROM THE PHASE SHIFTS DIRECTLY.

TABLE 2.5 PIPLUS-P SCATTERING

	PLAB = .1670 GEV/C	PCM = .1370 GEV/C	
Z	SFIP	SDCS	UF
.90	.528	.527	1.354
.80	.522	.521	1.273
.70	.517	.516	1.204
.60	.512	.511	1.153
.50	.508	.506	1.121
.40	.504	.501	1.112
.30	.500	.497	1.125
.20	.496	.493	1.160
.10	.493	.490	1.214
-.00	.491	.487	1.285
-.10	.488	.485	1.372
-.20	.486	.483	1.470
-.30	.484	.481	1.579
-.40	.483	.480	1.695
-.50	.481	.479	1.819
-.60	.481	.478	1.949
-.70	.480	.478	2.083
-.80	.480	.478	2.222
-.90	.480	.479	2.364

Z -COSINE OF THE SCATTERING ANGLE.

SF -THE RIGHT HAND SIDE OF EQ. (4.2.21).

SFIP -THE RIGHT HAND SIDE OF EQ. (4.2.1) WITH THE INTEGRAND (4.2.17) MAJORIZED BY (4.2.25), (4.2.27), (4.2.29), (4.2.31) AND (4.2.33) FOR DIFFERENT CASES.

SDCS -SQUARE ROOT OF THE DIFFERENTIAL CROSS SECTION.

UF -THE UPPER BOUND OF THE MODULI OF THE SPIN-NON-FLIP AMPLITUDE CALCULATED FROM EQ. (3.2.15A).

SG1 -THE RIGHT HAND SIDE OF EQ. (4.3.2) WITH (4.3.5).

SG2 -THE RIGHT HAND SIDE OF EQ. (4.3.2) WITH (4.3.17).

SGIP -THE RIGHT HAND SIDE OF EQ. (4.3.1) WITH THE INTEGRAND (4.3.6) MAJORIZED BY (4.3.10), (4.3.11) AND (4.3.12) FOR DIFFERENT CASES.

TABLE 2.6 PIPLUS-P SCATTERING

PLAB = .2110 GEV/C

PCM = .1680 GEV/C

Z	SF	SFIP	SDCS	UF	SG1	SGIP	SG2
.90	1.695	1.693	2.699	2.694	2.476	2.224	1.227
.80	1.678	1.674	2.508	2.497	2.588	2.276	1.591
.70	1.663	1.657	2.336	2.317	2.654	2.307	1.819
.60	1.650	1.642	2.187	2.160	2.700	2.327	1.979
.50	1.638	1.628	2.065	2.031	2.723	2.336	2.102
.40	1.628	1.616	1.975	1.935	2.745	2.350	2.205
.30	1.620	1.606	1.921	1.878	2.768	2.364	2.297
.20	1.613	1.598	1.905	1.865	2.772	2.363	2.384
.10	1.608	1.592	1.930	1.894	2.769	2.362	2.470
.00	1.604	1.588	1.992	1.965	2.780	2.366	2.555
-.10	1.602	1.586	2.090	2.070	2.760	2.355	2.640
-.20	1.601	1.586	2.218	2.204	2.753	2.348	2.731
-.30	1.602	1.588	2.372	2.363	2.739	2.341	2.820
-.40	1.605	1.592	2.547	2.541	2.708	2.319	2.914
-.50	1.609	1.598	2.739	2.736	2.677	2.298	3.007
-.60	1.615	1.606	2.946	2.945	2.643	2.281	3.100
-.70	1.623	1.615	3.166	3.165	2.589	2.253	3.188
-.80	1.632	1.626	3.395	3.395	2.515	2.213	3.263
-.90	1.642	1.639	3.633	3.633	2.396	2.154	3.319

Z -COSINE OF THE SCATTERING ANGLE.

SF -THE RIGHT HAND SIDE OF EQ. (4.2.21).

SFIP -THE RIGHT HAND SIDE OF EQ. (4.2.1) WITH THE INTEGRAND (4.2.17) MAJORIZED BY (4.2.25), (4.2.27), (4.2.29), (4.2.31) AND (4.2.33) FOR DIFFERENT CASES.

SDCS-SQUARE ROOT OF THE DIFFERENTIAL CROSS SECTION

UF -THE UPPER BOUND OF THE MODULI OF THE SPIN-NON-FLIP AMPLITUDE CALCULATED FROM EQ. (3.2.15A).

SG1 -THE RIGHT HAND SIDE OF EQ. (4.3.2) WITH (4.3.5).

SG2 -THE RIGHT HAND SIDE OF EQ. (4.3.2) WITH (4.3.17).

SGIP -THE RIGHT HAND SIDE OF EQ. (4.3.1) WITH THE INTEGRAND (4.3.6) MAJORIZED BY (4.3.10), (4.3.11) AND (4.3.12) FOR DIFFERENT CASES.

TABLE 2.7 PIPLUS-P SCATTERING

Z	PLAB = .2370 GEV/C	PCM = .1866 GEV/C					
		SF	SFIP	SDCS	UF	SGI	SGIP
.90	3.008	3.202	3.198	3.872	3.865	4.671	4.199
.80	2.688	3.168	3.161	3.588	3.573	4.881	4.296
.70	2.367	3.139	3.127	3.325	3.300	5.005	4.355
.60	2.046	3.113	3.096	3.086	3.051	5.091	4.395
.50	1.725	3.091	3.070	2.878	2.832	5.136	4.413
.40	1.405	3.073	3.047	2.708	2.651	5.179	4.441
.30	1.084	3.058	3.028	2.581	2.519	5.226	4.471
.20	0.763	3.047	3.014	2.506	2.442	5.238	4.473
.10	0.443	3.040	3.005	2.485	2.428	5.238	4.477
-.00	0.122	3.036	3.000	2.522	2.475	5.262	4.489
-.10	-0.199	3.036	3.000	2.612	2.578	5.232	4.472
-.20	-0.520	3.039	3.006	2.752	2.729	5.226	4.464
-.30	-0.840	3.047	3.016	2.935	2.921	5.207	4.457
-.40	-1.161	3.058	3.030	3.153	3.145	5.155	4.422
-.50	-1.482	3.072	3.049	3.399	3.395	5.105	4.388
-.60	-1.802	3.091	3.071	3.670	3.668	5.053	4.365
-.70	-2.123	3.113	3.098	3.959	3.958	4.962	4.319
-.80	-2.444	3.138	3.128	4.264	5.264	4.832	4.255
-.90	-2.765	3.167	3.162	4.583	4.583	4.617	4.153

Z -COSINE OF THE SCATTERING ANGLE.

IMF -THE IMAGINARY PART OF SPIN NON-FLIP AMPLITUDE CALCULATED FROM THE PHASE SHIFTS DIRECTLY.

SF -THE RIGHT HAND SIDE OF EQ. (4.2.21).

SFIP -THE RIGHT HAND SIDE OF EQ. (4.2.1) WITH THE INTEGRAND (4.2.17) MAJORIZED BY (4.2.25),

(4.2.27), (4.2.29), (4.2.31) AND (4.2.33) FOR DIFFERENT CASES.

SDCS -SQUARE ROOT OF THE DIFFERENTIAL CROSS SECTION.

UF -THE UPPER BOUND OF THE MODULI OF THE SPIN-NON-FLIP AMPLITUDE CALCULATED FROM EQ. (3.2.15A).

SG1 -THE RIGHT HAND SIDE OF EQ. (4.3.2) WITH (4.3.5).

SG2 -THE RIGHT HAND SIDE OF EQ. (4.3.2) WITH (4.3.17).

SGIP -THE RIGHT HAND SIDE OF EQ. (4.3.1) WITH THE INTEGRAND (4.3.6)° MAJORIZED BY (4.3.10),

(4.3.11) AND (4.3.12) FOR DIFFERENT CASES.

IMG -THE IMAGINARY PART OF SPIN FLIP AMPLITUDE CALCULATED FROM THE PHASE SHIFTS DIRECTLY.

TABLE 2.8 PIPLUS-P SCATTERING

Z	SF	SFIP.	S _D CS	UF	SGI	SG2
.90	4.445	4.440	4.674	4.666	6.480	5.828
.80	4.397	4.385	4.328	4.311	6.769	5.960
.70	4.354	4.335	4.003	3.975	6.939	6.041
.60	4.316	4.291	3.702	3.662	7.055	6.095
.50	4.285	4.253	3.432	3.379	7.118	6.120
.40	4.259	4.220	3.202	3.136	7.178	6.161
.30	4.239	4.194	3.018	2.943	7.243	6.204
.20	4.224	4.175	2.892	2.813	7.262	6.208
.10	4.215	4.162	2.829	2.756	7.264	6.215
.00	4.211	4.157	2.834	2.774	7.301	6.234
-.10	4.213	4.161	2.908	2.683	7.262	6.213
-.20	4.221	4.171	3.044	3.015	7.257	6.204
-.30	4.234	4.189	3.236	3.218	7.236	6.198
-.40	4.253	4.213	3.474	3.465	7.168	6.153
-.50	4.278	4.243	3.751	3.746	7.105	6.110
-.60	4.308	4.280	4.057	4.055	7.039	6.083
-.70	4.343	4.322	4.389	4.388	6.920	6.026
-.80	4.385	4.370	4.740	4.740	6.748	5.943
-.90	4.432	4.424	5.107	5.107	6.457	5.809

Z -COSINE OF THE SCATTERING ANGLE.

SF -THE RIGHT HAND SIDE OF EQ. (4.2.21).

SFIP -THE RIGHT HAND SIDE OF EQ. (4.2.1) WITH THE INTEGRAND (4.2.17) MAJORIZED BY (4.2.25), (4.2.27), (4.2.29), (4.2.31) AND (4.2.33) FOR DIFFERENT CASES.

S_DCS -SQUARE ROOT OF THE DIFFERENTIAL CROSS SECTION.

UF -THE UPPER BOUND OF THE MODULI OF THE SPIN-NON-FLIP AMPLITUDE CALCULATED FROM EQ. (3.2.15A).

SGI - THE RIGHT HAND SIDE OF EQ. (4.3.2) WITH (4.3.5).

SG2 - THE RIGHT HAND SIDE OF EQ. (4.3.2) WITH (4.3.17).

SGIP - THE RIGHT HAND SIDE OF EQ. (4.3.1) WITH THE INTEGRAND (4.3.6) MAJORIZED BY (4.3.10), (4.3.11) AND (4.3.12) FOR DIFFERENT CASES.

TABLE 2.9 PIPLUS-P SCATTERING
 $P_{LAB} = .2770 \text{ GEV/C}$ $PCM = .2130 \text{ GEV/C}$

Z	SF	SDCS	UF	SG1	SGIP	SG2
.90	5.321	5.314	5.188	7.750	6.972	3.957
.80	5.258	5.243	4.800	8.089	7.125	5.082
.70	5.203	5.179	4.431	8.403	8.286	5.763
.60	5.155	5.123	4.085	4.044	8.420	6.227
.50	5.115	5.074	3.769	3.713	8.492	6.581
.40	5.082	5.032	3.489	3.418	8.561	7.355
.30	5.056	4.999	3.255	3.172	8.639	7.406
.20	5.038	4.974	3.078	2.989	8.660	7.411
.10	5.027	4.959	2.969	2.882	8.664	7.421
.00	5.023	4.953	2.934	2.860	8.708	7.444
-.10	5.027	4.959	2.976	2.921	8.664	7.420
-.20	5.038	4.974	3.093	3.056	8.660	7.411
-.30	5.056	4.999	3.275	3.254	8.638	7.406
-.40	5.082	5.031	3.515	3.504	8.561	7.355
-.50	5.115	5.072	3.799	3.795	8.491	7.307
-.60	5.155	5.121	4.121	4.119	8.420	7.280
-.70	5.203	5.177	4.471	4.471	8.285	7.218
-.80	5.258	5.241	4.844	4.844	8.088	7.126
-.90	5.321	5.312	5.235	5.235	7.749	6.792

Z -COSINE OF THE SCATTERING ANGLE.

SF -THE RIGHT HAND SIDE OF EQ. (4.2.21).

SDCS -THE RIGHT HAND SIDE OF EQ. (4.2.1) WITH THE INTEGRAND (4.2.17) MAJORIZED BY (4.2.25), (4.2.27), (4.2.29), (4.2.31) AND (4.2.33) FOR DIFFERENT CASES.

SG1 -SQUARE ROOT OF THE DIFFERENTIAL CROSS SECTION.

SGIP -THE UPPER BOUND OF THE MODULI OF THE SPIN-NON-FLIP AMPLITUDE CALCULATED FROM EQ. (3.2.15A).

SG2 -THE RIGHT HAND SIDE OF EQ. (4.3.2) WITH (4.3.5).

SGIP -THE RIGHT HAND SIDE OF EQ. (4.3.2) WITH (4.3.17).

SG2 -THE RIGHT HAND SIDE OF EQ. (4.3.1) WITH THE INTEGRAND (4.3.6) MAJORIZED BY (4.3.10), (4.3.11) AND (4.3.12) FOR DIFFERENT CASES.

TABLE 3:1 PIMINUS-P SCATTERING

Z	PLAB = 0800 GEV/C	PCM = .0680 GEV/C	SFIP	SDCS	UF	SG1	SGIP	SG2
.90	.061	.053	.551	.551	.089	.080	.038	
.80	.061	.061	.541	.541	.094	.082	.052	
.70	.060	.060	.530	.530	.097	.083	.061	
.60	.060	.060	.519	.519	.099	.084	.069	
.50	.060	.060	.509	.509	.100	.085	.075	
.40	.060	.060	.498	.498	.101	.085	.080	
.30	.060	.060	.487	.487	.102	.086	.085	
.20	.059	.059	.477	.477	.102	.086	.089	
.10	.059	.059	.466	.466	.102	.086	.093	
-.00	.059	.059	.455	.455	.102	.086	.096	
-.10	.059	.059	.444	.444	.101	.085	.099	
-.20	.059	.059	.434	.434	.101	.085	.102	
-.30	.059	.059	.423	.423	.100	.084	.104	
-.40	.058	.058	.412	.412	.098	.083	.106	
-.50	.058	.058	.401	.401	.097	.082	.108	
-.60	.058	.058	.391	.391	.095	.081	.110	
-.70	.058	.058	.380	.380	.093	.080	.112	
-.80	.058	.058	.369	.369	.089	.078	.113	
-.90	.058	.058	.358	.358	.085	.076	.114	

Z - COSINE OF THE SCATTERING ANGLE.

SF - THE RIGHT HAND SIDE OF EQ. (4.2.21).

SFIP - THE RIGHT HAND SIDE OF EQ. (4.2.1) WITH THE INTEGRAND (4.2.17) MAJORIZED BY (4.2.25), (4.2.27), (4.2.29), (4.2.31) AND (4.2.33) FOR DIFFERENT CASES.

SDCS - SQUARE ROOT OF THE DIFFERENTIAL CROSS SECTION.

UF - THE UPPER BOUND OF THE MODULI OF THE SPIN-NON-FLIP AMPLITUDE CALCULATED FROM EQ. (3.2.15A).

SG1 - THE RIGHT HAND SIDE OF EQ. (4.3.2) WITH (4.3.5).

SG2 - THE RIGHT HAND SIDE OF EQ. (4.3.2) WITH (4.3.17).

SGIP - THE RIGHT HAND SIDE OF EQ. (4.3.1) WITH THE INTEGRAND (4.3.6) MAJORIZED BY (4.3.10), (4.3.11) AND (4.3.12) FOR DIFFERENT CASES.

TABLE 3.2 PIMINUS- \bar{p} SCATTERING

Z	SF	PLAB = 1000 GEV/C		PCM = .0850 GEV/C	
		SFIP	SDCS	UF	SG1
.90	.075	.075	.489	.489	.110
.80	.075	.075	.483	.483	.116
.70	.074	.074	.476	.476	.119
.60	.074	.074	.469	.468	.121
.50	.074	.074	.461	.461	.122
.40	.073	.073	.453	.452	.123
.30	.073	.073	.444	.444	.124
.20	.073	.072	.435	.434	.124
.10	.072	.072	.425	.424	.124
-.00	.072	.072	.415	.414	.124
-.10	.071	.071	.403	.403	.123
-.20	.071	.071	.391	.391	.122
-.30	.071	.071	.379	.378	.121
-.40	.070	.070	.365	.364	.119
-.50	.070	.070	.350	.349	.116
-.60	.070	.070	.334	.334	.114
-.70	.069	.069	.317	.316	.111
-.80	.069	.069	.298	.298	.107
-.90	.069	.069	.278	.277	.101

Z -COSINE OF THE SCATTERING ANGLE.

SF -THE RIGHT HAND SIDE OF EQ. (4.2.21).

SFIP -THE RIGHT HAND SIDE OF EQ. (4.2.1) WITH THE INTEGRAND (4.2.17) MAJORIZED BY (4.2.25), (4.2.27), (4.2.29), (4.2.31) AND (4.2.33) FOR DIFFERENT CASES.

SDCS -SQUARE ROOT OF THE DIFFERENTIAL CROSS SECTION.

UF -THE UPPER BOUND OF THE MODULI OF THE SPIN-NON-FLIP AMPLITUDE CALCULATED FROM EQ. (3.2.15A).

SG1 -THE RIGHT HAND SIDE OF EQ. (4.3.2) WITH (4.3.5).

SG2 -THE RIGHT HAND SIDE OF EQ. (4.3.2) WITH (4.3.17).

SGIP -THE RIGHT HAND SIDE OF EQ. (4.3.1) WITH THE INTEGRAND (4.3.6) MAJORIZED BY (4.3.10), (4.3.11) AND (4.3.12) FOR DIFFERENT CASES.

TABLE 3.3
 $P_{LAB} = .1150 \text{ GEV}/c$ $PCM = .9700 \text{ GEV}/c$
 PI MINUS-P SCATTERING

Z	SF	SFIP	SDCS	UF	SG1	SGIP	SG2
.90	.008	.008	.051	.051	.012	.011	.005
.80	.008	.008	.050	.050	.013	.011	.007
.70	.008	.008	.049	.049	.013	.011	.009
.60	.008	.008	.048	.048	.014	.012	.010
.50	.008	.008	.047	.047	.014	.012	.010
.40	.008	.008	.046	.046	.014	.012	.011
.30	.008	.008	.044	.044	.014	.012	.012
.20	.008	.008	.043	.043	.014	.012	.012
.10	.008	.008	.041	.041	.014	.012	.012
-.00	.008	.008	.040	.040	.014	.012	.012
-.10	.008	.008	.038	.038	.014	.011	.013
-.20	.008	.008	.036	.036	.013	.011	.014
-.30	.008	.008	.034	.034	.013	.011	.014
-.40	.008	.008	.032	.032	.013	.011	.014
-.50	.008	.008	.030	.030	.013	.011	.014
-.60	.008	.008	.027	.027	.013	.011	.014
-.70	.008	.008	.024	.024	.012	.011	.015
-.80	.008	.008	.021	.020	.012	.010	.015
-.90	.008	.008	.016	.016	.011	.010	.015

2 -COSINE OF THE SCATTERING ANGLE.

SF -THE RIGHT HAND SIDE OF EQ. (4.2.21).

SFIP -THE RIGHT HAND SIDE OF EQ. (4.2.1) WITH THE INTEGRAND (4.2.17) MAJORIZED BY (4.2.25), (4.2.27), (4.2.29), (4.2.31) $^\circ$ AND (4.2.33) FOR DIFFERENT CASES.

SDCS-SQUARE ROOT OF THE DIFFERENTIAL CROSS SECTION.

UF -THE UPPER BOUND OF THE MODULI OF THE SPIN-NON-FLIP AMPLITUDE CALCULATED FROM EQ. (3.2.15A).

SG1 -THE RIGHT HAND SIDE OF EQ. (4.3.2) WITH (4.3.5).

SG2 -THE RIGHT HAND SIDE OF EQ. (4.3.2) WITH (4.3.17).

SGIP -THE RIGHT HAND SIDE OF EQ. (4.3.1) WITH THE INTEGRAND (4.3.6) MAJORIZED BY (4.3.10), (4.3.11) AND (4.3.12) $^\circ$ FOR DIFFERENT CASES.

TABLE 3.4 PIMINUS-P SCATTERING

PLAB = .1420 GEV/c PCM = .1190 GEV/c

Z	IMF	SF	SFIP	SDCS	UF	SG1	SGIP	SG2	IMG
.90	.127	.128	.128	.537	.536	.188	.168	.086	.011
.80	.120	.125	.127	.528	.527	.197	.173	.114	.015
.70	.114	.126	.126	.519	.518	.202	.175	.147	.018
.60	.108	.125	.125	.509	.508	.205	.177	.147	.020
.50	.102	.124	.124	.499	.498	.206	.177	.158	.022
.40	.096	.123	.123	.489	.487	.207	.178	.167	.023
.30	.089	.122	.122	.477	.475	.209	.179	.175	.024
.20	.083	.121	.121	.464	.463	.208	.178	.181	.025
.10	.077	.121	.120	.451	.449	.207	.177	.188	.025
.00	.071	.120	.119	.436	.434	.207	.177	.193	.025
-.10	.064	.119	.118	.419	.417	.204	.175	.198	.025
-.20	.058	.118	.118	.500	.399	.203	.174	.202	.025
-.30	.052	.117	.117	.380	.378	.200	.172	.206	.024
-.40	.046	.116	.116	.356	.355	.196	.169	.210	.023
-.50	.040	.116	.115	.330	.329	.193	.167	.214	.022
-.60	.003	.115	.115	.299	.298	.188	.164	.217	.020
-.70	.027	.114	.114	.262	.262	.183	.160	.220	.018
-.80	.021	.114	.113	.217	.217	.176	.156	.222	.015
-.90	.015	.113	.113	.156	.156	.166	.150	.224	.011

Z - COSINE OF THE SCATTERING ANGLE.

IMF - THE IMAGINARY PART OF SPIN NON-FLIP AMPLITUDE CALCULATED FROM THE PHASE SHIFTS DIRECTLY.

SF - THE RIGHT HAND SIDE OF EQ. (4.2.21).

SFIP - THE RIGHT HAND SIDE OF EQ. (4.2.1) WITH THE INTEGRAND (4.2.17) MAJORIZED BY (4.2.25), (4.2.27), (4.2.29), (4.2.31) AND (4.2.33) FOR DIFFERENT CASES.

SDCS - SQUARE ROOT OF THE DIFFERENTIAL CROSS SECTION.

UF - THE UPPER BOUND OF THE MODULI OF THE SPIN-NON-FLIP AMPLITUDE CALCULATED FROM EQ. (3.2.15A).

SG1 - THE RIGHT HAND SIDE OF EQ. (4.3.2) WITH (4.3.5).

SG2 - THE RIGHT HAND SIDE OF EQ. (4.3.2) WITH (4.3.17).

SGIP - THE RIGHT HAND SIDE OF EQ. (4.3.1) WITH THE INTEGRAND (4.3.6) MAJORIZED BY (4.3.10), (4.3.11) AND (4.3.12) FOR DIFFERENT CASES.

IMG - THE IMAGINARY PART OF SPIN FLIP AMPLITUDE CALCULATED FROM THE PHASE SHIFTS DIRECTLY.

TABLE 3.5
KMINUS-P SCATTERING
PLAB = 1670 GEV/C PCM = 11370 GEV/C

Z	SF	SFIP	SDCS	UF	SGI	SGIP	SG2
.90	.271	.271	.873	.873	.398	.356	.186
.80	.269	.269	.836	.835	.416	.365	.245
.70	.267	.267	.800	.799	.427	.371	.284
.60	.265	.265	.764	.763	.435	.374	.313
.50	.264	.263	.728	.727	.439	.376	.336
.40	.262	.261	.694	.692	.442	.378	.355
.30	.261	.260	.659	.657	.445	.380	.372
.20	.259	.258	.625	.623	.446	.379	.387
.10	.258	.257	.591	.589	.444	.378	.401
-.09	.257	.256	.557	.555	.445	.378	.414
-.10	.256	.255	.523	.522	.441	.375	.426
-.20	.255	.254	.489	.488	.439	.373	.438
-.30	.254	.253	.455	.454	.435	.370	.449
-.40	.254	.253	.420	.419	.428	.366	.461
-.50	.253	.252	.384	.384	.422	.361	.471
-.60	.253	.252	.347	.347	.414	.357	.482
-.70	.252	.252	.307	.307	.404	.351	.491
-.80	.252	.252	.264	.264	.390	.343	.499
-.90	.252	.252	.215	.214	.369	.332	.504

Z -COSINE OF THE SCATTERING ANGLE:
SF -THE RIGHT HAND SIDE OF EQ. (4.2.21)

SFIP -THE RIGHT HAND SIDE OF EQ. (4.2.1) WITH THE INTEGRAND (4.2.17) MAJORIZED BY (4.2.25), (4.2.27), (4.2.29), (4.2.31) AND (4.2.33) FOR DIFFERENT CASES.

SDCS -SQUARE ROOT OF THE DIFFERENTIAL CROSS SECTION.

UF -THE UPPER BOUND OF THE MODULI OF THE SPIN-NON-FLIP AMPLITUDE CALCULATED FROM EQ. (3.2.15A).

SGI -THE RIGHT HAND SIDE OF EQ. (4.3.2) WITH (4.3.5).

SG2 -THE RIGHT HAND SIDE OF EQ. (4.3.2) WITH (4.3.17).

SGIP -THE RIGHT HAND SIDE OF EQ. (4.3.1) WITH THE INTEGRAND (4.3.6) MAJORIZED BY (4.3.10), (4.3.11) AND (4.3.12) FOR DIFFERENT CASES.

TABLE 3.6. PIMINUS-P SCATTERING

Z	SF	PCM = .2110 GEV/C			PCM = .1680 GEV/C		
		SFIP	SDCS	UF	SG1	SG2	UF
.90	.674	.673	1.280	1.280	.985	.886	.479
.80	.668	.667	1.202	1.202	1.031	.908	.625
.70	.662	.661	1.127	1.127	1.058	.921	.718
.60	.658	.655	1.055	1.055	1.077	.930	.784
.50	.654	.650	.986	.986	1.087	.934	.836
.40	.650	.646	.921	.920	1.096	.940	.880
.30	.647	.642	.859	.859	1.105	.945	.918
.20	.644	.639	.802	.802	1.107	.945	.955
.10	.642	.637	.750	.750	1.106	.944	.990
.00	.641	.635	.703	.703	1.110	.945	1.024
-.10	.640	.634	.662	.662	1.102	.940	1.058
-.20	.639	.634	.628	.628	1.099	.916	1.093
-.30	.639	.635	.603	.601	1.093	.932	1.128
-.40	.640	.636	.585	.582	1.080	.923	1.163
-.50	.641	.637	.576	.571	1.067	.914	1.198
-.60	.643	.640	.575	.569	1.053	.907	1.233
-.70	.645	.643	.582	.575	1.030	.895	1.265
-.80	.648	.646	.597	.591	1.000	.879	1.293
-.90	.651	.650	.618	.614	.952	.855	1.314

2 - COSINE OF THE SCATTERING ANGLE.

SF - THE RIGHT HAND SIDE OF EQ. (4.2.21).

SFIP - THE RIGHT HAND SIDE OF EQ. (4.2.1) WITH THE INTEGRAND (4.2.17) MAJORIZED BY (4.2.25), (4.2.27), (4.2.29), (4.2.31) AND (4.2.33) FOR DIFFERENT CASES.

SDCS - SQUARE ROOT OF THE DIFFERENTIAL CROSS SECTION.

UF - THE UPPER BOUND OF THE MODULI OF THE SPIN-NON-FLIP AMPLITUDE CALCULATED FROM EQ. (3.2.15A).

SG1 - THE RIGHT HAND SIDE OF EQ. (4.3.2) WITH (4.3.5).

SG2 - THE RIGHT HAND SIDE OF EQ. (4.3.2) WITH (4.3.17).

SGP - THE RIGHT HAND SIDE OF EQ. (4.3.1) WITH THE INTEGRAND (4.3.6) MAJORIZED BY (4.3.10), (4.3.11) AND (4.3.12) FOR DIFFERENT CASES.

TABLE 3.7 PIMIUS-P SCATTERING

	PLAB	2.376 GEV/C	PFM = 1866 GEV/C			
IMF	SDIP	SDCS	UP	SG1	SG2	IMG
.90	1.089	1.151	1.150	1.554	1.681	1.512
.80	0.982	1.140	1.137	1.444	1.444	1.549
.70	0.874	1.129	1.125	1.339	1.339	1.571
.60	0.767	1.121	1.115	1.239	1.239	1.586
.50	0.650	1.113	1.106	1.146	1.146	1.850
.40	0.552	1.106	1.098	1.060	1.060	1.865
.30	0.445	1.101	1.091	1.983	1.983	1.882
.20	0.338	1.097	1.086	1.916	1.916	1.886
.10	0.230	1.094	1.083	1.860	1.860	1.886
.00	0.123	1.093	1.081	1.818	1.817	1.894
-10	0.016	1.092	1.081	1.791	1.789	1.883
-20	-0.091	1.093	1.082	1.780	1.776	1.880
-30	-0.199	1.096	1.085	1.785	1.779	1.873
-40	-0.306	1.099	1.090	1.806	1.798	1.853
-50	-0.413	1.104	1.096	1.841	1.831	1.834
-60	-0.520	1.109	1.103	1.888	1.878	1.815
-70	-0.628	1.116	1.111	1.944	1.936	1.781
-80	-0.735	1.125	1.121	1.009	1.003	1.733
-90	-0.842	1.134	1.132	1.080	1.077	1.655

2. -COSINE OF THE SCATTERING ANGLE.

IMF - THE IMAGINARY PART OF SPIN NON-FLIP AMPLITUDE CALCULATED FROM THE PHASE SHIFTS DIRECTLY.

SF - THE RIGHT HAND SIDE OF EQ. (4.2.21).

SDIP - THE RIGHT HAND SIDE OF EQ. (4.2.1) WITH THE INTEGRAND (4.2.17) MAJORIZED BY (4.2.25), (4.2.27), (4.2.29), (4.2.31) AND (4.2.33) FOR DIFFERENT CASES.

SDCS - SQUARE ROOT OF THE DIFFERENTIAL CROSS SECTION.

UP - THE UPPER BOUND OF THE MODULUS OF THE SPIN-NON-FLIP AMPLITUDE CALCULATED FROM EQ. (3.2.15A).

SG1 - THE RIGHT HAND SIDE OF EQ. (4.3.2) WITH (4.3.5).

SG2 - THE RIGHT HAND SIDE OF EQ. (4.3.2) WITH (4.3.17).

SGIP - THE RIGHT HAND SIDE OF EQ. (4.3.1) WITH THE INTEGRAND (4.3.6) MAJORIZED BY (4.3.10), (4.3.11) AND (4.3.12) FOR DIFFERENT CASES.

IMG - THE IMAGINARY PART OF SPIN FLIP AMPLITUDE CALCULATED FROM THE PHASE SHIFTS DIRECTLY.

TABLE 3.6 PIMINUS-P SCATTERING
 $P_{LAB} = 2540 \text{ GeV}/c$ $PCM = 1980 \text{ GeV}/c$

Z	SF	SFIP	SDCS	UF	SG1	SG2
.90	1.537	1.535	1.764	1.764	2.241	1.131
.80	1.520	1.516	1.631	1.631	2.342	1.457
.70	1.506	1.500	1.505	1.505	2.401	1.659
.60	1.493	1.485	1.387	1.386	2.442	2.111
.50	1.483	1.472	1.277	1.277	2.464	2.120
.40	1.474	1.461	1.178	1.178	2.485	2.133
.30	1.467	1.452	1.092	1.092	2.508	2.147
.20	1.462	1.446	1.021	1.021	2.514	2.156
.10	1.459	1.442	.967	.967	2.515	2.237
.00	1.458	1.440	.934	.934	2.528	2.320
-.10	1.459	1.441	.922	.921	2.514	2.403
-.20	1.461	1.445	.933	.930	2.512	2.493
-.30	1.466	1.450	.964	.960	2.505	2.584
-.40	1.472	1.458	1.014	1.008	2.481	2.124
-.50	1.480	1.469	1.079	1.073	2.459	2.109
-.60	1.490	1.481	1.158	1.151	2.436	2.099
-.70	1.502	1.495	1.246	1.240	2.394	2.079
-.80	1.516	1.511	1.343	1.338	2.334	2.051
-.90	1.532	1.529	1.446	1.443	2.233	2.005

2 - COSINE OF THE SCATTERING ANGLE.

SF - THE RIGHT HAND SIDE OF EQ. (4.2.21).

SFIP - THE RIGHT HAND SIDE OF EQ. (4.2.1) WITH THE INTEGRAND (4.2.17) MAJORIZED BY (4.2.25), (4.2.27), (4.2.29), (4.2.31) AND (4.2.33) FOR DIFFERENT CASES.

SDCS - SQUARE ROOT OF THE DIFFERENTIAL CROSS SECTION.

UF - THE UPPER BOUND OF THE MODULI OF THE SPIN-NON-FLIP AMPLITUDE CALCULATED FROM EQ. (3.2.15A).

SG1 - THE RIGHT HAND SIDE OF EQ. (4.3.2) WITH (4.3.5).

SG2 - THE RIGHT HAND SIDE OF EQ. (4.3.2) WITH (4.3.17).

SGIP - THE RIGHT HAND SIDE OF EQ. (4.3.1) WITH THE INTEGRAND (4.3.6) MAJORIZED BY (4.3.10), (4.3.11) AND (4.3.12) FOR DIFFERENT CASES.

TABLE 3.9 PIMINUS-P SCATTERING

Z	PLAB = .2770 GEV/C	PCM = .2130 GEV/C				
	SFIP	SDCS	UF	SG1	SGIP	SG2
.90	1.848	1.846	1.893	1.893	2.694	2.426
.80	1.827	1.822	1.749	1.749	2.813	2.481
.70	1.809	1.801	1.611	1.611	2.882	2.514
.60	1.793	1.782	1.480	1.480	2.929	2.536
.50	1.779	1.765	1.357	1.357	2.955	2.545
.40	1.768	1.752	1.246	1.245	2.980	2.560
.30	1.760	1.740	1.147	1.147	3.007	2.577
.20	1.753	1.732	1.064	1.063	3.015	2.578
.10	1.750	1.727	1.001	1.000	3.016	2.580
.00	1.748	1.725	.961	.958	3.032	2.586
-.10	.750	.727	.946	.941	3.016	2.577
-.20	1.753	1.732	.958	.950	3.015	2.572
-.30	1.759	1.740	.995	.984	3.007	2.569
-.40	1.768	1.751	1.053	1.042	2.979	2.551
-.50	1.779	1.765	1.131	1.119	2.955	2.533
-.60	1.793	1.781	1.223	1.212	2.929	2.523
-.70	1.809	1.800	1.326	1.317	2.882	2.502
-.80	1.827	1.822	1.439	1.433	2.812	2.470
-.90	1.848	1.845	1.559	1.555	2.693	2.418

Z -COSINE OF THE SCATTERING ANGLE.

SF -THE RIGHT HAND SIDE OF EQ. (4.2.21).

SFIP -THE RIGHT HAND SIDE OF EQ. (4.2.1) WITH THE INTEGRAND (4.2.17) MAJORIZED BY (4.2.25), (4.2.27), (4.2.29), (4.2.31) AND (4.2.33) FOR DIFFERENT CASES.

SDCS -SQUARE ROOT OF THE DIFFERENTIAL CROSS SECTION.

UF -THE UPPER BOUND OF THE MODULI OF THE SPIN-NON-FLIP AMPLITUDE CALCULATED FROM EQ. (3.2.15A).

SG1 -THE RIGHT HAND SIDE OF EQ. (4.3.2) WITH (4.3.5).

SG2 -THE RIGHT HAND SIDE OF EQ. (4.3.2) WITH (4.3.17).

SGIP -THE RIGHT HAND SIDE OF EQ. (4.3.1) WITH THE INTEGRAND (4.3.6) MAJORIZED BY (4.3.10), (4.3.11) AND (4.3.12) FOR DIFFERENT CASES.

TABLE 4.1 KPLUS-P SCATTERING
 $P_{LAB} = .1400 \text{ GEV/C}$ $PCM = .0910 \text{ GEV/C}$

Z	SF	SFIP	SDCS	UF	SG1	SGIP	SG2
.90	.087	.087	.877	.877	.128	.114	.054
.80	.086	.086	.866	.866	.134	.117	.073
.70	.086	.086	.854	.854	.139	.120	.087
.60	.086	.086	.843	.843	.142	.121	.098
.50	.086	.086	.831	.831	.144	.122	.108
.40	.086	.086	.820	.820	.146	.123	.116
.30	.086	.086	.808	.808	.147	.124	.123
.20	.086	.086	.796	.796	.148	.124	.129
.10	.086	.086	.785	.785	.148	.125	.135
.00	.086	.086	.773	.773	.149	.125	.140
-.10	.086	.086	.762	.762	.148	.124	.145
-.20	.086	.086	.750	.750	.147	.124	.149
-.30	.086	.086	.738	.738	.146	.123	.153
-.40	.086	.086	.727	.727	.145	.123	.156
-.50	.086	.086	.715	.715	.143	.121	.160
-.60	.086	.086	.704	.704	.141	.120	.163
-.70	.086	.086	.692	.692	.137	.118	.165
-.80	.085	.085	.681	.681	.133	.116	.168
-.90	.085	.085	.669	.669	.126	.113	.170

Z -COSINE OF THE SCATTERING ANGLE.

SF -THE RIGHT HAND SIDE OF EQ. (4.2.21).

SFIP-THE RIGHT HAND SIDE OF EQ. (4.2.1) WITH THE INTEGRAND (4.2.17) MAJORIZED BY (4.2.25), (4.2.27), (4.2.29), (4.2.31) AND (4.2.33) FOR DIFFERENT CASES.

SDCS-SQUARE ROOT OF THE DIFFERENTIAL CROSS SECTION.

UF -THE UPPER BOUND OF THE MODULI OF THE SPIN-NON-FLIP AMPLITUDE CALCULATED FROM EQ. (3.2.15A).

SG1 -THE RIGHT HAND SIDE OF EQ. (4.3.2) WITH (4.3.5).

SG2 -THE RIGHT HAND SIDE OF EQ. (4.3.2) WITH (4.3.17).

SGIP-THE RIGHT HAND SIDE OF EQ. (4.3.1) WITH THE INTEGRAND (4.3.6) MAJORIZED BY (4.3.10), (4.3.11) AND (4.3.12) FOR DIFFERENT CASES.

TABLE 4.2 KPLUS-P SCATTERING
 $P_{LAB} = .1750 \text{ GEV/C}$ $PCM = .1130 \text{ GEV/C}$

Z	SF	SFIP	SDCS	UF	SGL	SGIP	SG2
.90	.143	.143	.920	.920	.212	.189	.089
.80	.143	.143	.917	.917	.223	.195	.121
.70	.143	.143	.915	.915	.230	.198	.144
.60	.143	.143	.912	.912	.235	.201	.163
.50	.143	.143	.910	.910	.239	.203	.178
.40	.143	.143	.907	.907	.242	.205	.192
.30	.143	.143	.904	.904	.245	.206	.204
.20	.143	.143	.902	.902	.246	.207	.215
.10	.143	.143	.899	.899	.247	.207	.224
-.00	.143	.143	.896	.896	.248	.208	.233
-.10	.143	.143	.893	.893	.247	.207	.241
-.20	.143	.143	.891	.891	.246	.207	.249
-.30	.143	.143	.888	.888	.245	.206	.255
-.40	.143	.143	.885	.885	.242	.205	.262
-.50	.143	.143	.882	.882	.239	.203	.268
-.60	.143	.143	.879	.879	.235	.201	.273
-.70	.143	.143	.877	.877	.230	.198	.277
-.80	.143	.143	.874	.874	.223	.195	.281
-.90	.143	.143	.871	.871	.212	.189	.285

Z -COSINE OF THE SCATTERING ANGLE.

SF -THE RIGHT HAND SIDE OF EQ. (4.2.21).

SFIP-THE RIGHT HAND SIDE OF EQ. (4.2.1) WITH THE INTEGRAND (4.2.17) MAJORIZED BY (4.2.25), (4.2.27), (4.2.29), (4.2.31) AND (4.2.33) FOR DIFFERENT CASES.

SDCS-SQUARE ROOT OF THE DIFFERENTIAL CROSS SECTION.

UF -THE UPPER BOUND OF THE MODULI OF THE SPIN-NON-FLIP AMPLITUDE CALCULATED FROM EQ. (3.2.15A).

SGL -THE RIGHT HAND SIDE OF EQ. (4.3.2) WITH (4.3.5).

SG2 -THE RIGHT HAND SIDE OF EQ. (4.3.2) WITH (4.3.17).

SGIP-THE RIGHT HAND SIDE OF EQ. (4.3.1) WITH THE INTEGRAND (4.3.6) MAJORIZED BY (4.3.10), (4.3.11) AND (4.3.12) FOR DIFFERENT CASES.

TABLE 4.3. KPLUS-P SCATTERING
 $P_{LAB} = .2050 \text{ GEV/C}$ $PCM = .1320 \text{ GEV/C}$

Z	SF	SFIP	SDCS	UF	SG1	SG2
.90	.181	.181	.856	.856	.268	.240
.80	.181	.181	.864	.864	.282	.246
.70	.181	.181	.873	.873	.291	.251
.60	.181	.181	.881	.881	.297	.254
.50	.181	.181	.889	.889	.302	.257
.40	.181	.181	.898	.898	.306	.259
.36	.181	.181	.906	.906	.309	.260
.20	.181	.181	.915	.915	.311	.261
.10	.181	.181	.923	.923	.312	.262
-.00	.181	.181	.931	.931	.312	.262
-.10	.181	.181	.940	.940	.312	.262
-.20	.181	.181	.948	.948	.310	.261
-.30	.181	.181	.956	.956	.309	.260
-.40	.181	.181	.965	.965	.306	.258
-.50	.181	.181	.973	.973	.302	.256
-.60	.181	.181	.981	.981	.296	.253
-.70	.180	.180	.989	.989	.290	.250
-.80	.180	.180	.998	.998	.280	.245
-.90	.180	.180	1.006	1.006	.266	.238

Z -COSINE OF THE SCATTERING ANGLE.

SF -THE RIGHT HAND SIDE OF EQ. (4.2.21).

SFIP -THE RIGHT HAND SIDE OF EQ. (4.2.1) WITH THE INTEGRAND (4.2.17) MAJORIZED BY (4.2.25), (4.2.27), (4.2.29), (4.2.31) AND (4.2.33) FOR DIFFERENT CASES.

SDCS -SQUARE ROOT OF THE DIFFERENTIAL CROSS SECTION.

UF -THE UPPER BOUND OF THE MODULI OF THE SPIN-NON-FLIP AMPLITUDE CALCULATED FROM EQ. (3.2.15A).

SG1 -THE RIGHT HAND SIDE OF EQ. (4.3.2) WITH (4.3.5).

SG2 -THE RIGHT HAND SIDE OF EQ. (4.3.2) WITH (4.3.17).

SGIP -THE RIGHT HAND SIDE OF EQ. (4.3.1) WITH THE INTEGRAND (4.3.6) MAJORIZED BY (4.3.10), (4.3.11) AND (4.3.12) FOR DIFFERENT CASES.

TABLE 4.4 KPLUS-P SCATTERING.

Z	SF	SFIP	SDCS	UF	SG1	SG2
.90	.192	.192	.918	.918	.284	.254
.80	.192	.192	.916	.916	.298	.261
.70	.192	.192	.914	.914	.308	.266
.60	.192	.192	.912	.912	.315	.269
.50	.192	.192	.910	.910	.321	.272
.40	.192	.192	.908	.908	.325	.274
.30	.192	.192	.906	.906	.328	.276
.20	.192	.192	.904	.904	.330	.277
.10	.192	.192	.902	.902	.331	.278
-.00	.192	.192	.900	.900	.332	.278
-.10	.192	.192	.898	.898	.331	.278
-.20	.192	.192	.896	.896	.330	.277
-.30	.192	.192	.894	.894	.328	.276
-.40	.192	.192	.892	.892	.325	.274
-.50	.192	.192	.890	.890	.321	.272
-.60	.192	.192	.888	.888	.315	.269
-.70	.192	.192	.886	.886	.308	.266
-.80	.192	.192	.883	.883	.298	.261
-.90	.192	.192	.881	.881	.283	.254

Z -COSINE OF THE SCATTERING ANGLE.

SF -THE RIGHT HAND SIDE OF EQ. (4.2.21).

SFIP -THE RIGHT HAND SIDE OF EQ. (4.2.1) WITH THE INTEGRAND (4.2.17) MAJORIZED BY (4.2.27), (4.2.29), (4.2.31) AND (4.2.33) FOR DIFFERENT CASES.

SDCS -SQUARE ROOT OF THE DIFFERENTIAL CROSS SECTION.

UF -THE UPPER BOUND OF THE MODULI OF THE SPIN-NON-FLIP AMPLITUDE CALCULATED FROM EQ. (3.2.15A).

SG1 -THE RIGHT HAND SIDE OF EQ. (4.3.2) WITH (4.3.5).

SG2 -THE RIGHT HAND SIDE OF EQ. (4.3.2) WITH (4.3.17).

SGIP -THE RIGHT HAND SIDE OF EQ. (4.3.1) WITH THE INTEGRAND (4.3.6) MAJORIZED BY (4.3.10), (4.3.11) AND (4.3.12) FOR DIFFERENT CASES.

TABLE 4.5 KPLUS-P SCATTERING
 $P_{LAB} = .2650 \text{ GEV/C}$ $PCM = .1690 \text{ GEV/C}$

Z	SF	SFIP	SDCS	UF	SG1	SG2
.90	.214	.214	.925	.925	.315	.282
.80	.214	.213	.923	.923	.331	.290
.70	.213	.213	.920	.920	.342	.295
.60	.213	.213	.918	.917	.350	.299
.50	.213	.213	.915	.914	.356	.302
.40	.213	.213	.912	.911	.361	.305
.30	.213	.213	.909	.908	.364	.307
.20	.213	.213	.905	.905	.366	.308
.10	.213	.213	.901	.901	.368	.309
-.00	.213	.213	.898	.897	.368	.309
-.10	.213	.213	.894	.893	.368	.309
-.20	.213	.213	.889	.889	.366	.308
-.30	.213	.213	.885	.884	.364	.307
-.40	.213	.213	.880	.879	.361	.305
-.50	.213	.213	.875	.875	.356	.302
-.60	.213	.213	.870	.869	.350	.299
-.70	.213	.213	.864	.864	.342	.295
-.80	.213	.213	.858	.858	.331	.289
-.90	.213	.213	.853	.852	.315	.282

Z -COSINE OF THE SCATTERING ANGLE.

SF -THE RIGHT HAND SIDE OF EQ. (4.2.21).

SFIP -THE RIGHT HAND SIDE OF EQ. (4.2.1) WITH THE INTEGRAND (4.2.17) MAJORIZED BY (4.2.25), (4.2.27), (4.2.29), (4.2.31) AND (4.2.33) FOR DIFFERENT CASES.

SDCS -SQUARE ROOT OF THE DIFFERENTIAL CROSS SECTION.

UF -THE UPPER BOUND OF THE MODULI OF THE SPIN-NON-FLIP AMPLITUDE CALCULATED FROM EQ. (3.2.15A).

SG1 -THE RIGHT HAND SIDE OF EQ. (4.3.2) WITH (4.3.5).

SG2 -THE RIGHT HAND SIDE OF EQ. (4.3.2) WITH (4.3.17).

SGIP -THE RIGHT HAND SIDE OF EQ. (4.3.1) WITH THE INTEGRAND (4.3.6) MAJORIZED BY (4.3.10), (4.3.11) AND (4.3.12) FOR DIFFERENT CASES.

TABLE 4.6
K⁺ PLUS-P SCATTERING

Z	SF	SFIP	SDCS	UF	SG1	SG2
.90	.335	.335	.966	.965	.493	.442
.80	.335	.335	.971	.970	.518	.454
.70	.335	.335	.975	.973	.535	.462
.60	.335	.335	.979	.977	.548	.468
.50	.335	.335	.982	.979	.557	.473
.40	.335	.334	.984	.982	.564	.477
.30	.335	.334	.986	.984	.570	.480
.20	.335	.334	.987	.985	.573	.482
.10	.335	.334	.988	.986	.575	.483
.00	.335	.334	.989	.986	.576	.484
-.10	.335	.334	.988	.986	.575	.483
-.20	.335	.334	.988	.985	.573	.482
-.30	.335	.334	.986	.984	.570	.480
-.40	.335	.334	.984	.982	.564	.477
-.50	.335	.335	.982	.980	.557	.473
-.60	.335	.335	.979	.977	.548	.468
-.70	.335	.335	.976	.974	.535	.462
-.80	.335	.335	.972	.971	.518	.454
-.90	.335	.335	.967	.966	.493	.442

Z - COSINE OF THE SCATTERING ANGLE.

SF - THE RIGHT HAND SIDE OF EQ. (4.2.21).

SFIP - THE RIGHT HAND SIDE OF EQ. (4.2.1) WITH THE INTEGRAND (4.2.17) MAJORIZED BY (4.2.25), (4.2.27), (4.2.29), (4.2.31) AND (4.2.33) FOR DIFFERENT CASES.

SDCS - SQUARE ROOT OF THE DIFFERENTIAL CROSS SECTION.

UF - THE UPPER BOUND OF THE MODULI OF THE SPIN-NON-FLIP AMPLITUDE CALCULATED FROM EQ. (3.2.15A).

SG1 - THE RIGHT HAND SIDE OF EQ. (4.3.2) WITH (4.3.5).

SG2 - THE RIGHT HAND SIDE OF EQ. (4.3.2) WITH (4.3.17).

SGIP - THE RIGHT HAND SIDE OF EQ. (4.3.1) WITH THE INTEGRAND (4.3.6) MAJORIZED BY (4.3.10), (4.3.11) AND (4.3.12) FOR DIFFERENT CASES.

TABLE 4.7 KPLUS-P SCATTERING
 $P_{LAB} = .5200 \text{ GEV/C}$ $PCM = .3100 \text{ GEV/C}$

Z	IMF	SF	SDCS	UF	SG1	SGIP	SG2	IMG
.90	.515	.515	.514	1.023	1.021	.750	.674	.308
.80	.511	.515	.514	1.029	1.026	.789	.692	.421
.70	.507	.515	.513	1.035	1.029	.815	.705	.503
.60	.503	.515	.512	1.039	1.032	.834	.715	.569
.50	.499	.515	.512	1.042	1.035	.848	.722	.624
.40	.495	.515	.511	1.044	1.036	.859	.728	.672
.30	.491	.515	.511	1.045	1.037	.867	.733	.714
.20	.487	.515	.511	1.045	1.036	.871	.735	.752
.10	.483	.515	.510	1.045	1.035	.875	.738	.787
.00	.479	.515	.510	1.043	1.033	.877	.738	.818
-.10	.475	.515	.510	1.039	1.030	.875	.738	.847
-.20	.471	.515	.511	1.035	1.026	.871	.735	.873
-.30	.467	.515	.511	1.030	1.022	.867	.733	.897
-.40	.463	.515	.511	1.024	1.016	.859	.728	.919
-.50	.459	.515	.512	1.017	1.010	.847	.722	.940
-.60	.455	.515	.512	1.008	1.002	.833	.715	.958
-.70	.451	.515	.513	.999	.994	.815	.705	.975
-.80	.447	.515	.513	.988	.984	.789	.692	.990
-.90	.443	.515	.514	.976	.974	.750	.674	1.003

Z -COSINE OF THE SCATTERING ANGLE.

IMF -THE IMAGINARY PART OF SPIN NON-FLIP AMPLITUDE CALCULATED FROM THE PHASE SHIFTS DIRECTLY.

SF -THE RIGHT HAND SIDE OF EQ. (4.2.21).

SFIP -THE RIGHT HAND SIDE OF EQ. (4.2.1) WITH THE INTEGRAND (4.2.17) MAJORIZED BY (4.2.25), (4.2.27), (4.2.29), (4.2.31) AND (4.2.33) FOR DIFFERENT CASES.

SDCS-SQUARE ROOT OF THE DIFFERENTIAL CROSS SECTION.

UF -THE UPPER BOUND OF THE MODULI OF THE SPIN-NON-FLIP AMPLITUDE CALCULATED FROM EQ. (3.2.15A).

SG1 -THE RIGHT HAND SIDE OF EQ. (4.3.2) WITH (4.3.5).

SG2 -THE RIGHT HAND SIDE OF EQ. (4.3.2) WITH (4.3.17).

SGIP -THE RIGHT HAND SIDE OF EQ. (4.3.1) WITH THE INTEGRAND (4.3.6) MAJORIZED BY (4.3.10), (4.3.11) AND (4.3.12) FOR DIFFERENT CASES.

IMG -THE IMAGINARY PART OF SPIN FLIP AMPLITUDE CALCULATED FROM THE PHASE SHIFTS DIRECTLY.

SUMMARY AND DISCUSSION

In this thesis we have compared Cutkosky phase shifts and CERN α , β , γ phase shifts for $K^+ p$ scattering at 13 different energies between $P_{lab.} = 0.87$ Gev/c and 1.89 Gev/c with the bounds of the theoretical quantities relative moduli of the spin non-flip and spin flip amplitude r , relative phase α , moduli of spin non-flip amplitude $|f|$ and spin flip amplitude $|g| \sin \theta$, product of the moduli of spin non-flip amplitude and spin flip amplitude m and sum of the moduli of spin non-flip amplitude and spin flip amplitude s . The comparisons are shown in figures 2, 3, 4, 5 and 6. The features are discussed. Using these inequalities also in the unitarity condition different majorizations for the imaginary parts of spin non-flip and spin flip amplitudes are obtained. For the imaginary part of the spin non-flip amplitude the results of the majorizations are shown in (4.2.22), (4.2.16), (4.2.21). Expression (4.2.17) is majorized for different cases which are possible with forms (4.2.25), (4.2.27), (4.2.29), (4.2.31), (4.2.33). Those expressions represent an improvement over the form (4.2.21). For the imaginary part of the spin flip amplitude the bound is shown in (4.3.2) one factor of which is majorized alternately by (4.3.5) or (4.3.17). Expression (4.3.6) is majorized by (4.3.10), (4.3.11), (4.3.12) in different cases respectively. The numerical results for $\pi^+ p$, $\pi^- p$ and $K^+ p$ below the inelastic threshold are presented in tables 2, 3 and 4.

In our majorization program there is still room for improvement. For example, when we majorize F of (4.2.17) we replace $\cos(\Delta\alpha + \beta)$ and $\cos \beta$ by one. This is a complete loss of information about relative

phase. If one considers F as a function of three variables $|f(z')|$, $|f(z'')|$ and β (instead of only moduli) using bounds both of $|f|$ and relative phase one would expect better bounds. However the process is very complicated being a three variable case. If one considers the fact that everything we have done is in two variables the complications can be appreciated.

On the other hand the inequalities of f , $\sin \alpha$, $|f|$, $|g|\sin \theta$, m and s are obtained by using the relations of the scattering amplitudes and experimental measurable quantities D , P , R and A . Those inequalities are rigorous and model independent. The upper bounds of the imaginary parts of the scattering amplitudes are found by using these inequalities in the unitarity condition. But the analyticity property of the scattering amplitude and Mandelstam representation etc., have not been used. Adding these properties one can expect that better bound will be obtained.

APPENDIX I

THE PARTIAL WAVES IN THE CASE OF THE ANTI-LINEAR TRANSFORMATION

From the partial wave expansion of the spin non-flip and spin flip amplitudes (2.2.4) and (2.2.5)

$$f(\theta) = \frac{1}{q_{\text{C.M.}}} \sum_{l=0}^L [(\ell + 1)f'_{\ell+} + \ell f'_{\ell-}] P_{\ell}(\cos \theta) \quad (2.2.4)$$

$$g(\theta) = \frac{\sin \theta}{q_{\text{C.M.}}} \sum_{l=0}^L (f'_{\ell+} - f'_{\ell-}) P'_{\ell}(\cos \theta) \quad (2.2.5)$$

the anti-linear transformation (2.2.8)

$$f(\theta) \rightarrow -f^*(\theta) \quad (2.2.8)$$

$$g(\theta) \rightarrow g^*(\theta)$$

is equivalent to

$$\sum_{l=0}^L [(\ell + 1)f'_{\ell+} + \ell f'_{\ell-}] P_{\ell}(\cos \theta) = - \sum_{l=0}^L [(\ell + 1)f'^*_{\ell+} + \ell f'^*_{\ell-}] P_{\ell}(\cos \theta) \quad (\text{A.1.1})$$

$$\sum_{l=0}^L (f'_{\ell+} - f'_{\ell-}) P'_{\ell}(\cos \theta) = \sum_{l=0}^L (f'^*_{\ell+} - f'^*_{\ell-}) P'_{\ell}(\cos \theta) \quad (\text{A.1.2})$$

This means

$$(\ell + 1)f'_{\ell+} + \ell f'_{\ell-} = -(\ell + 1)f'^*_{\ell+} - \ell f'^*_{\ell-} \quad (\text{A.1.3})$$

(A.1.4)

Solve (A.1.3) and (A.1.4) we have,

$$\hat{v}_+^* = -(\hat{v}_+^* + 2\epsilon v_0)/(\Delta + 1)$$

(2.2.10)

$$\hat{v}_-^* = -12(\epsilon + 1)\hat{v}_+^* + \epsilon_-^* 1/(2\Delta + 1)$$

APPENDIX 2

THE PARTIAL WAVES IN THE CASE OF THE LINEAR TRANSFORMATION

The linear transformation (2.2.4) with $\psi = 0$.

$$\begin{pmatrix} f'(\theta) \\ g(\theta) \end{pmatrix} = \begin{pmatrix} \cos \theta & \sin \theta \\ -\sin \theta & \cos \theta \end{pmatrix} \begin{pmatrix} f(\theta) \\ g(\theta) \end{pmatrix} \quad (2.2.9)$$

means

$$f'(\theta) = \cos \theta f(\theta) + \sin \theta g(\theta) \quad (A.2.1)$$

$$g'(\theta) = -\sin \theta f(\theta) + \cos \theta g(\theta) \quad (A.2.2)$$

In terms of partial wave amplitudes (A.2.1) becomes

$$\begin{aligned} \sum_{\ell} [(\ell+1)f'_{\ell+} + \ell f'_{\ell-}] P_{\ell}(\cos \theta) &= \cos \theta \sum_{\ell} [(\ell+1)f_{\ell+} + \ell f_{\ell-}] \\ &\times P_{\ell}(\cos \theta) + \sin^2 \theta \sum_{\ell} (f_{\ell+} - f_{\ell-}) \frac{d P_{\ell}(\cos \theta)}{d \cos \theta} \end{aligned} \quad (A.2.3)$$

We use the recursion relation for Legendre Polynomials.

$$\sin^2 \theta \frac{d P_{\ell}(\cos \theta)}{d \cos \theta} = (\ell+1)[\cos \theta P_{\ell}(\cos \theta) - P_{\ell+1}(\cos \theta)] \quad (A.2.4)$$

$$\cos \theta P_\ell(\cos \theta) = \frac{1}{2\ell + 1} [(\ell + 1)P_{\ell+1}(\cos \theta) + \ell P_{\ell-1}(\cos \theta)] \quad (\text{A.2.5})$$

$$P_\ell(\cos \theta) = \frac{1}{2\ell + 1} \left[\frac{d P_{\ell+1}(\cos \theta)}{d \cos \theta} - \frac{d P_{\ell-1}(\cos \theta)}{d \cos \theta} \right] \quad (\text{A.2.6})$$

Then the right hand side of (A.2.3) has

$$\begin{aligned} & \cos \theta \sum [(\ell + 1)f_{\ell+1}^+ + \ell f_{\ell-1}^-] P_\ell(\cos \theta) + \sum (\ell + 1)(f_{\ell+1}^+ - f_{\ell-1}^-) \\ & \times [\cos \theta P_\ell(\cos \theta)^2 - P_{\ell+1}(\cos \theta)] \\ &= \cos \theta \sum [(2\ell + 2)f_{\ell+1}^+ - f_{\ell-2}^-] P_\ell(\cos \theta) - \sum (\ell + 1)(f_{\ell+1}^+ - f_{\ell-1}^-) \\ & \times P_{\ell+1}(\cos \theta) \\ &= \sum [(2\ell + 2)f_{\ell+1}^+ - f_{\ell-2}^-] \frac{1}{2\ell + 1} [(\ell + 1)P_{\ell+1}(\cos \theta) \\ & + \ell P_{\ell-1}(\cos \theta)] - \sum (\ell + 1)(f_{\ell+1}^+ - f_{\ell-1}^-) P_{\ell+1}(\cos \theta) \\ &= \sum \left[\frac{\ell + 1}{2\ell + 1} f_{\ell+1}^+ + \frac{2\ell(\ell + 1)}{2\ell + 1} f_{\ell-2}^- \right] P_{\ell+1}(\cos \theta) + \sum \frac{2\ell(\ell + 1)}{2\ell + 1} f_{\ell+1}^+ \\ & - \frac{\ell}{2\ell + 1} f_{\ell-1}^- P_{\ell-1}(\cos \theta) \\ &= \sum \left[\frac{\ell}{2\ell - 1} f_{(\ell-1)+}^+ + \frac{2(\ell - 1)}{2\ell - 1} f_{(\ell-1)-}^- \right] P_\ell(\cos \theta) \\ & + \left[\frac{2(\ell + 1)(\ell + 2)}{2\ell + 3} f_{(\ell+1)+}^+ - \frac{1 + 1}{2\ell + 3} f_{(\ell+1)-}^- \right] P_\ell(\cos \theta) \end{aligned}$$

Compare with the left hand side of (A.2.3) we have

$$\begin{aligned} (\ell + 1) f'_{\ell+} + \ell f'_{\ell-} &= \frac{\ell}{2\ell - 1} f_{(\ell-1)+} + \frac{2\ell(\ell - 1)}{2\ell - 1} f_{(\ell-1)-} \\ &\quad + \frac{2(\ell + 1)(\ell + 2)}{2\ell + 3} f_{(\ell+1)+} - \frac{\ell + 1}{2\ell + 3} f_{(\ell+1)-} \end{aligned} \quad (\text{A.2.7})$$

Also, in terms of partial wave amplitudes (A.2.2) becomes

$$\begin{aligned} \sin \theta \sum_{\ell} (f'_{\ell+} - f'_{\ell-}) \frac{d P_{\ell}(\cos \theta)}{d(\cos \theta)} &= -\sin \theta \sum_{\ell} [(\ell + 1) f'_{\ell+} + \ell f'_{\ell-}] \\ &\quad \times P_{\ell}(\cos \theta) + \cos \theta \sin \theta \sum_{\ell} (f'_{\ell+} - f'_{\ell-}) \frac{d P_{\ell}(\cos \theta)}{d \cos \theta} \end{aligned}$$

Using (A.2.4), (A.2.5) and (A.2.6) and doing some simplifications we have

$$\begin{aligned} f'_{\ell+} - f'_{\ell-} &= -\frac{1}{2\ell + 1} f_{(\ell-1)+} - \frac{2(\ell - 1)}{2\ell - 1} f_{(\ell-1)-} \\ &\quad + \frac{2(\ell + 2)}{2\ell + 3} f_{(\ell+1)+} - \frac{1}{2\ell + 3} f_{(\ell+1)-} \end{aligned} \quad (\text{A.2.8})$$

Solving equations (A.2.7) and (A.2.8) for $f'_{\ell+}$ and $f'_{\ell-}$ we get

$$f'_{\ell+} = [2(\ell + 2)f_{(\ell+1)+} - f_{(\ell+1)-}] / (2\ell + 3) \quad (2.2.11)$$

$$f'_{\ell-} = [2(\ell - 1)f_{(\ell-1)+} + f_{(\ell-1)-}] / (2\ell - 1)$$

APPENDIX 3

THE BOUNDS FOR THE MODULI OF THE SPIN NON-FLIP AND SPIN FLIP AMPLITUDES

For the right hand side of the inequality (2.2.13) we have

$$\begin{aligned}
 \frac{D}{1 + \frac{\sin^2 \theta}{r_+^2}} &= \frac{D}{1 + \frac{\sin^2 \theta}{\frac{\sin^2 \theta}{|P|^2} (1 + \sqrt{1 - P^2})^2}} \\
 &= \frac{D(1 + \sqrt{1 - P^2})^2}{(1 + \sqrt{1 - P^2})^2 + P^2} \\
 &= \frac{D(1 + \sqrt{1 - P^2})^2}{2(1 + \sqrt{1 - P^2})} \\
 &= \frac{D}{2}(1 + \sqrt{1 - P^2}) \tag{A.3.1}
 \end{aligned}$$

For the right hand side of the inequality (2.2.14) we have

$$\begin{aligned}
 \frac{D}{1 + \frac{r_-^2}{\sin^2 \theta}} &= \frac{D}{1 + \frac{\sin^2 \theta}{\frac{|P|^2}{\sin^2 \theta} (1 - \sqrt{1 - P^2})^2}} \\
 &= \frac{D |P|^2}{|P|^2 + (1 - \sqrt{1 - P^2})^2} \\
 &= \frac{D |P|^2}{2(1 - \sqrt{1 - P^2})}
 \end{aligned}$$

$$\begin{aligned}
 &= \frac{D|P|^2(1 + \sqrt{1 - P^2})}{2[1 - (1 - P^2)]} \\
 &= \frac{D(1 + \sqrt{1 - P^2})}{2} \tag{A.3.2}
 \end{aligned}$$

and then we get

$$|f|_+ = |g|_+ \sin \theta = \sqrt{\frac{D}{2}(1 + \sqrt{1 - P^2})} \tag{2.2.15a}$$

For the right hand side of the inequality (2.2.13) we have

$$\begin{aligned}
 \frac{D}{1 + \frac{\sin^2 \theta}{2}} &= \frac{D}{1 + \frac{\sin^2 \theta}{\frac{|P|^2}{2}(1 - \sqrt{1 - P^2})^2}} \\
 &= \frac{D(1 - \sqrt{1 - P^2})^2}{(1 - \sqrt{1 - P^2})^2 + |P|^2} \\
 &= \frac{D(1 - \sqrt{1 - P^2})^2}{2(1 - \sqrt{1 - P^2})} \\
 &= \frac{D}{2}(1 - \sqrt{1 - P^2}) \tag{A.3.3}
 \end{aligned}$$

For the left hand side of the inequality (2.2.14) we have

$$\begin{aligned}
 \frac{D}{1 + \frac{r^2}{\sin^2 \theta}} &= \frac{D}{1 + \frac{\sin^2 \theta (1 + \sqrt{1 - P^2})^2}{\sin^2 \theta}} \\
 &= \frac{D|P|^2}{|P|^2 + (1 + \sqrt{1 - P^2})^2} \\
 &= \frac{D|P|^2}{2(1 + \sqrt{1 - P^2})} \\
 &= \frac{D}{2}(1 - \sqrt{1 - P^2}) \quad (\text{A.3.4})
 \end{aligned}$$

Finally we get

$$|f| \cdot |g| \cdot \sin \theta = \sqrt{\frac{D}{2}(1 - \sqrt{1 - P^2})} \quad (2.2.15b)$$

APPENDIX 4
THE BOUNDS OF s DEFINED AS (3.2.6)

We solve

$$\frac{\partial s}{\partial |f|} = 0 \quad \text{where } s = |f| + \sqrt{D - |f|^2}$$

$$|f| = \sqrt{\frac{D}{2}}$$

$$\text{and } s = \sqrt{2D}$$

It is the extreme point of s

The other extreme points are on the boundary

$$|f| = |f|_+ = \sqrt{\frac{D}{2}(1 + \sqrt{1 - P^2})}$$

$$s = |f| + \sqrt{D - |f|^2}$$

$$= \sqrt{D(1 + |P|)}$$

$$\text{and } |f| = |f|_- + \sqrt{\frac{D}{2}(1 - \sqrt{1 + P^2})}$$

$$\text{also } s = \sqrt{D(1 + |P|)}$$

It turns out s are the same in the boundary points of $|f|$. It is easy to see that $s = \sqrt{2D}$ is the maximum and $s = \sqrt{D(1 + |P|)}$ is the minimum.

APPENDIX 5

THE DERIVATION OF THE COUPLED UNITARITY EQUATIONS FOR SPIN 0
AND SPIN $\frac{1}{2}$ SCATTERING

From equation (4.1.31)

$$\operatorname{Im} \begin{pmatrix} f(\theta) & g(\theta)\sin\theta \\ -g(\theta)\sin\theta & f(\theta) \end{pmatrix} = \frac{q_{\text{C.M.}}}{4\pi} \int d\vec{n} \begin{pmatrix} M_{11} & M_{12} \\ M_{21} & M_{22} \end{pmatrix} \begin{pmatrix} N_{11} & N_{12} \\ N_{21} & N_{22} \end{pmatrix}$$

so we have four equations

$$\operatorname{Im} f(\theta) = \frac{q_{\text{C.M.}}}{4\pi} \int d\vec{n} (M_{11}N_{11} + M_{12}N_{21}) \quad (\text{A.5.1})$$

$$\operatorname{Im} g(\theta)\sin\theta = \frac{q_{\text{C.M.}}}{4\pi} \int d\vec{n} (M_{12}N_{12} + M_{12}N_{22}) \quad (\text{A.5.2})$$

$$-\operatorname{Im} g(\theta)\sin\theta = \frac{q_{\text{C.M.}}}{4\pi} \int d\vec{n} (M_{21}N_{11} + M_{22}N_{21}) \quad (\text{A.5.3})$$

$$\operatorname{Im} f(\theta) = \frac{q_{\text{C.M.}}}{4\pi} \int d\vec{n} (M_{21}N_{12} + M_{22}N_{22}) \quad (\text{A.5.4})$$

where $M_{11}, M_{12}, M_{21}, M_{22}, N_{11}, N_{12}, N_{21}, N_{22}$ are defined in (4.1.32), (4.1.33), (4.1.34), (4.1.32), (4.1.26), (4.1.27), (4.1.28) and (4.1.29) respectively

$$M_{11} = M_{22} = f^*(\theta'')$$

$$M_{12} = g^*(\theta)(\sin\theta''\cos\phi'' - i\sin\theta''\sin\phi'')$$

$$M_{21} = -g^*(\theta)(\sin \theta'' \cos \phi'' + i \sin \theta'' \sin \phi'')$$

$$N_{11} = f(\theta') - i' g(\theta') \sin \theta \sin \theta'' \sin \theta''$$

$$\begin{aligned} N_{12} = & -g(\theta') (\sin \theta'' \cos \theta \cos \phi'' - \sin \theta \cos \theta'') \\ & + i g(\theta') \cos \theta \sin \theta'' \sin \phi'' \end{aligned}$$

$$\begin{aligned} N_{21} = & g(\theta') (\sin \theta'' \cos \theta \cos \phi'' - \sin \theta \cos \theta'') \\ & + i g(\theta') \cos \theta \sin \theta'' \sin \phi'' \end{aligned}$$

$$N_{22} = f(\theta') + i g(\theta') \sin \theta \sin \theta'' \sin \phi''$$

Then

$$M_{11} N_{11} + M_{12} N_{21}$$

$$= f^*(\theta'') [f(\theta') - i g(\theta') \sin \theta \sin \theta'' \sin \phi'']$$

$$+ g^*(\theta'') g(\theta') (\sin \theta'' \cos \phi'' - i \sin \theta'' \sin \phi'')$$

$$\times [(\sin \theta'' \cos \theta \cos \phi'' - \sin \theta \cos \theta'') + i \cos \theta \sin \theta'' \sin \phi'']$$

$$= f^*(\theta'') f(\theta') + g^*(\theta'') g(\theta') [\cos \theta \sin^2 \theta'' \cos^2 \phi'']$$

$$+ \sin \theta \sin \theta'' \cos \theta'' \cos \phi'' + \cos \theta \sin^2 \theta'' \sin^2 \phi'']$$

$$\begin{aligned}
 & - i f^*(\theta'') g(\theta') \sin \theta \sin \theta'' \sin \phi'' + i g^*(\theta'') g(\theta') \sin \theta \sin \theta'' \\
 & \quad \times \cos \theta'' \sin \phi'' \\
 & = f^*(\theta'') f(\theta') + g^*(\theta'') g(\theta') [z(1 - z''^2) - z''(z' - zz'')] + B \\
 & = f^*(\theta'') f(\theta') + g^*(\theta'') g(\theta') (z - z'z'') + B
 \end{aligned}$$

where $B = i g^*(\theta'') g(\theta') \sin \theta \sin \theta'' \cos \theta'' \sin \phi''$

$$\begin{aligned}
 & - i f^*(\theta'') g(\theta') \sin \theta \sin \theta'' \sin \phi''
 \end{aligned}$$

and we have used the relation

$$\cos \theta' = \cos \theta \cos \theta'' + \sin \theta \sin \theta'' \cos \phi''$$

Substitute it in equation (A.5.1), we have

$$\begin{aligned}
 \text{Im } f(\theta) &= \frac{q \text{C.M.}}{4\pi} \int d\vec{n} [f^*(\theta'') f(\theta') + g^*(\theta'') g(\theta') (z - z'z'')] \\
 &+ \frac{q \text{C.M.}}{4\pi} \int d\vec{n} \cdot B
 \end{aligned} \tag{A.5.5}$$

Next we calculate

$$M_{21} N_{12} + M_{22} N_{22}$$

$$= g^*(\theta'') g(\theta') (\sin \theta'' \cos \phi'' + i \sin \theta'' \sin \phi'') [\sin \theta'' \cos \theta \cos \phi'']$$

$$\begin{aligned}
& - \sin \theta \cos \theta'') - i \cos \theta \sin \theta'' \sin \phi''] + f^*(\theta'') [f(\theta') \\
& + ig(\theta') \sin \theta \sin \theta'' \sin \phi''] \\
& = f^*(\theta'') f(\theta') + g^*(\theta'') g(\theta') [\cos \theta \sin^2 \theta'' \cos^2 \phi'' \\
& - \sin \theta \sin \theta'' \cos \theta'' \cos \phi'' + \cos \theta \sin^2 \theta'' \sin^2 \phi''] \\
& + ig^*(\theta'') g(\theta') \sin \theta'' \sin \theta \sin \phi'' - ig^*(\theta'') g(\theta') \sin \theta \sin \theta'' \\
& \times \cos \theta'' \sin \phi''] \\
& = f^*(\theta'') f(\theta') + g^*(\theta'') g(\theta') (z - z' z'') - B
\end{aligned}$$

and substitute in (A.5.4) we have

$$\begin{aligned}
\text{Im } f(\theta) &= \frac{q_{\text{C.M.}}}{4\pi} \int d\vec{n} [f^*(\theta'') f(\theta') + g^*(\theta'') g(\theta') (z - z' z'')] \\
&= \frac{q_{\text{C.M.}}}{4\pi} \int d\vec{n} B
\end{aligned} \tag{A.5.6}$$

Compare (A.5.5) and (A.5.6) then the last term of the right hand side must be vanished. Finally we get

$$\text{Im } f(\theta) = \frac{q_{\text{C.M.}}}{4\pi} \int d\vec{n} [f^*(\theta'') f(\theta') + g^*(\theta'') g(\theta') (z - z' z'')] \tag{4.1.35}$$

We calculate

$$M_{11}N_{12} + M_{12}N_{22}$$

$$= -f^*(\theta'')g(\theta') [(\sin \theta'' \cos \theta \cos \phi'' - \sin \theta \cos \theta'')$$

$$- i \cos \theta \sin \theta'' \sin \phi''] + g^*(\theta'') (\sin \theta'' \cos \phi'' - i \sin \theta'' \sin \theta'')$$

$$\times [f(\theta') + ig(\theta') \sin \theta \sin \theta'' \sin \phi'']$$

$$= f^*(\theta'')g(\theta') \frac{\sin^2 \theta \cos \theta'' - \cos \theta \sin \theta \sin \theta'' \cos \phi''}{\sin \theta}$$

$$+ g^*(\theta'')f(\theta') \frac{\sin \theta \sin \theta'' \cos \phi''}{\sin \theta}$$

$$+ g^*(\theta'')g(\theta') \frac{\sin^2 \theta \sin^2 \theta'' \sin^2 \phi''}{\sin \theta} + if^*(\theta'')g(\theta') \cos \theta \sin \theta''$$

$$\times \sin \phi'' - ig^*(\theta'')f(\theta') \sin \theta'' \sin \phi''$$

$$+ ig^*(\theta'')g(\theta') \sin \theta \sin^2 \theta'' \sin \phi'' \cos \phi''$$

$$= f^*(\theta'')g(\theta') \frac{(1 - z^2)z'' - z(z' - zz'')}{\sqrt{1 - z^2}} + g^*(\theta'')f(\theta') \frac{z' - zz''}{\sqrt{1 - z^2}}$$

$$+ g^*(\theta'')g(\theta') \frac{(1 - z^2)(1 - z''^2) - (z' - zz'')^2}{\sqrt{1 - z^2}} + c$$

$$= f^*(\theta'')g(\theta') \frac{z'' - zz'}{\sqrt{1 - z^2}} + g^*(\theta'')f(\theta') \frac{z' - zz''}{\sqrt{1 - z^2}}$$

$$+ g^*(\theta')g(\theta') \frac{1 - z^2 - z'^2 - z''^2 + 2zz'z''}{\sqrt{1 - z^2}}$$

where $C = i f^*(\theta')g(\theta')\cos \theta'' \sin \theta'' \sin \phi'' - i g^*(\theta')f(\theta')\sin \theta'' \sin \theta'' \sin \phi''$

$$+ i g^*(\theta')g(\theta')\sin \theta'' \sin^2 \theta'' \sin \phi'' \cos \phi''.$$

Substitute in (A.5.2) we have

$$\begin{aligned} \operatorname{Im} g(\theta) \sin \theta &= \frac{q_{C.M.}}{4\pi} \int d\theta [f^*(\theta')g(\theta') \frac{z'' - zz'}{\sqrt{1 - z^2}} \\ &\quad + g^*(\theta')f(\theta') \frac{z' - zz''}{\sqrt{1 - z^2}} + g^*(\theta')g(\theta')] \\ &\quad - \frac{1 - z^2 - z'^2 - z''^2 + 2zz'z''}{\sqrt{1 - z^2}}] + \frac{q_{C.M.}}{4\pi} \int d\theta [c_1 e^{iz\theta}] \end{aligned} \quad (\text{A.5.7})$$

Next we calculate

$$M_{21}N_{11} + M_{22}N_{21}$$

$$= -g^*(\theta)(\sin \theta'' \cos \phi'' + i \sin \theta'' \sin \phi'') [f(\theta')]$$

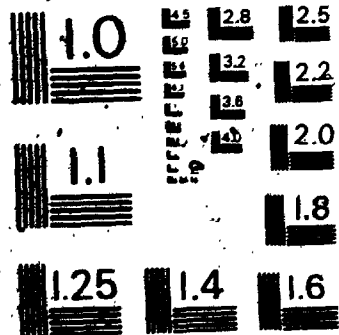
$$- ig(\theta)\sin \theta'' \sin \theta'' \sin \phi'') + f''(\theta')g(\theta')[(\sin \theta'' \cos \theta'' \cos \phi''$$

$$- \sin \theta'' \cos \theta'') + i \cos \theta'' \sin \theta'' \sin \phi'')$$

3

3

OF/DE



35Y-RESOLUTION TEST CHART
AL BUREAU OF STANDARDS 1963-A

$$\begin{aligned}
&= -f^*(\theta'')g(\theta')(\sin \theta \cos \theta'' + \cos \theta \sin \theta'' \cos \phi'') \\
&\quad - g^*(\theta'')f(\theta')\sin \theta'' \cos \phi'' - g^*(\theta'')g(\theta')\sin \theta \sin^2 \theta'' \sin^2 \phi'' \\
&\quad + i f^*(\theta'')g(\theta')\cos \theta \sin \theta'' \sin \phi'' - i g^*(\theta'')f(\theta')\sin \theta'' \sin \phi'' \\
&\quad + i g^*(\theta'')g(\theta')\sin \theta \sin^2 \theta'' \sin \phi'' \cos \phi'' \\
&= -[f^*(\theta'')g(\theta') \frac{z'' - zz'}{\sqrt{1-z^2}} + g^*(\theta'')f(\theta') \frac{z' - zz''}{\sqrt{1-z^2}} \\
&\quad + g^*(\theta'')g(\theta') \frac{1 - z^2 - z'^2 - z''^2 + 2zz'z''}{\sqrt{1-z^2}} - c]
\end{aligned}$$

Substitute in (A.5.3) we have

$$\begin{aligned}
\text{Im } g(\theta) &\stackrel{q \text{C.M.}}{=} \frac{q \text{C.M.}}{4\pi} \int d\vec{n} [f^*(\theta'')g(\theta') \frac{z'' - zz'}{\sqrt{1-z^2}} \\
&\quad + g^*(\theta'')f(\theta') \frac{z' - zz''}{\sqrt{1-z^2}} + g^*(\theta'')g(\theta') \\
&\quad \times \frac{1 - z^2 - z'^2 - z''^2 + 2zz'z''}{\sqrt{1-z^2}}] \frac{q \text{C.M.}}{4\pi} \int d\vec{n} \cdot c
\end{aligned} \tag{A.5.8}$$

Compare (A.5.7) and (A.5.8) then the last term of the right hand side must be zero. Finally we get

$$\begin{aligned} \text{Im } g(\theta) = & \frac{q_{C.M.}}{4\pi} \int d\vec{n} [f^*(\theta'')g(\theta')] \frac{z'' - zz'}{\sqrt{1 - z^2}} \\ & + g^*(\theta'')f(\theta') \frac{z' - zz''}{\sqrt{1 - z^2}} \\ & + g^*(\theta'')g(\theta') \frac{1 - z^2 - z'^2 - z''^2 + 2zz'z''}{\sqrt{1 - z^2}}. \end{aligned}$$

(4.1.36a)

APPENDIX 6

THE MAXIMUM VALUE OF $F(\beta)$ DEFINED AS (4.2.8) WITH $a = 1$

From (4.2.9)

$$\tan \beta = \frac{\sin \Delta\alpha}{\pm 1 - \cos \Delta\alpha} \quad (4.2.9)$$

there are two cases

<1>

$$\begin{aligned}\tan \beta &= \frac{\sin \Delta\alpha}{1 - \cos \Delta\alpha} \\ &= \cot \frac{\Delta\alpha}{2}\end{aligned}$$

Hence

$$\cos \beta = \pm \sin \frac{\Delta\alpha}{2} \quad \sin \beta = \pm \cos \frac{\Delta\alpha}{2}$$

then

$$|\cos \beta| = \sqrt{\frac{1 - \cos \Delta\alpha}{2}} \quad (A.6.1)$$

and $\cos(\Delta\alpha + \beta) = \cos \Delta\alpha \cos \beta - \sin \Delta\alpha \sin \beta$

$$= \mp \sin \frac{\Delta\alpha}{2}$$

$$|\cos(\Delta\alpha + \beta)| = \sqrt{\frac{1 - \cos \Delta\alpha}{2}} \quad (\text{A.6.2})$$

So

$$F(\beta) = |\cos(\Delta\alpha + \beta)| + |\cos \beta|$$

$$= \sqrt{2(1 - \cos \Delta\alpha)} \quad (\text{A.6.3})$$

<2>

$$\tan \beta = \frac{\sin \Delta\alpha}{-1 - \cos \Delta\alpha}$$

$$= -\tan \frac{\Delta\alpha}{2}$$

$$\text{Hence } \cos \beta = \pm \cos \frac{\Delta\alpha}{2} \quad \sin \beta = \sin \frac{\Delta\alpha}{2}$$

$$\text{then } |\cos \beta| = \sqrt{\frac{1 + \cos \Delta\alpha}{2}} \quad (\text{A.6.4})$$

and

$$\cos(\beta + \Delta\alpha) = \pm \cos \frac{\Delta\alpha}{2}$$

$$\text{then } |\cos(\beta + \Delta\alpha)| = \sqrt{\frac{1 + \cos \Delta\alpha}{2}} \quad (\text{A.6.5})$$

So

$$F(\beta) = |\cos(\beta + \Delta\alpha)| + |\cos \beta|$$

$$= \sqrt{2(1 + \cos \Delta\alpha)} \quad (\text{A.6.6})$$

Combine (A.6.3) and (A.6.6) we have

$$F(\beta) = \sqrt{2(1 \pm \cos \Delta\alpha)} \quad (4.2.10a)$$

APPENDIX 7

THE MAXIMUM VALUE OF $F(\beta)$ IN (4.2.8) WITH $a \leq 1$

The maximum of

$$F(\beta) = |\cos(\Delta\alpha + \beta)| + a|\cos \beta|$$

occurs at

$$-\sin(\Delta\alpha + \beta) + a \sin \beta = 0$$

this leads to

$$|\cos \beta| = \frac{|\cos \Delta\alpha + a|}{\sqrt{1 + a^2 - 2a \cos \Delta\alpha}}$$

$F(\beta)$ then becomes

$$F(\beta) = \frac{1 + a \cos \Delta\alpha + a|\cos \Delta\alpha + a|}{\sqrt{1 + a^2 - 2a \cos \Delta\alpha}}$$

The following cases arise:

(I) (a) sign (-), $\cos \Delta\alpha > 0$ $a < \cos \Delta\alpha$:

In this case

$$F(\beta) = \frac{1 - a^2}{\sqrt{1 + a^2 - 2a \cos \Delta\alpha}}$$

(b) sign (-) $\cos \Delta\alpha > 0$ $a > |\cos \Delta\alpha|$

In this case

$$F(\beta) = \sqrt{1 + a^2 - 2a \cos \Delta\alpha}$$

(c) sign (-) $\cos \Delta\alpha < 0$

$$F(\beta) = \sqrt{1 + a^2 + 2a|\cos \Delta\alpha|}$$

(II) (a) sign (+) $\cos \Delta\alpha > 0$

$$F(\beta) = \sqrt{1 + a^2 + 2a|\cos \Delta\alpha|}$$

(b) sign (+) $\cos \Delta\alpha < 0$ $a < |\cos \Delta\alpha|$

$$F(\beta) = \frac{1 - a^2}{\sqrt{1 + a^2 - 2a|\cos \Delta\alpha|}}$$

(c) sign (+) $\cos \Delta\alpha < 0$ $a > |\cos \Delta\alpha|$

$$F(\beta) = \sqrt{1 + a^2 - 2a|\cos \Delta\alpha|}$$

It is readily shown that if $\cos \Delta\alpha > 0$, II (a) gives a larger $F(\beta)$

than I (a) or I (b). Similarly if $\cos \Delta\alpha < 0$, I (c) gives a larger $F(\beta)$ than II (b) or II (c). Thus when $\cos \Delta\alpha > 0$ we choose II (a); when $\cos \Delta\alpha < 0$ we choose I (c). In the either case

$$F(\beta) = \sqrt{1 + a^2 + 2a|\cos \Delta\alpha|}$$

APPENDIX 8

THE DISCUSSION OF THE FUNCTION G DEFINED AS (4.2.18)

We investigate the function

$$G = xy + a \sqrt{1 - x^2} \sqrt{1 - y^2} \quad (A.8.1)$$

in the domain

$$0 \leq x \leq 1$$

$$\text{and } 0 \leq a \leq 1$$

$$0 \leq y \leq 1$$

And

$$\frac{\partial G}{\partial x} = y - ax(1 - y^2)^{\frac{1}{2}}(1 - x^2)^{-\frac{1}{2}} \quad (A.8.2)$$

$$\frac{\partial^2 G}{\partial x^2} = -a(1 - y^2)^{\frac{1}{2}}(1 - x^2)^{-\frac{3}{2}} \leq 0 \quad (A.8.3)$$

Since this function is symmetric with respect to x and y we find from the equation above

$$\frac{\partial G}{\partial y} = x - ay(1 - x^2)^{\frac{1}{2}}(1 - y^2)^{-\frac{1}{2}} \quad (A.8.4)$$

$$\frac{\partial^2 G}{\partial y^2} = -a(1 - x^2)^{\frac{1}{2}}(1 - y^2)^{-\frac{3}{2}} \leq 0 \quad (A.8.5)$$

and $\frac{\partial^2 G}{\partial x \partial y} = 1 + axy(1 - x^2)^{-\frac{1}{2}}(1 - y^2)^{-\frac{1}{2}}$ (A.8.6)

So the point $x = 0, y = 0$ is a saddle point for $a < 1$. When $a = 1$ G becomes G' , where G' is

$$G' = xy + \frac{1}{2}(1-x^2)^{\frac{1}{2}}(1-y^2)^{\frac{1}{2}} \quad (\text{A.8.11})$$

The maximum value of this function is at $x = y$ for a fixed value of y . In that case

$$G' = y^2 + (1-y^2) = 1$$

This means that G' is a constant and equals one on $x = y$ line. That is

$$G_{\max} = 1 \quad (\text{A.8.12})$$

From (A.8.2) and (A.8.3) when $a < 1$ the extremum of G when y is fixed is at

$$x = \sqrt{\frac{y^2}{y^2(1-a^2) + a^2}}$$

and

$$G_{(\text{y fixed})}^{\max} = \sqrt{y^2(1-a^2) + a^2}$$

This function is an increasing function in the region $0 \leq y \leq 1$.

Hence the largest value of G is at $y = 1$ (also $x = 1$) and

We are looking for the extremum. So we solve the equations

$$\frac{\partial F}{\partial x} = 0 \quad \text{and} \quad \frac{\partial F}{\partial y} = 0$$

From (A.8.2) and (A.8.4) we have

$$y = ax(1 - y^2)^{\frac{1}{2}}(1 - x^2)^{-\frac{1}{2}} \quad (\text{A.8.7})$$

$$x = zy(1 - x^2)^{\frac{1}{2}}(1 - y^2)^{-\frac{1}{2}} \quad (\text{A.8.8})$$

We square both sides of (A.8.7) and (A.8.8), and then multiply them with $(1 - x^2)$ and $(1 - y^2)$ respectively. We find

$$y^2(1 - x^2) = a^2 x^2(1 - y^2) \quad (\text{A.8.9})$$

$$x^2(1 - y^2) = a^2 y^2(1 - x^2) \quad (\text{A.8.10})$$

The roots of these coupled equations are:

$$x = 0 \quad y = 0 \quad \text{and} \quad x = 1 \quad y = 1$$

But from (A.8.7) and (A.8.8) to (A.8.9) and (A.8.10) we multiply $(1 - x^2)$ and $(1 - y^2)$ in both sides of (A.8.7) and (A.8.8) respectively. It creates a root $x = 1$ and $y = 1$. Actually $x = 1$ and $y = 1$ is not the solution of (A.8.7) and (A.8.8).

Substitute $x = 0$ and $y = 0$ into

$$\frac{\partial^2 G}{\partial x^2} - \frac{\partial^2 G}{\partial y^2} - \left(\frac{\partial^2 G}{\partial x \partial y}\right)^2 = a^2 - 1 < 0 \quad \text{when } a < 1.$$

$$G_{\max} = 1 \quad (A.8.13)$$

Finally from (A.8.12) and (A.8.13) we have

$$G_{\max} = 1$$

$$\text{when } 0 \leq \alpha \leq 1 \quad \text{and} \quad 0 \leq x \leq 1 \quad 0 \leq y \leq 1$$

REFERENCES

1. J.H. Crichton, Nuovo Cimento 45A (1966) 256.
2. D. Atkinson, P.W. Johnson, N. Mehta and M. de Roo, Nucl. Phys. B55 (1973) 125-131.
3. F.A. Berends and S.N.M. Ruijsenaars, Nucl. Phys. B56 (1973) 507-524.
4. A. Gersten, Nucl. Phys. B12 (1969) 537-548.
5. D. Atkinson and L.P. Kok, Z Physik 266 (1974) 373.
6. M. Cornille and J.M. Drouffe, Nuovo Cimento A20 (1974) 401.
7. C. Itzykson and A. Martin, Nuovo Cimento 17A (1973) 245.
8. A. Martin, Preprint CERN TH. 1764 (1973).
9. H. Burkhardt, Nuovo Cimento 10A (1972) 379.
10. M.J. Moracsik and W.Y. Yu, J. of Math. Phys. 10 (1969) 925.
11. L. Puzikov, R. Ryndin and Ya. Smorodinskii, Sov. Phys. JETP 5 (1957) 489.

12. F.A. Berends and S.N.M. Ruijsenaars, Nucl. Phys. B56 (1973) 525.
13. R.C. Brunet, L. Gauthier and P. Winternitz, Phys. Rev. P13 (1976) 1390.
14. N.W. Dean and P. Lee, Phys. Rev. D5 (1972) 2741.
15. N.P. Klepikov, Sov. Phys. JETP 14 (1962) 846, 17 (1963) 257, 20 (1969) 505.
16. N.P. Klepikov and Ya Smorodinskii, Sov. Phys. JETP 16 (1963) 1536.
17. C. Efimiu, J. of Math. Phys. 12 (1971) 2, 12 (1971) 2047, 13 (1972) 458.
18. M. Tortorella and J.A. Leise, SIAM J. Appl. Math. 30 (1976) 407.
19. A. Martin, Nuovo Cimento A59 (1969) 131-151.
20. R.G. Newton, J. of Math. Phys. 9 (1968) 2050.
21. Pogorzelski: "Integral Equations and their Applications"
Polish Scientific Publishers.

22. D. Atkinson, P.W. Johnson and R.L. Warnock, Commun. Math. Phys. 28 (1972) 133.
23. D. Atkinson, G. Mahoux and F.J. Yndurain, Nucl. Phys. B54 (1973) 263.
24. I.A. Sakmar, Nuovo Cimento Lett. 2 (1969) 256.
25. H. Goldberg, Phys. Rev. D1 (1970) 1242.
26. R.F. Alvarez-Estrada and B. Carreras, Nucl. Phys. B54 (1973) 237.
27. D. Atkinson, G. Mahoux and F.J. Yndurain, Nucl. Phys. B66 (1973) 429.
28. R.F. Alvarez-Estrada, B. Carreras and M.A. Goni, Nucl. Phys. B62 (1973) 221.
29. M. Manolesson-Grainmaticon, Nucl. Phys. B98 (1975) 298.
30. I.A. Sakmar, Progr. Theor. Phys. 55 (1976) 896.
31. I.A. Sakmar, Progr. Theor. Phys. 48 (1972) 235.
32. I.A. Sakmar, Phys. Rev. D3 (1971) 1675.

33. Y.C. Liu and I.A. Sakmar, Annals of Phys. 77 (1973) 414.
34. S.K. Chan and I.A. Sakmar, Nuovo Cimento 35A (1976) 234.
35. I.A. Sakmar and S.K. Chan, Phys. Rev. D13 (1976) 603.
36. C. Daum, F.C. Erne, J.P. Lagnaux, J.C. Sens, M. Steuer and F. Udo, Nucl. Phys. B6 (1968) 273..
37. M.G. Albrow, S. Andersson/Almehed, B. Bosnjakovic, C. Daum, F.C. Erne, J.P. Lagnaux, J.C. Sens and F. Udo, Nucl. Phys. B25 (1970) 9.
38. M.G. Albrow, S. Andersson/Almehed, B. Bosnjakovic, F.C. Erne, Y. Kimura, J.P. Lagnaux, J.C. Sens and F. Udo, Nucl. Phys. B29 (1971) 413.
39. M.G. Albrow, S. Andersson/Almehed, B. Bosnjakovic, C. Daum, F.C. Erne, Y. Kimura, J.P. Lagnaux, J.C. Sens, F. Udo and F. Wagner, Nucl. Phys. 30B (1971) 273.
40. M.G. Albrow, S. Andersson/Almehed, B. Bosnjakovic, C. Daum, F.C. Erne, Y. Kimura, J.P. Lagnaux, J.C. Sens and F. Udo, Nucl. Phys. B37 (1972) 594.
41. A. DeLesquen, B. Amblard, R. Beurtey, G. Cozzika, J. Bystricky, J. Deregel, Y. Ductos, J.M. Fontaine, A. Gardot, M. Hansroul.

F. Lehar, J.P. Merlo, S. Miyashita, J. Morchet and L. Van Rossum, Phys. Lett. 40B (1972) 277.

42. F. Wagner and C. Lovelace, Nucl. Phys. B25 (1971) 411.

43. L.D. Roper and R.M. Wright, Phys. Rev. 138 (1965) B921.

44. R.E. Cutkosky and B.B. Deo, Phys. Rev. 174 (1968) 1859.

45. R.C. Miller, T.B. Norey, A. Yokosawa, R.E. Cutkosky, H.R. Hicks, R.L. Kelly, C.C. Shih and G. Burleson, Nucl. Phys. 37B (1972) 401.

46. R.E. Cutkosky, private communication.

47. A.M. Sachs, H. Winick and B.A. Wooten, Phys. Rev. 109 (1958) 1750.

48. G. Giacomelli, P. Pini and S. Stagni, CERN Report No. CERN/HERA 69-1.

49. S. Almehed and C. Lovelace, CERN Report No. CERN TH 1408, 1971.